Universität Bremen

Universität Bremen

ATMOSPHERIC AND BIOSPHERIC METHANOL FLUX MEASUREMENTS:

DEVELOPMENT AND APPLICATION OF A NOVEL TECHNIQUE

Vom Fachbereich für Physik und Electrotechnik
der Universität Bremen
zur Erlangung des akademischen Grades eines
Doktor der naturwissenschaften (Dr. rer. nat.)
genehmigte Dissertation

von

Sheena Juliet Solomon

1. Gutachter : Prof. Dr. John Burrows
2. Gutachter : Prof. Dr. Gunnar Schade
1. Prüfer : Prof. Dr. Justus Notholt
2. Prüfer : Prof. Dr. Peter Richter
1. Beisitzer : Dr. Annette Ladstaetter Weissenmayer
2. Beisitzer : Anja Schoenhardt

Submitted on : April 2007
Defended (awarded) on : May 2007

A

Dedication:

This thesis is the fulfilment of a noble and humble wish of my beloved parents:

Joseph David Solomon and Aleyamma Joseph Solomon!

Contents

Abstract

A novel atmospheric methanol (CH_3OH) measurement technique (M&M), employing selective gas-phase catalytic conversion of CH_3OH to formaldehyde (HCHO) followed by detection of the HCHO product, is developed, tested, and applied for various studies. The effects of temperature, gas flow rate, gas composition, reactor-bed length, and reactor-bed composition on the CH_3OH conversion efficiency of iron molybdate catalyst [Mo-Fe-O] were studied. Best results were achieved using a 1:4 mixture (w/w) of the catalyst in quartz sand. Optimal CH_3OH to HCHO conversion (>95% efficiency) achieved at a catalyst housing temperature of 345°C and an estimated sample-air/catalyst contact time of <0.2 seconds. The CH_3OH and HCHO measurement accuracy was better than 6.4% at 1-75 ppb (parts per billion). Potential interferences arising from conversion of methane (CH_4), carbon dioxide (CO_2), ammonia (NH_3), sulphur dioxide (SO_2) and a suit of other VOCs (Volatile Organic Compounds) to HCHO were found to be negligible under most atmospheric conditions and catalyst housing temperatures.

Applying the method, measurements of CH_3OH under different atmospheric backdrops were made during various measurement campaigns and thus, are validated; whereby suggest that the new method is an inexpensive and effective way to monitor atmospheric CH_3OH.

Tropospheric ozone effects on plant physiological cycle and how ozone fumigated plants react against CH_3OH and HCHO emissions were studied in order to identify the process based relationships arising from negative global change effects. The measured emissions of CH_3OH exhibited near-exponential temperature dependence at 10°C-32°C and a strong dependence on light and stomatal conductance. During the acute ozone experiments (~170 ppb $4h^{-1}$ day^{-1}) CH_3OH and HCHO were emitted with maximum rates of about 100 µg gw^{-1} h^{-1} (micrograms per gram fresh weight per hour) and 22 µg gw^{-1} h^{-1} from plants which were 2-5 fold greater than the normal emission rates. The increase in HCHO flux and decrease in CH_3OH observed during the plant recovery period clearly showed that CH_3OH produced inside the plant cell was converted to HCHO as suggested by the formate cycle in plants. The increased CH_3OH emission, as seen in this study, in response to higher temperatures has high correlation with climate change as the present warming climate milieu can encourage more plant growth, and therefore increased levels of VOCs in areas where VOC-emitting plants grow abundantly. So the future global climate change will have a profound impact on the emissions of these compounds and thus, will affect the chemistry of the troposphere.

The in house indoor air quality measurement and assessment using M&M and PTR-MS reveals that the breathing air in our office premises is contaminated to stir disturbing problems in health and comfort of the occupant. Therefore, the study demands a serious revision of air quality standards in the working environments.

Publications

Parts of this work have been used in the following journal articles.

Peer reviewed

1. **Solomon, S. J**., T. Custer, G. Schade, A. P. Soares Dias, and J. P. Burrows: Atmospheric methanol measurement using selective catalytic methanol to formaldehyde conversion, *Atmos. Chem. Phys.,* 5, 2787–2796, 2005.

2. **Solomon, S. J**., G. Schade, A. Ladstätter-Weissenmayer, J. Kuttippurath and J. P. Burrows: VOC concentrations in an indoor workplace environment of a university building *Indoor and Built Environment*, Vol. 17, No. 3, 260-268, DOI: 10.1177/1420326X08090822, 2008.

3. G. W. Schade, **S. J. Solomon**, E. Dellwik, K. Pilegaard, and A. Ladstätter-Weissenmayer: Methanol and other VOC fluxes from a Danish beech forest during springtime, *Biogeosciences*, Page(s) 4315-4352. SRef-ID: 1810-6285/bgd/2008-5-4315, 2008.

4. Wisthaler, A., E. C. Apel, J. Bossmeyer, A. Hansel, W. Junkermann, R. Koppmann, R. Meier, K. Müller**, S. J. Solomon**, R. Steinbrecher, R. Tillmann, and T. Brauers: Technical Note: Intercomparison of formaldehyde measurements at the atmosphere simulation chamber SAPHIR, *Atmos. Chem. Phys*., 8, 2189-2200, 2008.

5. Apel, E.C., T. Brauers, R. Koppmann, R. Tillmann, C. Holzke, R. Wegener, J. Boßmeyer, A. Brunner, T. Ruuskanen, M. Jocher, C. Spirig, R. Steinbrecher, R. Meier, D. Steigner, E. Gomez Alvarez, K. Müller, **S. J. Solomon**, G. Schade, D. Young, P. Simmonds, J.R. Hopkins, A.C. Lewis, G. Legreid, S. Reimann, A. Wisthaler, A. Hansel, R. Blake, K. Wyche, A. Ellis, and P.S. Monks, Intercomparison of oxygenated volatile organic (OVOC) measurements at the SAPHIR atmosphere simulation chamber, *J. Geophys. Res., 113*, D20307, 2008.

In preparation

6. **Solomon, S. J.**, C. Cojocariu, J. P. Burrows, and C. N. Hewitt: Effect of ozone fumigation on leaf level emission of methanol and formaldehyde from Grey Poplar plants: Global climate change effects, to be sumitted to *Plant Phys.*

7. **Solomon, S. J.**, A. P. Soares and G. W. Schade: Investigation of chemical interferences on iron-molybdate catalyst applied for atmospheric MeOH measurement, in preparation *Appl. Cataly. B.*

8. **Solomon, S. J**., J. Kuttippurath and A. Ladstätter-Weissenmayer: Modelling environmental tobacco smoke in a non-industrial workplace environment, to be submitted to special issue of *International Journal of Environmental Research and Public Health* (ISSN 1660-4601).

Conference contributions

1. **Solomon**, **S. J**., C. Cojocariu, J. P. Burrows, and C. N. Hewitt: Effect of ozone fumigation on methanol and formaldehyde emission by the leaves of Grey poplar: Global Climate Change Effects, *ACCENT Symposium, Urbino*, *Italy*, 23-27 July 2007.

2. **Solomon, S. J**. and J. P. Burrows: Air quality and health risk assessment in non-industrial indoor environment: A case study, *The Third International Conference on Environmental Science and Technology, Houston TX, USA,* 6-9 August 2007.

3. **Solomon, S. J**., J. P. Burrows, J. Kuttippurath, A. Ladstätter-Wissenmayer, and G. Schade: Evaluation of occupational exposure to VOC concentrations in an indoor workplace environment, *ACCENT Symposium, Urbino,Italy,* 23-27 July 2007.

4. **Solomon, S. J.** and J. P. Burrows: Biogenic (O)VOCs – Global Climate Change Effects, *The 3rd ACCENT Barnsdale Expert workshop on VOC, Barnsdale, UK,* 30 October - 01 November 2006.

5. **Solomon, S. J**., J. Kuttippurath, A. Ladstätter-Weissenmayer and J. Burrows: Exposure assessment of VOCs in an indoor workplace environment of a university building in Germany, *Geophysical Research Abstracts,* Vol. 8, 09266, 2006.

6. **Solomon, S. J**., T. Custer, G. Schade, and A. P. Soares Dias: A new method for semi-continuous atmospheric methanol measurements and its application to measure soil-atmosphere methanol exchange, *Geophys. Res. Abs.,* Vol. 7, 00825, 2005.

7. **Solomon, S. J**., T. Custer, G. Schade, and J. P. Burrows: Semi-continuos measurements of methanol and formaldehyde during the ACCENT OVOC intercomparison campaign, *First ACCENT Symposium, Urbino, Italy,* 12-16 September 2005.

8. **Solomon, S. J**., T. Custer, G. Schade and J. Burrows: Application of a selective catalytic convertor for atmospheric methanol measurements: First results*, Faraday Discuss., University*

of Leeds, UK, 130 p, 11-13 April 2005.

9. Apel, E., T. Brauers, R. Koppmann, R.Tillmann, C. Holzke, R. Wegener, J. Boßmeyer, A. Brunner, T. Ruuskanen, M. Jocher, C. Spirig, R. Steinbrecher, R. Meier, D. Steigner, E. Alvarez, K. Müller, **S. J. Solomon**, D. Young, P. Simmonds, G. Legreid, A. Wisthaler, A. Hansel, R. Blake, K. Wyche, P. S. Monks: Intercomparison of oxygenated volatile organic (OVOC) measurements at the SAPHIR atmosphere simulation chamber, *Amer. Geophys. Union, SanFrancisco, USA,* 11–15 December 2006.

10. Cojocariu, C., **S. J. Solomon**, J. Burrows and C. N. Hewitt: Effect of ozone fumigation on isoprene and methanol emission by the leaves of Grey poplar (*Populus x canescens*), *Geophys. Res. Abs.,* Vol. 8, 03615, 2006.

11. Wisthaler, A., A. Hansel, R. Koppmann, T. Brauers, J. Boßmeier, R. Steinbrecher, W. Junkermann, R. Meier, K. Müller, **S. J. Solomon**, and A. Bjerke: PTR-MS measurements of HCHO and results from HCHO intercomparison measurements in the atmosphere simulation chamber SAPHIR, *Deutschen Physikalischen Gesellschaft (DPG), Hiedelberg, Germany,* 13-16 March 2006.

12. Wisthaler, A., A. Hansel, R. Koppmann, T. Brauers, J. Bossmeyer, R. Steinbrecher, W. Junkermann, K. Müller, **S. J. Solomon,** and E. Apel: PTR-MS measurements of HCHO and results from HCHO intercomparison measurements in the atmosphere simulation chamber SAPHIR, *Geophys. Res. Abs.,* Vol. 8, 04776, 2006.

13. Wegener, R., T. Brauers, J. Bossmeyer, C. Holzke, R. Tillmann, R. Koppmann, A. Brunner, M. Jocher, C. Spirig, R. Steinbrecher, R. Meier, D. Steigner, E. Alvarez, K. Müller, **S. J. Solomon,** D. Young, J. Hopkins, G. Legreid, A. Wisthaler, A. Hansel, R. Blake, K. Wyche, T. Ruuskanen, A. Bjerke, E. Apel: Intercomparison of oxygenated volatile organic compounds (OVOC) measurements in the atmosphere simulation chamber SAPHIR, *Geophys. Res. Abs.*, Vol. 8, 04427, 2006.

14. Koppmann, R., T. Brauers, R. Bossmeyer, J. Bossmeyer, C. Holzke, R. Tillmann, A. Brunner, M. Jocher, C. Spirig, R. Steinbrecher, R. Meier, D. Steigner, E. Alvarez, K. Müller, **S. J. Solomon,** D. Young, J. Hopkins, G. Legreid, A. Wisthaler, A. Hansel, R. Blake, K. Wyche, T. Ruuskanen, A. Bjerke, E. Apel: Intercomparison of oxygenated volatile organic compounds (OVOC) measurements, *First ACCENT Symposium, Urbino, Italy,* 12-16 September 2005.

Acronym

ACCENT	Atmospheric Composition Change the European Network of Excellence
BVOC	Biogenic Volatile Organic Compound
CEAM	Centro de Estudios Ambientales del Mediterraneo
DNPH	Dinitrophenylhydrazine
DOAS	Differential Optical Absorption Spectroscopy
DWD	DeutscheWetterdienst
EMPA	Swiss Federal Laboratories for Materials Testing and Research
ETS	Environmental Tobacco Smoke
EU	European Union
FAL	Forschunganstalt für Agrarökologie und Landbau
FEP	Perfluorethylenpropylene
FID	Flame Ionisation Detector
FTIR	Fourier Transform Infrared Spectroscopy
GM	Geometric Mean
HPLC	High Performance Liquid Chromatography
HYSPLIT	HYbrid Single- Particle Lagrangian Integrated Trajectory model
IAQ	Indoor Air Quality
IARC	International Agency for Research on Cancer
IFT	Leibniz-Institute for Tropospheric Research
IMK-FZK	The Institut für Meteorologie und Klimaforschung of the Forschungszentrum Karlsruhe
ICG-II	Institut für Chemie und Dynamik der Geosphäre-II
I/O ratio	Indoor/Outdoor ratio
IUP-B	Institute für Umwelt Physik- University of Bremen
J_{CO2}	Net carbon assimilation
J_{H2O}	Transpiration rate
g_{H2O}	Stomatal conductance
MAC	Maximum Accepted Concentration
M&M	Methanol and Methanalyser
MV	Median Value
m/z	Mass to Charge ratio
NILU	Norsk Institutt for Luftforsknin
NCAR	National Center for Atmospheric Research
NMHC	Non-methane Hydrocarbon
NMVOC	Non-methane Volatile Organic Compound
NOAA	National Oceanic and Atmospheric Administration
OPFTIR	Open Path FTIR
OVOC	Oxygenated volatile organic compound
OVOCCOMP	OVOC Comparisons
PAR	Photosynthetically Active Radiation
PFA	Perfluoroalkoxy
PPB	Parts Per Billion
PPFD	Photosynthetic Photon Flux Density
PPT	Parts Per Trillion
PTFE	Polytetrafluoroethylene
PTR-MS	Proton Transfer Reaction Mass Spectrometry
PTR-TOF-MS	Proton Transfer Reaction- Time of Flight-Mass Spectrometry
QA/QC	Quality Assurance/Quality Control
SAPHIR	Simulation of Atmospheric PHotochemistry In a large Reaction Chamber
Tg	Teragram

T_{LA}	Total leaf area
UK	United Kingdom
USEPA	United States Environment Protection Agency
VMR	Volume Mixing Ratio
VOC	Volatile Organic Compound

II. Chemical compounds

C_6 compounds	6 carbon compounds
C_8 compounds	8 carbon compounds
$CH_3C(O)CH_3$	Acetone
CH_3OH	Methanol
CH_4	Methane
CO	Carbonmonoxide
CO_2	Carbondioxide
$FeMoO_4$	Ferrous Iron molybdate
$Fe_2 (MoO_4)_3$	Ferric Iron molybdate
$Fe_2 (MoO_4)_3.3MoO_3$	Iron molybdate
HCHO	Formaldehyde
H_2O	Water
HO_x	OH+ HO_2 +H
m/z 33	Methanol
m/z 69	Isoprene
m/z 137	Monoterpene
m/z 107	C_8-aromatics and benzaldehyde
m/z 105	Styrene
m/z 121	C_9 aromatics
NH_3	Ammonia
NO_x	NO+NO_2
O_3	Ozone
O_x	O_2+O_3
PAN	Peroxy acetyl nitrate
SO_2	Sulphurdioxide
H_2SO_4	Sulphuric acid
MSA	Methane Sulphonate

Acknowledgement

I wish to thank *Prof. Dr. John Burrows* for giving me the opportunity to pursue my thesis at the Institute of Environmental Physics (IUP), University of Bremen. He was instrumental in making this thesis, when there was time when thesis work was in a stand still. I do really appreciate his kindness and comfort during the hard times! It should also be mentioned that he could raise some funds for my plant emission studies conducted at the Lancaster University.

I would like to thank *Prof. Dr. Gunnar Schade,* who selected me for the Ph D. programme in his esteemed research group. His timely advice, support, comments and scientific discussions on several manuscripts are very much appreciated. I indebted to him for inseminating the great scientific spirit during the short period I had with him at IUP.

Prof. Dr. Jorn Bleck-Neuhaus is one of the reasons to have my presence in IUP, who guided me to win the DAAD scholarship to carryout my Postgraduate certificate course in Environmental Physics. I take this opportunity to thank him.

It is a real comfort when Annette (*Dr. Annette Ladstatter-Weissenmayer*) is around. She had always a smile on her face and cheerful words for me. I thank for her help in various administrative issues, and making a friendly atmosphere in the office. She is just more than a colleague; more than a friend as well!!

Tom (*Dr. Thomas Custer*) is an encyclopaedia of technical details of PTR-MS and general laboratory methods. He was very helpful in the development of the M&M. He was always a source of true uninterrupted inspiration apart from being one of my best friends!!

Ngwa Martin. He helped a lot during the Indoor Air measurements. He also taught me to use the PTRMS instrument effectively. I thank his valuable help and support, especially at a period, when the research group was reduced to two of us!

I had a wonderful research team in Lancaster University with *Prof. Dr. Nick Hewitt.* I am very much pleased that my research proposal was accepted as a part of the VOCBAS project by Prof. Hewitt. I thank him for allowing me to use his office, laboratories, other relevant facilities, and for stimulating scientific discussions I had with him.

Dr. Christian Cojocariu is an expert in plant emission studies. He did a few critical studies on our plant emission project. He was my research colleague in my studies at Lancaster. I appreciate his help, co-operation and friendly chats.

I had a great time together with *Dr. Eric Apel* (NCAR, USA), *Prof. Dr. Ralf Koppmann, Dr. Armin Wisthaler* (University of Innsbrück, Austria), and *Eleana Gomez Alvarez*, during the ACCENT OVOC campaign. I also thank *Dr. Theo Braeurs* for providing ACCENT data for our intercomparison and validation studies.

It is really a blessing that we have *Frau Petra Horn* in the administrative departments. She is just rather more than a staff in the secretariat: a real friend in need. I do appreciate her kindness and support during my tenure at IUP. Her smiling face and unsaid words were a real comfort.

I am very much thankful to *Herr. Heiko Shröchter and Herr. Heiko Schellhorn* for their tremendous help and support in maintaining my computers and backup routines.

I am grateful to *Steffani Bhueler, Sabine Packeiser, Susanne Themm and Petra Schumacher* for their administrative support during the course of my thesis.

I would like to extend my sincere thanks to *Rev. Dr. Hans Jürgen Steubing, Rev. Dr. Detlev Knoche and Rev. Musiolik* for their powerful prayers and immense blessings.

Support and prayers from my best friends are beyond words; my childhood friend *Reshmi, Sreeja, and Kairali* were always there for me. I also acknowledge all my friends and teachers in CMS College and Peet Memorial Training College, whose help and support paved the path for my higher studies in Germany.

My parents and siblings are the ones behind the scene for the whole process!! My parent's prayers are the only factor that helped me to face many a problem during the stay at IUP. I formally acknowledge the help and support from my dearest and loving brothers and adorable sister-in-law; *Jacob, Jayan, Jayan (Dr. Jayan. Kuttippurath, CNRS, France) and Richu*. A special word of gratitude to *Dr. Jayan*, my mentor and guide, as it would have been an impossible task without him. I also thank my dearest husband, *Prasanth Kurian (Concordia University, Canada) and, my "precious" son Johan*, for their help, patience and unconditional support in publishing the thesis. I wish to thank my dear uncles and aunts for being the source of inspiration throughout my life. Last but not least, I acknowledge my cute niece *Anna* for being a non-stop entertainment; she was just there when I was in need of her!!

This research was made possible by the Deutsche Forschungsgemeinschaft (DFG) under grant SCHA922/2-1.

Motivation

Methanol is the second most abundant biogenic trace gas in the atmosphere after CH_4, having ubiquitous presence throughout the depth of the troposphere. It is present at typical mixing ratios of 1-10 ppb in the planetary boundary layer and 0.1-1 ppb in the remote atmosphere [*Singh et. al., 1995*]. Being a significant source of atmospheric formaldehyde [*Palmer et al., 2003a*] and CO [*Duncan et al 2004*] it plays an important role in the upper tropospheric photooxidant chemistry of ozone and HO_x [*Singh et al., 2004*]. Having a lifetime of days in the planetary boundary layer, CH_3OH is also often used as a tracer for biogenic emissions.

Although the groundwork for understanding the global cycling of CH_3OH has been laid, the distribution and magnitude of sources and sinks and environmental factors affecting them are still uncertain. Given its comparatively short lifetimes and geographically varying sources, it is not possible to derive a global atmospheric burden or mean abundance from current measurements. Thus, it is clear that the organic chemistry of CH_3OH is not well understood and therefore a great need exists for instrumentation that can reliably identify even low levels in complex mixture and quantify CH_3OH in both field and laboratory studies.

In spite of an impressive array of tools, the experimental measurement of CH_3OH at typical tropospheric abundances can still be quite challenging. The Open-path and Photoacoustic Fourier Transform Infrared instruments (OPFTIR) are artefact-free and are well suited for identification and quantification of most trace gases including CH_3OH, but not below the ppb levels needed to probe the clean troposphere [*Goode et al., 1999*]. Methods designed to preconcentrate/trap CH_3OH, such as carbon based adsorption cartridges, exhibit low trapping efficiency compared to other VOCs at ppt (parts per trillion) levels [*Qin et al., 1997*] though they have been used widely [*Montzka et al., 1993*].

Even though gas or liquid chromatography can readily separate CH_3OH from other species, detection of the CH_3OH following separation can be inefficient due to sampling and storage artefacts [*Kelly and Holdren, 1995*]. While, chemical ionisation mass spectrometry (CIMS) has fast measurement time, it shows linear response up to ppm (parts per million) levels and ppt detection limits without preconcentration, which is an adequate sensitivity for many species in clean air. There are also certain disadvantages using CIMS since compound losses can occur on the sample line or within the instrument, and species identification and quantification can be complicated by the presence of other compounds and fragments with the same mass to charge ratio. It is quite expensive and not yet easily field transportable as well.

In short, each technique has its own strengths and weakness and detection of low molecular weight ambient CH_3OH at trace levels is still a difficult problem!. Methods that will improve sensitivity, portability, and less expensive ambient CH_3OH mixing ratio measurements are clearly desirable, which is the need of the hour and hence, the M&M instrument!!.

Research on direct emissions from the vegetation has focused largely on isoprene and monoterpenes, and available data focusing on the direct biogenic exchange of CH_3OH and HCHO are still sparse. Formaldehyde is central to tropospheric chemistry as when oxidized volatile organic compounds (VOCs) are often broken down into HCHO, making it a viable proxy for overall VOC oxidation. Experiments were carried out using the M&M to identify the pattern and variability in CH_3OH and HCHO emitted from plants to quantify fluctuations of these emissions in relation to environmental factors and physiological factors towards the atmospheric budget of the gases. The emission responses from plants are studied in tune with changes in the physico-chemical factors, which are based on an enforced climate change scenario with a negative feedback. The soil emission studies are planned to meet the requirements to fill in the gaps of current emission budget analysis of CH_3OH (this is an on going work), which is a pilot study in the respective area too.

Thus the overall objective of this work is to study CH_3OH and HCHO in ambient air, develop and validate determination methods for them, characterize their concentrations and estimate the contributions of different VOC sources.

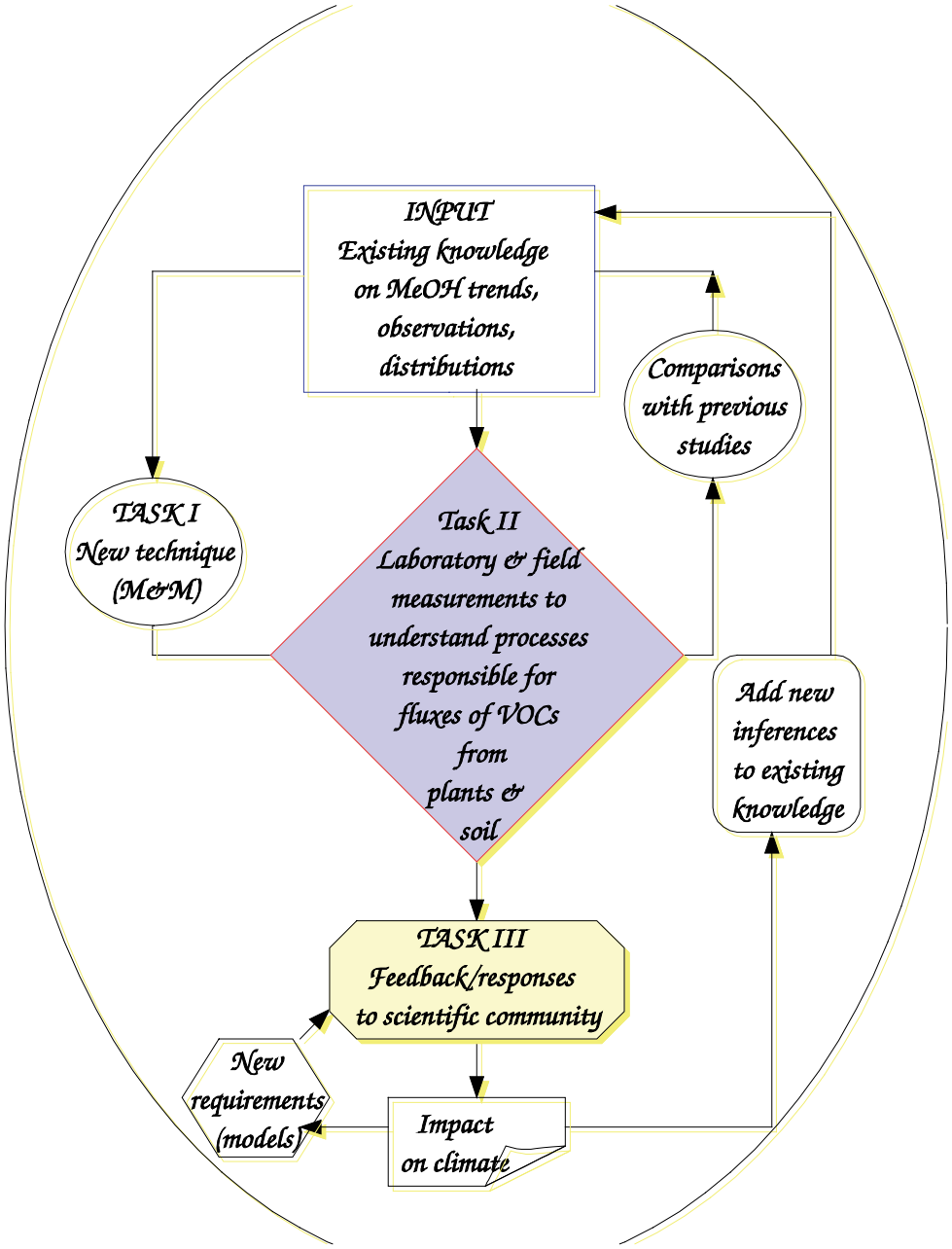

The specific aims of the study were (the publications related to each study are given in bracket with article number, which can be found in the publication list of the author, page 7):

1. To develop a selective method for atmospheric methanol measurements (*paper 1*).
2. To characterise M&M instrument under varying physical and chemical parameters (*paper 7*).
3. To validate the M&M results with other state-of-the-art instruments (*papers 4, 6*).
4. To study the effect of plant physiological and environmental parameters on CH_3OH and HCHO emission from Grey Poplars (*paper 6*).
5. To determine profiles of different VOC sources in indoors, including CH_3OH (*paper 2, 8*).
6. To study the fluxes of CH_3OH from different soil types and identify the parameters that control emissions (*this work is not included in the thesis as it is beyond the scope of this work*).

Chapter 01

Prologue

This thesis deals with the development, characterisation, validation and application of a novel measurement technique, Methanol and Methanalyser (M&M), for atmospheric methanol (CH_3OH) measurements.

What is the significance of atmospheric CH_3OH measurements?
Do we really need another technique to scale atmospheric CH_3OH?
What is the advantage of the new technique over the other existing methods?
How biosphere-atmosphere interaction affects the atmospheric budget of CH_3OH?
How atmospheric CH_3OH cycle influence global tropospheric chemistry and hence, our climate?

These interesting questions are the definite motivation and possible answers for the queries constitute backbone of this doctoral dissertation.

As the study concentrates on the planetary boundary layer (PBL) of the atmosphere, the second chapter lays the foundation for the basic physics, chemistry and dynamics of the lowest atmospheric layer.

The third chapter explains the necessity of development of the new atmospheric methanol measurement technique. Calibration and characterisation of the instrument are also discussed there.

Since any newly developed method needs to be validated against well checked and proven instruments or methods, the fourth chapter is dedicated to the validation activities of the M&M CH_3OH and HCHO measurements. The validation data were amassed from a large intercomparison exercise performed in a simulation chamber.

Application, affordability and feasibility of a technique underline the true value of an instrument. The succeeding chapters deal with various applications of the novel method, which are aimed to help to unveil unknown vistas of various atmospheric processes involving CH_3OH and HCHO.

Perturbation of biogenic trace gas emission on plants and how it affects the physical and chemical aspects of atmosphere is one of the most concerning issues in the environmental science research. VOC emissions are currently modelled using empirical algorithms based on the emission response to environmental factors. However, a thorough understanding of VOC synthesis mechanisms and plant and ecosystem responses to global climate change is required if future emissions are to be reliably predicted on the regional scale. The fifth chapter revolves round the issues of tropospheric ozone (O_3)

and its effect on oxygenated volatile organic compounds (OVOCs), in particular CH_3OH and HCHO emissions from plants. This pilot work was envisaged in a global climate change impact on tropospheric ozone perspective.

Quality of indoor air in our day-to-day working environment has a tremendous impact on our health. Human emissions of VOCs are negligible on a regional (less than 4%) and global scale (less than 0.3%). And as “measurement is fundamental to control” it is necessary to check the pollutant levels in indoor air for both health and environmental reasons. High levels of spurious gases like BTEX (benzene, toluene, ethylbenzene, xylene), VOCs and HCHO, which can act as carcinogens are a real threat to occupant health and comfort. Towards a better understanding of our indoor premises, an experiment was conducted to measure the gas concentration levels. A statistical analysis was also carried out in comparison with previous studies and threshold values of the gases. Apart from the measurements of M&M, supplementary observations from PTR-MS (Proton Transfer Reaction Mass Spectrometry) were also availed for the analysis. The work is presented in the sixth chapter.

A gist of the thesis with important conclusions from various studies is noted in the last chapter.

Introduction

Chapter 02

Physics and Chemistry of the Atmosphere

The earth's atmosphere is a thin layer of gases of varying composition that surrounds the earth. It is a remarkably complex system governed by dynamical and radiative processes within which a myriad of complex chemical processes take place. This chapter mainly features the general structure of earth's atmosphere, starting with the major structure and composition of the atmosphere followed by the biosphere-atmosphere interactions. A laconic description of tropospheric ozone chemistry and climate change issues related to increasing trend of trace gas emissions are also addressed.

2.1 Atmospheric layer

The atmosphere is divided into regions of different typical vertical temperature gradients, -dT/dh, or lapse rates. The troposphere is the lowest layer of the atmosphere extending from surface to 15-17 km in the tropics, 10-12 km in the mid-latitudes and 8-10 km in polar latitudes, which varies with respect to space and time. Temperature decreases uniformly with altitude in the troposphere due to expansive cooling, with warmer air near the earth's surface. About 80% of the total mass of the atmosphere is contained in the troposphere and this region of atmosphere is often dynamically unstable with rapid vertical exchanges of energy and mass associated with turbulent atmospheric mixing. Most of the atmospheric processes and variability's leading to weather pattern occur in this region. There is a thin buffer zone between the troposphere and the next layer called the tropopause. Since the thesis doesn't deal with the stratospheric or mesospheric process, the reader is referred to *Brasseur et al., [1999] and Seinfeld and Pandis, [1998]* for further discussions on the rest of atmospheric layers.

2.2 Atmospheric composition

The chemical composition of earth's atmosphere plays an important role in determining the climate, air quality and existence of the biosphere. The gases in the atmosphere in small amounts are called trace gases. Over the past 40 years atmospheric pollutants of anthropogenic origin were found to increase atmospheric concentration of carbon dioxide at a rate of more than 1% (~1.5 ppm) per year. Similarly other trace gases, such as ozone (O_3), methane (CH_4), nitrous oxide [N_2O] and carbon monoxide (CO) are also increasing proportionally with increasing emissions and population growth. Several processes, including surface emissions and deposition, chemical and photochemical reactions, and transport determine the spatial and temporal distribution of these chemical species in the atmosphere. Therefore it is important to monitor and understand the temporal and spatial changes in the atmospheric composition.

The abundance of a given chemical constituent in the atmosphere can be expressed in terms of number density n_i [number of molecules (N_i) per unit volume (cm^3)]. The mass per unit volume (ρ_i), the partial pressure, P_i, or volume mixing ratios ($VMR)_i$ are the other units to express trace gas concentration. The

VMR_i is often expressed in parts per million (ppm), ppb, and parts per trillion (ppt) in volume (v) or mass (m) corresponding to mixing ratios of 10^{-6}, 10^{-9}, and 10^{-12} respectively.

2.3 General dynamics

The movements of particles and chemical species within the atmosphere are collectively called atmospheric transport. Chemical constituents are redistributed in the atmosphere by the transport processes caused by dynamical disturbances in the atmosphere. Most of the atmospheric motions are driven by the geostrophic equilibrium between the horizontal pressure gradient and Coriolis force. The property that distinguishes the troposphere from stratosphere is the disparity in vertical mixing timescales. The vertical transport of air and chemical species throughout the depth of troposphere occurs via convective updrafts.

The planetary boundary layer (PBL), also known as the atmospheric boundary layer (ABL), is the lowest part of the atmosphere. It responds to surface forcing (heat conduction, friction, pollutant emission, evaporation etc) at a timescale of an hour or less [*Stull, 1993*]. PBL depth can vary from approximately 50 m to 2000 m. In this layer, physical quantities such as flow velocity, temperature, moisture etc., display rapid fluctuations (turbulence) and vertical mixing is strong. Above the PBL is the free atmosphere where the wind is approximately geostrophic (parallel to the isobars i.e., lines of constant pressure) while within the PBL the wind is affected by surface drag and veers. The planetary boundary layer turbulence is produced in the layer with the largest velocity gradients that is at the very surface proximity. This layer - conventionally called a surface layer - constitutes about 10% of the total PBL depth.

2.4 The Terrestrial biosphere and trace gas exchange

The biosphere is the global ecological system integrating all living beings and their relationships, including their interaction with the elements of the lithosphere, hydrosphere, and atmosphere. The structure of the biosphere is strongly dependent on climate interaction of soil, topography and geographic location. Numerous atmospheric trace gases are exchanged at the soil and plant surfaces i.e. they are emitted from the soil/plant to the lower atmosphere or they are deposited to the soil/plant surfaces. Soils and plants all over the terrestrial biosphere play a significant role in the budget of many atmospheric trace gases, wherefore the exchange flux (defined as the mass, heat, or momentum transfer through the surface) of these trace gases with the soil and plant surface is of continued interest to the scientific community.

The pathway for trace gas uptake can be through the stomata or via surface reactions on leaves and the soil or wet surfaces. The deposition of chemical compounds to the surface (e.g., acid rain, O_3 deposition on vegetation) is an important process that directly affects the biosphere. A schematic representation of interaction of biosphere with the free atmosphere is shown in figure 2.1.

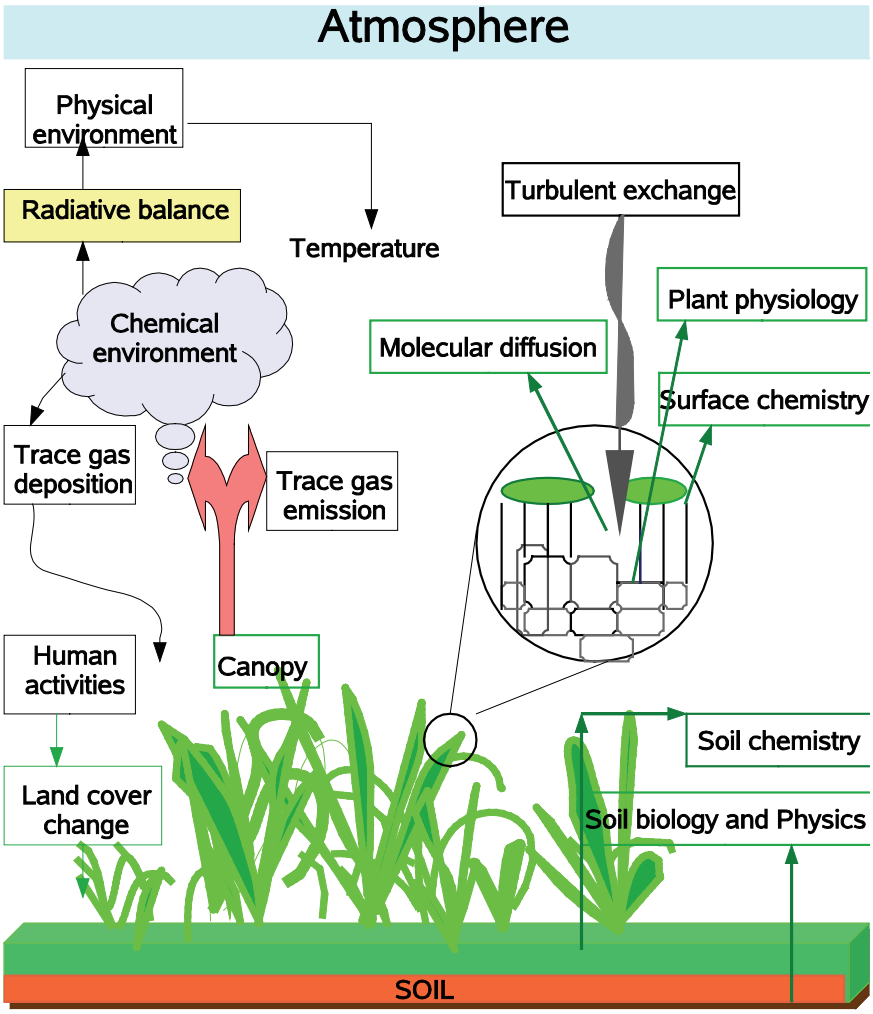

Figure 2.1. *Schematic representation of biosphere-atmosphere interaction and factors influencing trace gas fluxes.*

Natural trace gas emissions are higher in the tropics than in the mid-latitudes to high latitudes, due to variation in vegetation, temperature and soil patterns. The circulation of chemical compounds affecting the chemistry and biology of the earth system are termed biogeochemical cycles (water, carbon, nitrogen, sulphur etc.), which are described in terms of reservoirs (ocean, atmosphere, terrestrial ecosystem) and exchange fluxes between the reservoirs. For the atmosphere, the earth's surface acts both as a source and sink for trace gases and particles. The meteorological conditions in the boundary layer substantially affect the exchange flux of chemical compounds between the surface and free atmosphere. Consequently, the production, consumption and transport of atmospheric trace gases are subject to a suite of biotic and abiotic controls and pathways as they travel between the biosphere and atmosphere.

2.5 Tropospheric chemistry of VOCs

Hydrocarbons (C_nH_m) are organic compounds that consist of only C and H atoms. Substituted hydrocarbons most often contain oxygen, nitrogen, halogens or sulphur. Volatile organic compounds (VOCs) are hydrocarbons (with 2-10 carbon atoms) that have vapour pressures high enough to

significantly vaporize and enter the atmosphere. VOCs are generally grouped into methane and non-methane VOCs (NMVOC) also termed as non-methane hydrocarbons (NMHC). The NMVOC include oxygenated and non-oxygenated compounds. Anthropogenic NMVOC originates usually from vehicle exhausts, from industrial activities (point and area sources) and from atmospheric chemical loss reactions of non-oxygenated VOCs. VOCs produced from biogenic sources such as plants, animals, microbiota and microbial processes in soil and the oceans are termed Biogenic Volatile Organic compounds (BVOC). These include isoprenoids (isoprene and monterpenes) as well as alkanes, alkenes, carbonyls, alcohols, esters, ethers, and acids. The reaction products of VOCs may also take part the in formation and growth of new particles, with possible climate and health consequences [*Griffin et al.*, 1999; *Hoffmann et al.*, 1997]. Knowing the sources and concentrations of different VOCs is essential for the development of O_3 control strategies and for studies of secondary organic aerosols.

2.5.1 The role of VOCs: Tropospheric O_3 formation

The terrestrial biosphere is a major source of VOCs, emitted by the vegetation, and these compounds are highly reactive and thus play a key role in O_3 cycle as well as in the chemical composition of the troposphere. Moreover, VOC involvement in tropospheric chemistry does not only concern gas phase reactions but also particulate formation, and several studies demonstrated that monoterpenes, but also isoprene, oxidation contributes to secondary aerosols formation in the troposphere. [*Sillman, 1999; Chameides et al., 1987; McKeen et al., 1991; Fehsenfeld et al., 1992; Andreae and Crutzen, 1996*]. Several measurements have shown that oxygenated volatile organic compounds (OVOCs) can constitute a significant amount of total VOC loading in the troposphere [*Arey et al. 1991; Fukui and Doskey, 1998; Fall et al., 1999; Schade and Goldstein, 2001; Karl et al., 2001*]. They are sufficiently reactive to impact tropospheric chemistry by contributing ~260 Tg C yr^{-1} to the overall budget of BVOC emissions [*Guenther et al., 1995*].

Many of these OVOCs participate in a series of reactions that produces O_3 as one of several significant products [*Atkinson, 2000; Lightfoot, 1992; Tyndall et al., 2001; Atkinson and Arey, 1998*]. These reactions may also cause a decrease in the concentrations of the hydroxyl radical (OH) and so lead to the accumulation of methane and other greenhouse gases. The atmospheric OVOC reactivity is coupled to the O_x-HO_x-NO_x [$O_x = O_2+O_3$, $HO_x = OH+HO_2+H$, $NO_x = NO+NO_2$] chemistry in the atmosphere that controls the oxidizing capacity of the troposphere. Oxidation of primary VOC molecules is initiated by the OH radical, which is also therefore called the “atmospheric detergent”. By this reaction OH controls the lifetime of most VOC in the atmosphere. The lifetime is the time for the concentration of an organic compound to fall to 1/e of its initial value [*Finlayson-Pitts and Pitts*, 2000].

Natural lifetime [τ] is defined as,

$$\tau = \frac{1}{K_p}[X] \qquad \text{----------2.1}$$

where K_p is the reaction rate of the compound and [X] is the concentration of the oxidant. This reaction is also a key process in tropospheric O_3 formation, where it is initially photolysed and in the end it is produced. The HO_2 radicals produced are recycled to produce OH, which in turn could run more oxidation cycles before it is consumed in other processes. Thus, this cycle effectively produces O_3, which in periods of intensive solar radiation may cause "summer smog" episodes.

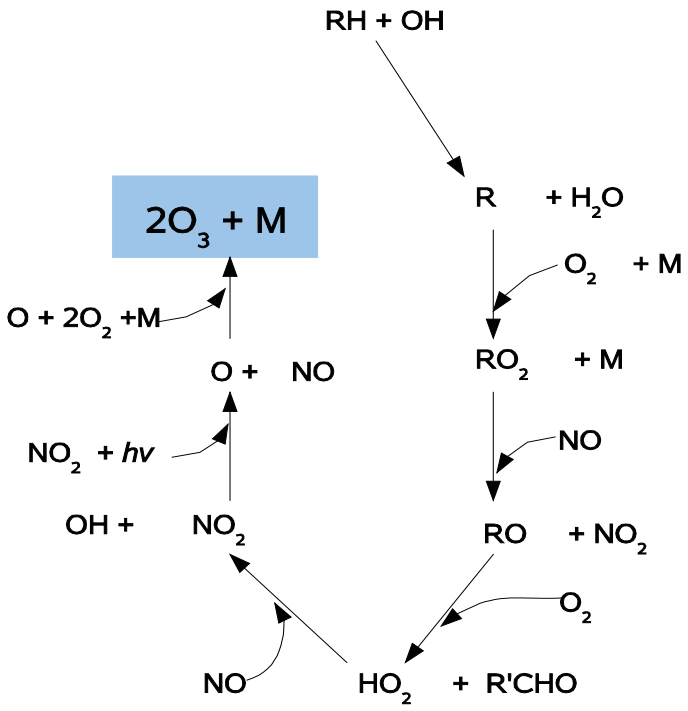

Overall: $RH + 4O_2 + h\nu \longrightarrow R'CHO + H_2O + 2O_3$ ---------- 2.2

Here in equation 2.2, OVOC is abbreviated as *R*H. In addition carbonyl products (aldehyde or ketone) are denoted *R'*CHO, where *R'* denotes an organic fragment having one carbon atom fewer than *R*. Of these OVOCs methanol (CH_3OH) has come under scrutiny due to its ubiquity and relative abundance in the atmosphere and their particularly close chemical connections to hydroperoxy radical (HO_2), formaldehyde (HCHO), and peroxy acetyl nitrate (PAN) [*Grosjean, 1997; McKeen et al., 1997*]. It also has a significant impact upon the oxidising capacity of the atmosphere and can oxidise sulphuric acid (H_2SO_4) to methane sulphonate (MSA) in cloud droplets [*Singh et al., 2000*].

2.5.2 VOCs and climate change

Non-methane volatile organic compounds influence climate change mainly through their production of organic aerosols and their involvement in the production of tropospheric O_3 [*IPCC, 2001*]. About 90 percent of O_3 in the atmosphere on the Earth is found in the stratosphere, with approximately the remaining 10 percent in the troposphere. Although both are O_3, its effects on the global environment are quite different depending on where it is found. In contrast to stratospheric O_3which is regarded as the "good O_3", tropospheric O_3 absorbs infrared rays emanating from Earth's surface and act as a powerful greenhouse gas after methane and CO. Other VOCs than halogenated hydrocarbons have only a small direct impact on radiative forcing. The halogenated HCs with the largest potential to influence climate are CFC-11 ($CFCl_3$), CFC-12 (CF_2Cl_2), and CFC-113 ($CF_2ClCFCl_2$). The radiative forcing due to these three halocarbons is approximately 13% of the total radiative forcing due to carbon dioxide, methane and nitrous oxide.

2.6 Source, sink and budget of CH_3OH and HCHO

2.6.1 Biosynthesis of CH_3OH in plants

The largest methanol source is biogenic in origin. Further analysis of the emissions of volatile organic compounds from leaves has revealed that most plants emit CH_3OH, especially during early stages of leaf expansion. It is probably produced as a by-product of pectin metabolism during cell wall synthesis, and a fraction of this pool is then emitted through stomata during transpiration [*Galbally and Kirstine, 2002; Fall and Benson, 1996*]. Methanol production in plants as a by-product of pectin demethylation is shown in figure 2.2. Methanol emission rate varies significantly during leaf development due to higher rates of pectin demethylation being required during leaf expansion, a period of rapid cell wall synthesis, and then declining demethylation and CH_3OH production in older leaves. The methanol produced in flowering plants can be stored in water and tissue within the plant cells, it can diffuse out through stomata to the atmosphere, or it can be oxidised to HCHO by CH_3OH oxidase. The methanol content of bean leaves has been measured as 10 to 27 $\mu g\ g^{-1}$ (fresh mass) for old and young leaves, respectively [*Nemecek-Marshall et al., 1995*]. The leaf CH_3OH emissions measured by *Nemecek-Marshall et al. [1995]* indicate that if the plant cell emission rate remained constant and no new CH_3OH were produced, all of the CH_3OH in the leaf would be lost to the atmosphere in three hours.

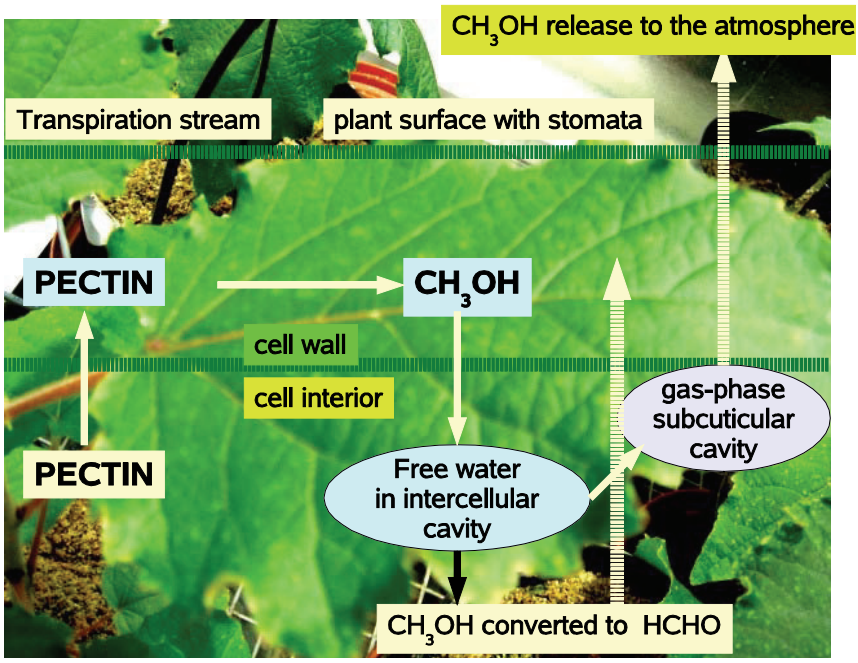

Figure 2.2: *The pectin-methylesterase-catalyzed reaction in plant cell walls is a source of* CH_3OH *formation in plants.*

2.6.2. Other major sources and sink

Methanol can also be produced from methane as shown in equation 2.3. CH_4 is generated and oxidised in ruminating animals, paddies, wetlands, sewage and landfills. Methanol (along with HCHO and formate) is an intermediate in the methane oxidation process [*Higgins et al., 1984*],

$$CH_4 \rightarrow CH_3OH \rightarrow HCHO \rightarrow HCOOH \rightarrow CO_2 . \qquad \text{---------- 2.3}$$

Methanol, thus formed, is utilised for growth by methylotrophs, and is readily converted to HCHO and then formate, by the enzyme alcohol dehydrogenase. So far, uptake by methylotrophs on plant leaves [*Fall, 1996*], production by methanotrophs [*Sluis et al., 2002; Mancinelli, 1995*], and degradation of plant matter by fungi and other microorganisms [*Galbally and Kirstine, 2002*] can easily be imagined, but their effect on biosphere-atmosphere exchange remain to be explored in depth experimentally. Anthropogenic source of CH_3OH result from biomass burning and human activity (for the production of HCHO, acetic acid, chloromethanes, and methyl methacrylate) as CH_3OH is a widely used industrial chemical. Based on concentrations measured in the troposphere and lower stratosphere [*Singh et al., 2000*] and the conclusions of budgetary modeling studies [*Heikes et al., 2002*], it has been suggested that the ocean may be a substantial source of CH_3OH. However, recent results indicate that the North Atlantic may in fact be a net sink for CH_3OH [*Carpenter et al., 2004*]. Observations of CH_3OH in biomass burning plumes and in clouds suggest that cloud-based heterogeneous reactions might be a significant CH_3OH sink [*Tabazadeh et al., 2004*], while ongoing production in biomass burning plumes is observed as well [*Singh et al., 2004; Holzinger et al., 2005*].

Studies show that CH_3OH has an average chemical lifetime due to gas phase removal of 16 days in the free troposphere [*Singh et al., 1995*], and a shorter lifetime of 69 daylight hours in the planetary boundary-layer [*Jacob et al., 1989*]. The chief process for removal of atmospheric CH_3OH is oxidation by hydroxyl radicals (*OH) in the gaseous phase (equation 2.4).

$$CH_3OH + *OH \rightarrow CH_2OH \text{ or } CH_3O + H_2O \quad \text{---------- 2.4}$$

$$CH_2OH \text{ or } CH_3O + O_2 \rightarrow HO_2 + CH_2O \quad \text{---------- 2.5}$$

Methanol serves as a significant source of odd hydrogen radicals (HO) via the production of HCHO (2.5) followed by the production of CHO, especially in the upper troposphere [*Singh et al., 1995*]. A similar reaction of CH_3OH and hydroxyl radicals occurs in the aqueous phase too where cloud droplets provide an aqueous medium for the chemical reaction of CH_3OH with hydroxyl radicals [*Monad and Carlier, 1999*]. The two other possible mechanisms for the gas phase production of CH_3OH in the atmosphere are through the reaction of methoxy radicals ($*CH_3O_2$).

$$*CH_3O_2 + *CH_3O_2 \rightarrow CH_3OH + *CH_2O + O_2 \quad \text{---------- 2.6}$$

$$HOCH_2CHO + h\nu \rightarrow CH_3OH + CO. \quad \text{---------- 2.7}$$

The reaction products of Equation 2.6 represent a minor pathway for the loss of methylperoxy radicals by self-reaction [*Tyndall et al., 2001*]. Methanol is also produced from glycolaldehyde which is formed in the atmosphere from isoprene and ethene oxidation (equation 2.7). Recent budget analysis of CH_3OH based on best knowledge of processes show an estimate of 128 Tg yr^{-1} (teragram per year) from plant growth, 38 Tg yr^{-1} from atmospheric production by CH_3O_2 radical reactions, 23 Tg yr^{-1} from plant decay, 13 Tg yr^{-1} from biomass burning and biofuels, and 4 Tg yr^{-1} from fossil fuel combustion and industrial activities [*Jacob et al., 2005*].

2.6.3 Sources and sinks of HCHO

HCHO is an important intermediate product of atmospheric methane oxidation, but is also produced from numerous other hydrocarbons, such as 1-alkenes, and in particular isoprene, the dominant BVOC emission. It is a primary emission product from biomass burning [*Carlier et al., 1986; Lipari et al., 1984*] and from fossil fuel combustion [*Anderson et al., 1996*]. Formaldehyde is involved in acidification of rain and it is considered a precursor of hydrogen peroxide. Formalehyde is a significant component of photochemical smog but is not transported far due to its short lifetime (<5h during daytime in mid-latitudes). Mixing ratios are measured as high as 100 ppb (Los Angeles smog) and as low as 0.1 ppb in marine background environments [*Warnecke, 2000*]. In clean or remote areas, the major natural source of HCHO is photooxidation and ozonolysis of naturally emitted nonmethane

hydrocarbons (NMHCs). It photolyses readily at wavelengths below 400 nm and reacts rapidly with the hydroxyl radical (OH) providing an average tropospheric lifetime for HCHO of about 5 hours [*Arlander et al., 1995*]. The main removal processes in the troposphere during daylight are the reaction with OH radicals and photolysis as shown in equation 2.8.

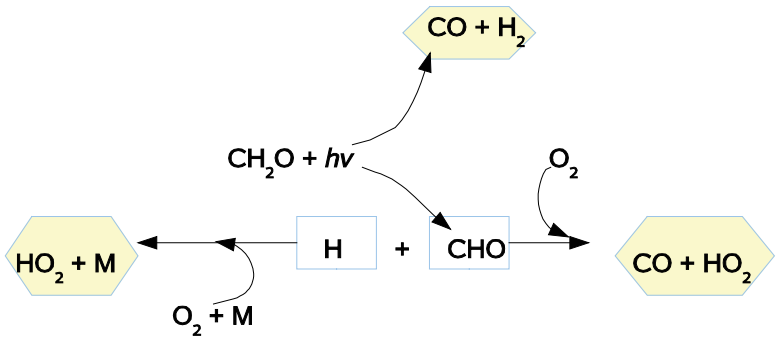

---------- 2.8

Formaldehyde is photo dissociated to form CHO, which reacts with oxygen primarily to form CO, precursor of CO_2. Formaldehyde photolysis and its oxidation by OH radicals also generate hydro peroxy radical (HO_2) which react with NO producing NO_2, a precursor of O_3. Removal by wet and dry deposition can be important during the night [*Altschuller, 1993; Lowe and Schmidt, 1983*]. It is also involved in acidification of rain and is considered as a precursor of hydrogen peroxide.

2.7 Effects and influences of BVOC emission on plants

BVOCs are synthesized in many different plant tissues and by various physiological processes, but the knowledge on how they affect plant functions and ecology is still scarce. They are emitted by plants as attractors of pollinators and herbivore predators thereby influencing the species distribution in ecosystems [*Penuelas et al., 1995: Shulaev et al., 1997*]. However, the most interesting hypothesis of recent studies is that BVOCs, i.e. isoprene and monoterpene, can have an important function in plant thermo tolerance. This is supported by the finding that monoterpene emission by several Mediterranean tree species confers protection against high temperature [*Loreto et al., 1998*], whereas other studies indicated a connection between photorespiration and BVOC emissions [*Jones et al., 1975; Penuelas and Llusia, 2003*]. The thermotolerance function of BVOCs is particularly important for forest ecosystems in the context of global warming, since it is known that emissions generally increase with temperature. However, it is not well established if the increased emissions will cool or warm the environment and how forest ecosystems will be affected by an enhanced BVOC emission.

Although on a regional scale the balance between natural and anthropogenic sources may be different, modeling studies as well as field observations indicate that BVOC play a significant, often dominating, role in the photochemical O_3 formation in the troposphere in both rural and urban environments. Still, the release of the VOCs other than isoprenoids has been poorly investigated and there are many gaps of knowledge on the factors controlling the emission of these compounds. Besides internal factors like genetic and biochemical, external factors of biotic and/or abiotic origin like

temperature, relative humidity, water availability all play a role in controlling and determining BVOC synthesis [*Kreuzweiser et al., 2001; Karl et al., 2004; Cojocariu et al., 2004*]. BVOC emission is thus limited by both physiological and physicochemical factors. The physiological factors determine the availability of VOC precursors and rate-controlling enzymes. The physicochemical factors limit the volatility (air-phase partial pressure, aqueous- and lipid-phase concentrations), the diffusion within gaseous, aqueous and lipid phases of organic compounds within the leaves, and the gas-phase diffusion at the leaf-atmosphere interface [*Staudt et al., 2001; Niinemets et al., 2004*]

2.8 Tropospheric O_3 and its impact on BVOC emission

There has been an increasing concern in recent years that O3 in the troposphere may be affecting the health and productivity of forests around the globe [*Skarby et al., 1998; Braun et al., 1999; Sanz and Millan, 1999*]. Increasing atmospheric O_3 concentration in the troposphere result in greenhouse warming of the lower atmosphere which might lead to higher emissions of VOCs from plants. On the other hand increasing O_3 on regional and hemispheric scales might suppress net productivity and growth in ecosystems. A schematic representation of these interactive processes is shown in Figure 2.3.

Although, ambient concentrations of O_3 typically range from 20 to 60 ppb, peak episodes of 100-150 ppb have also been found in photochemical smog regions [*Lorenzini and Panattoni, 1986*]. Ozone enters plants through leaf stomata and oxidizes plant tissue to produce reactive oxygen species, causing changes in biochemical and physiological processes that contribute to VOCs emission to the atmosphere. Because biogenic VOC emissions exert a very significant influence on atmospheric chemistry, it is crucial to identify the responses and feedbacks of the terrestrial vegetation to anthropogenically induced climate change. Acute dosages of O_3 cause severe foliar injuries [*Chappelka and Samuelson, 1998*], accelerated senescence, premature leaf loss and reduced photosynthesis which make plants more susceptible to pests and environmental stresses [*Peel and Dann, 1991*]. As a rule of nature plants use several strategies to combat O_3 stress, which include O_3 tolerance and avoidance to its byproducts. The pollutants can be avoided by stomatal closure and membrane impermeability [*Heath, 1994*]. Out of several factors such as light, humidity, and temperature that can affect emissions of VOCs from plants, the effect of O_3 on the emission signalling system still remains unexplored [*Penuelas and Llusia, 2001a*].

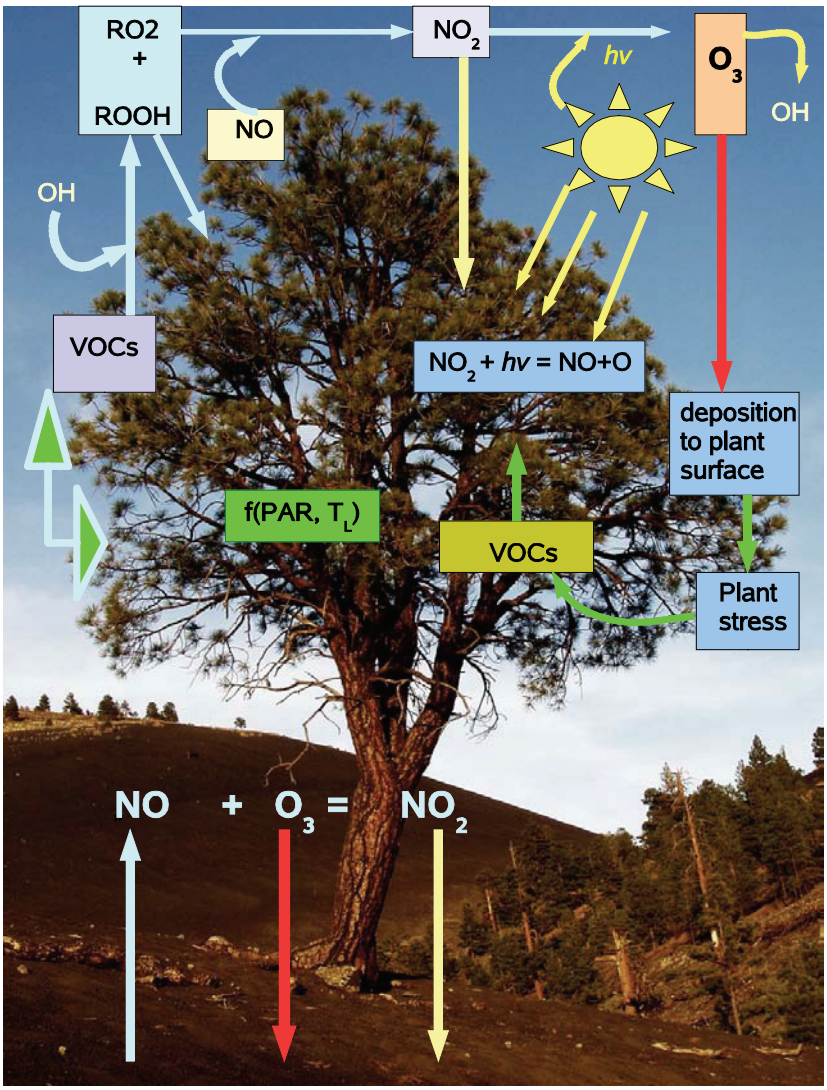

Figure 2.3: *Interaction of VOCs in the atmosphere-biosphere system leading to the formation/deposition of tropospheric O_3.*

The recent studies by *Loreto et a.l, [2001]* on O_3 fumigated plant types show that plants become resistant to acute and short exposure of O_3 if they are fumigated with isoprene and this isoprene-emitting plant do not suffer damage when exposed to O_3. According to *Beauchamp et al., [2005]* increased CH_3OH emissions were observed together with leaf alcohols and aldehydes when tobacco varieties of plants were exposed to short pulses of high concentration ozone. Furthermore, it remains to be tested other possible O_3 effects on the structure and the biochemical components of plants.

The development of M&M

Chapter 03

Development of a new method for atmospheric CH_3OH measurement using selective catalytic CH_3OH to HCHO conversion

Apart from being an important VOC in the troposphere, CH_3OH is also an important intermediate used in the chemical industry for the synthesis of various hydrocarbons and oxidation products. In the chemical industry, oxidative dehydrogenation of CH_3OH is a key to the manufacture of HCHO [Gerberich et al., 1980], which is accomplished by passing CH_3OH vapour in air over a heated, chemically selective catalyst and collecting the resulting HCHO product from the exhaust stream. The development and characterization of a new technique (M&M) based on this selective catalysis method is explained in this chapter.

3.1 The method

Using the catalytic process for atmospheric measurements, if gas-phase CH_3OH in the troposphere can efficiently and selectively be converted to HCHO, then capabilities of existing atmospheric HCHO measurement instrumentation can be expanded, simply and at low cost, to include CH_3OH. A variety of measurement techniques also exist for the measurement of HCHO including colorimetric techniques, fluorescent and derivatization techniques and are reviewed in *Kleindienst et al.,* [*1988*] and briefly in *Clemitshaw* [*2004*]. Intercomparisons among various HCHO detection methods have also been carried out in *Gilpin et al.,* [*1997*] and *C´ardenas et al., [2000]*. Although HCHO can also be a challenge to analyse, over the last 20 years high quality measurements of HCHO have been established using wet-chemical techniques [*Dong and Dasgupta, 1987; Fan and Dasgupta, 1994; Heikes et al., 1996; Dasgupta et al., 1999; Li et al., 2001*]. Such instruments are relatively inexpensive, have a detection limit in the mid-ppt range, are commercially available, run essentially continuously, and are highly selective for HCHO. This method was developed based on this simple but elegant idea of incorporating a selective catalytic converter to a HCHO instrument for semi-continuous measurements of both compounds. A simple flow diagram of the new technique for CH_3OH measurement is shown in figure 3.1.

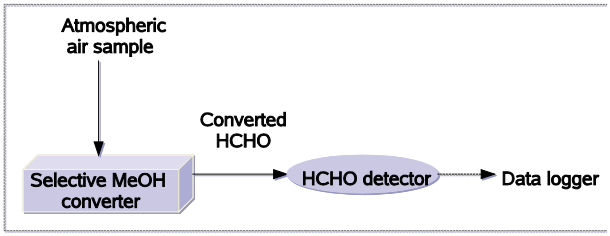

Figure 3.1*: A schematic representation of the M&M detection technique where atmospheric CH_3OH is passed through heated the catalyst and the converted HCHO is further sampled by the HCHO detector.*

3.2 Iron molybdate catalyst

In 1931, it was *Adkins and Peterson* who first pointed out the use of iron molybdenum oxides as a catalyst for CH_3OH to HCHO oxidation. The Adkins-Peterson reaction is the air oxidation of CH_3OH to HCHO with metal oxide catalysts such as iron oxide, molybdenum trioxide or combinations thereof. Of the two existing stoichiometric iron-molybdates, ferric [$Fe_2 (MoO_4)_3$] and ferrous [$FeMoO_4$], ferric molybdate is more effective in catalysing the selective oxidation of CH_3OH to HCHO. Current industrial production of HCHO is based on heterogeneous catalytic processes using CH_3OH as feedstock.

3.2.1 Catalyst preparation

All of the iron molybdate catalyst used for this study was prepared in laboratories at the Universidade Tecnica de Lisboa, Portugal and a full description of its preparation and characterisation are given elsewhere [*Soares et al., 2001, 2003*]. Briefly, the molybdenum (Mo) rich iron molybdate catalyst (atomic ratio = Mo/Fe = 3; [$Fe_2 (MoO_4)_3.3MoO_3$]) was co-precipitated from aqueous solutions of iron nitrate and ammonium heptamolybdate. The yellow-green precipitate was ripened in contact with mother liquors at 373 K for 3 h. Finally, the precipitate is filtered, dried at 393 K overnight and calcinated. Calcinations were performed at 648 K for 10 h in a flow of air.

3.2.2 Reaction Mechanism: CH_3OH conversion to HCHO

The mechanism of CH_3OH oxidation is widely believed to occur through the dissociative reactive adsorption of CH_3OH with a surface oxygen atom to form methoxy and hydroxyl groups, followed by the reaction of the methoxy intermediate with a second surface oxygen atom to form HCHO and a second hydroxyl as shown in the chemical equation (equation 3.1). Reaction of the two hydroxyl groups leads to the formation of water. Dissociative adsorption of dioxygen completes the redox cycle. This reaction mechanism is in general agreement with the mechanism of partial oxidation of hydrocarbons catalyzed by metal oxides first proposed by Mars and van Krevelen [*Jiru et al., 1983; Pernicone et al. 1969*].

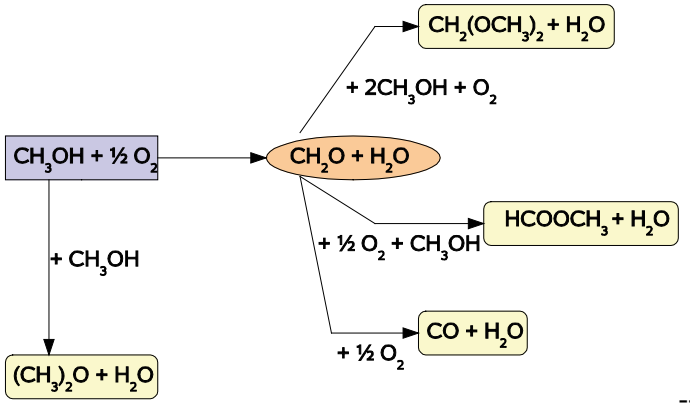

---------- 3.1

A variety of specific steps has been proposed regarding the details of the bonding of CH_3OH and hydroxyl groups on the surface [Pernicone et al., 1969, Allison and Goddard, Ohuchi et al., 1991, Chowdhry et al., 1998]. Irrespective of the specific identity of the adsorption site, the CH_3OH adsorption process involves two entities, a metal atom site to which the methoxy group is bound and an oxygen atom site to which the hydrogen atom is bound as a hydroxyl group. The rate-determining step in the oxidation of CH_3OH to HCHO is the conversion of the methoxy intermediate to HCHO through abstraction of a hydrogen atom.

3.2.3 The catalytic reactor

The reactor constructed for catalytic conversion of gas-phase CH_3OH to HCHO consisted of a stainless steel tube 15 cm in length and having 1 cm ID (inner diameter) and 1.27cm OD (outer diameter) embedded in a heated aluminium block. The block diagram of the catalytic convertor filled with the catalyst is depicted in figure 3.2. The tube, through which sample air was passed, was partially filled with a catalyst bed consisting of a mixture by weight of iron molybdate catalyst and quartz sand (0.5 mm average grain diameter). The quartz sand served as an inert substrate that evenly distributes the catalyst and that allows the sample air to flow evenly across the diameter of the tube, thereby increasing catalyst/ CH_3OH contact.

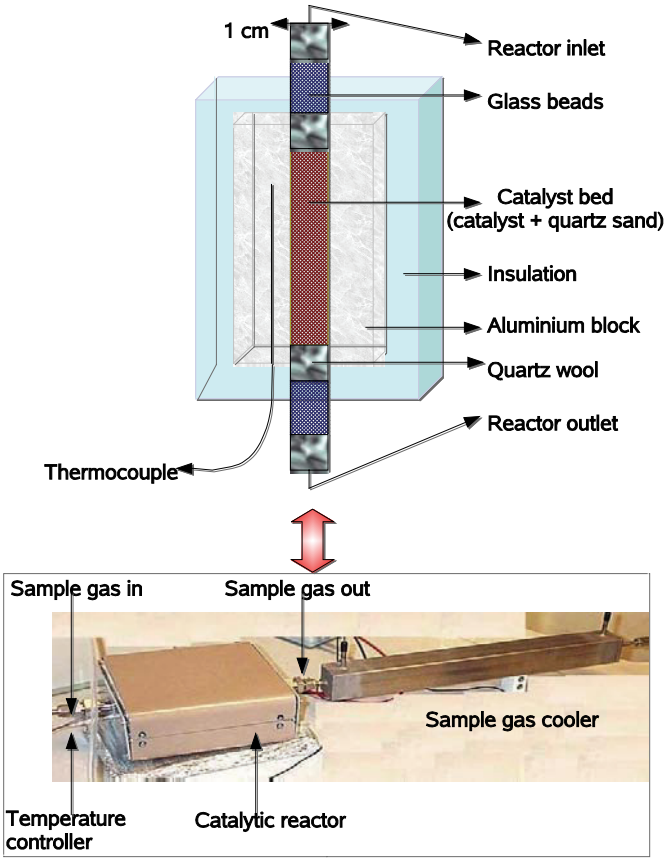

Figure 3.2: *The block diagram depicting the internal structure of catalytic convertor constructed for selective CH_3OH conversion. The picture also shows the constructed reactor with gas cooler attachment.*

The catalyst bed, filling various fractions of the total tube length, was held in place at the middle of the tube by filling the remainder with glass beads and glass wool. The ends of the tube were then fixed using 1/2" to 1/4" swagelok reducing unions.The aluminium block for the reactor bed was heated with a commercial cartridge heater with embedded thermocouple (350W, Ihne&Tesch HPS 10D, 100L). The temperature of the block was maintained using an electronic temperature controller (TC-Direct, Germany). The catalyst assembly was surrounded by Silcapor ultra 100-23 insulation and placed inside a metal box.

3.3 HCHO detection

A commercial, wet-chemical HCHO measurement instrument (Alpha Omega Power Technologies, Model MA-100) was employed for all measurements and is hereafter referred to as the methanalyser. A more thorough description of this and related instruments are given in [*Li et al., 2000; Fan and Dasgupta, 1994*]. This particular instrument consists of a Nafion-membrane diffusion scrubber integrated with an automated, liquid reactor. A schematic representation of the diffusion scrubber is shown in figure 3.3. Air is passed through the scrubber at a constant flow of 1 $Lmin^{-1}$ and HCHO in the air diffuses through the membrane into a counter-flow of water. HCHO in the water is then transferred continuously to the liquid reactor where it is combined with 2,4-pentanedione reagent and ammonium acetate buffer. The ensuing Hanztsch reaction with HCHO leads to a strongly UV-absorbent dihydrolutidine product (DDL), which is continuously monitored via its fluorescence. The reaction and fluorescent product formation occurs as shown in the equation 3.2. For these experiments, the scrubbing water and all reactor solutions were prepared using high purity Millipore water. Analytical grade 2,4-pentanedione, ammonium acetate, and glacial acetic acid were purchased from ALDRICH, Germany and were used without further purification. Solutions for the methanalyser were prepared according to specifications provided by the instrument manufacturer.

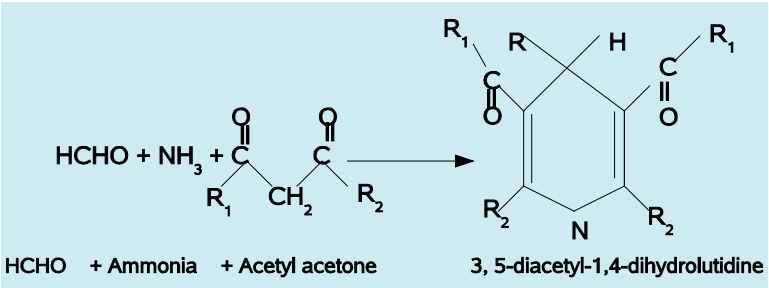

---------- 3.2

3.4 Calibration and air sampling

3.4.1 Permeation source

A KIN-TEK (LaMarque, Texas, USA) gas standard generator was used to generate a trace HCHO standard with mixing ratios between 2 and 20 ppb used to calibrate the response of the methanalyser to HCHO. The standard laboratory measurement setup for M&M detection system together with the calibration instruments are shown in figure 3.4. A permeation tube (VICI Metronic), rated to release

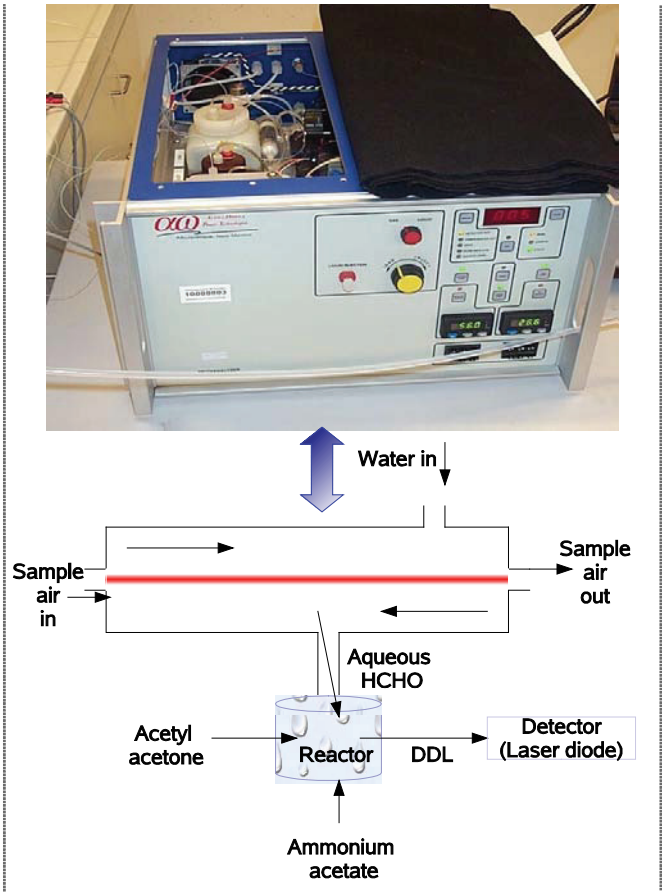

Figure 3.3: *Schematic of Nafion diffusion scrubber. Sample air is passed through the scrubber and HCHO in the air diffuses through the membrane into a counter-flow of water.*

12 $ngmin^{-1}$ ±15% HCHO was maintained at 50°C under a steady flow of N_2 gas. The quoted permeation rate was further verified by periodic weightings and revealed a loss of mass over time of 11.4± 0.2 $ngmin^{-1}$, in good agreement with the quoted value. Output of the permeation source, diluted by N_2 gas, was fed to the calibration gas port of the methanalyser for periodic sampling or could be fed directly to the sample inlet of the methanalyser.

3.4.2 CH_3OH standard

Trace CH_3OH mixing ratios were produced by dilution of a standard of CH_3OH in N_2 having a certified concentration of 20.4 $nmolmol^{-1}$ (Messer Griesheim, Germany). Diluting gas was either compressed air or a high purity O_2/N_2 mixture first passed through a cartridge containing an oxidation catalyst (1/8" Carulite 200, Carus Chemical Company) to remove HCHO impurities from the gas stream. Standard tank and dilution gas flow rates were controlled using appropriate mass flow controllers from MKS instruments.

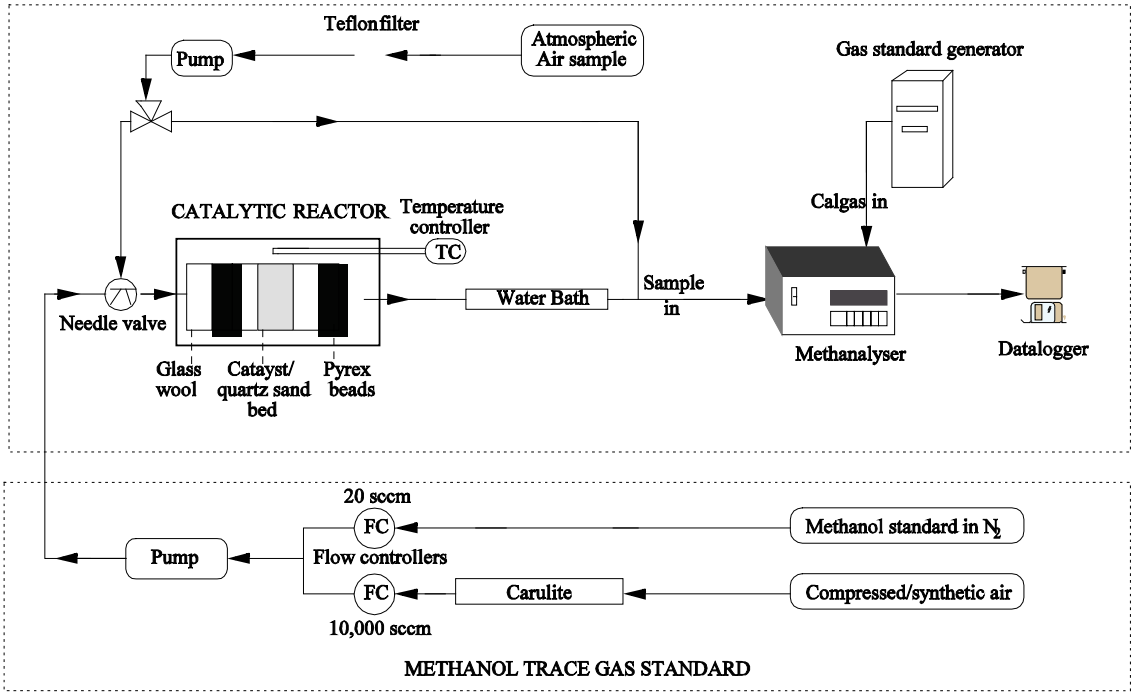

Figure 3.4: *The standard laboratory measurement setup for M&M detection system together with the calibration instruments.*

3.5 Air sampling

Ambient air was sampled at approximately 1.6 $Lmin^{-1}$ through a 2 m long 0.63 cm OD PFA Teflon line using a Teflon pump (KNF Model N86 KTDC B). The pump air output could be automatically diverted, using a 3-way PFA Teflon valve (Metron Technologies, Germany), to pass either through or around the catalytic converter. For CH_3OH measurement, air was pushed through the heated catalyst bed, cooled, and the effluent sub-sampled at 1 $Lmin^{-1}$ into the methanalyser. For HCHO measurement, the valve was switched so that sampled air bypassed the catalytic converter and again was sub-sampled at 1 $Lmin^{-1}$ into the methanalyser. The output of the methanalyser instrument was collected using a PCMCIA data collection card (NI DAQ 6024E, National Instruments Inc.) installed in a portable computer and controlled using a custom Lab View 6.1 programme. Timing of valve switching was also coordinated by the Lab View programme.

3.6 Air residence time and cooling

Under optimum conditions, the catalyst/quartz sand mixture filled 12 cm of the tubing or a volume of ~9.4 cm^3. Of this volume the sand/catalyst mixture itself occupies approximately half as calculated from the density of quartz (~2.7 gcm^3) and the mass of sand/catalyst mixture added (~13.0 g). Using this interstitial air volume and sample airflow of 1.6 $Lmin^{-1}$ yields an estimated air/catalyst contact time of less than 0.2 seconds. Although this residence time is short, at high flow rates, sample air is quite hot upon exit from the catalytic converter. High air temperatures negatively affected the performance of the methanalyser instrument for HCHO detection. Therefore, hot effluent was first sent

through 41 cm of a 0.63 cm OD stainless steel tubing immersed in a container filled with non-circulating water. Increased radiative cooling due to this bath was sufficient to cool the air to a temperature of approximately 40°C prior to sampling by the methanalyser.

3.7 Results and discussion

3.7.1 Catalyst characterization

Conversion efficiency: For this CH_3OH monitoring scheme, it is important that CH_3OH be quantitatively converted to HCHO and that none of the HCHO product be lost en-route to the HCHO detector. The efficiency or yield (equations 3.3 and 3.6) of the reactor, defined here as the ratio of the number of moles of HCHO detected to the number of moles of CH_3OH entering the catalytic converter, needs to be as close as possible to 1 in order to provide maximum sensitivity for a measurement of atmospheric CH_3OH. Among other factors, the catalyst bed temperature, the number of moles of catalyst accessible for conversion, HCHO selectivity (equation 3.4), the number of moles of CH_3OH present in sample air, air/catalyst contact time and composition of the gas passed through the converter all influence conversion efficiency.

CH_3OH conversion efficiency (%) $= C_{CH3OH}$

$$= \frac{[(n_{CH_3OH})_{in} - (n_{CH_3OH})_{out}]}{(n_{CH_3OH})_{in}} \times 100 \qquad \text{---------- 3.3}$$

HCHO selectivity (%) $= S_{HCHO}$

$$= \frac{(n_{HCHO})}{[(n_{CH_3OH})_{in} - (n_{CH_3OH})_{out}]} \times 100 \qquad \text{---------- 3.4}$$

$$= \frac{(n_{HCHO})_{out}}{[(n_{CH_3OH})_{in} \times C_{CH_3OH}]} \times 100 \qquad \text{---------- 3.5}$$

HCHO Yield (%) $$= [\frac{S_{HCHO}}{100}] \times C_{CH_3OH} \qquad \text{----------3.6}$$

$$= [\frac{(n_{HCHO})_{out}}{(n_{CH_3OH})_{in}}] \times 100 \qquad \text{---------- 3.7}$$

3.7.2 Effects of reaction temperature, flow rate, and catalyst mass

Figure 3.5 depicts catalyst conversion efficiency as a function of the temperature of the reaction bed housing for two different catalyst/quartz sand mixtures and for two different bed lengths of these mixtures. For these experiments, the CH_3OH standard was diluted with compressed air to a CH_3OH mixing ratio of 10.5±0.04 $nmolmol^{-1}$ and sub sampled through the catalytic converter at a flow rate of ~1.6 $Lmin^{-1}$. While sampling this CH_3OH standard, the temperature of the catalyst bed housing was systematically changed and the resulting HCHO concentrations observed with the methanalyser. For both 1:4 and 1:5 catalyst/quartz sand mixtures and both 8 and 12 cm bed lengths, a broad maximum of conversion efficiencies was observed for catalytic converter temperatures between 325 and 440°C. This result is consistent with previous studies [*Soares et al., 2001; Chu et al., 1997*]. Increasing the catalyst bed length from 8 to12 cm, using a 1:5 catalyst/quartz sand mixture, increased the efficiency in this temperature range from approximately 75 to 80%. With all other variables being constant, the increase in bed length increased the catalyst/sample interaction time and showed the expected efficiency increase. Further improvement, with an ultimate efficiency greater than 95%, was achieved for a 1:4 catalyst/quartz sand mixture and 12 cm catalyst bed length. Thus, increasing the amount of catalyst accessible for conversion also showed the expected increase in conversion efficiency. CH_3OH conversion efficiency was also examined as a function of gas flow rate through the catalytic converter as this parameter directly affects the catalyst/sample interaction time and therefore efficiency. In these experiments, CH_3OH standard gas flow rate through the catalytic converter was varied while maintaining a constant CH_3OH mixing ratio of 10.5±0.04 $nmolmol^{-1}$ and a constant catalytic converter housing temperature of 345°C.

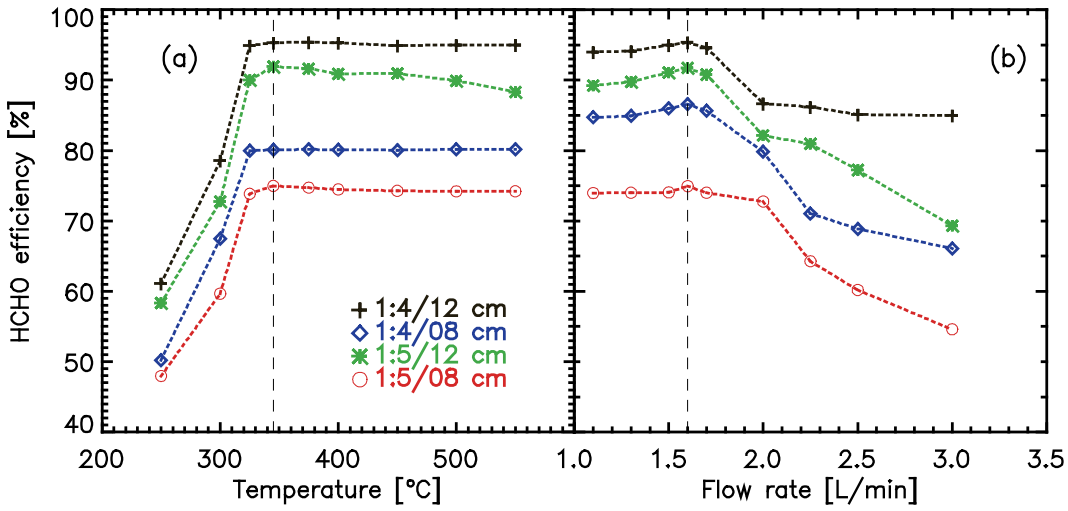

Figure. 3.5: *(a) HCHO yield as a function of catalyst housing temperature (°C) using combinations of two different catalyst mixtures and catalyst bed lengths (cm). The selected temperature range was 250°C to 550°C. (b) HCHO yield as a function of flow rate of CH_3OH mixture through the catalytic converter. The catalyst housing temperature was regulated to an optimal 345°C in all four cases. The vertical dashed lines represent 345°C or 1.6 $Lmin^{-1}$.*

The results are shown in Figure 3.5 b. Maximum conversion efficiency was 91±0.1% and 95±0.1% for the 1:5 and 1:4 mixtures respectively at 1.6 $Lmin^{-1}$. Methanol to HCHO conversion efficiency varied little at low flow rates, but decreased suddenly as flow rates exceeded 2 $Lmin^{-1}$. At flow rates lower than the 1.6 $Lmin^{-1}$ optimum, conversion efficiency also decreased slightly.

Although CH_3OH may have been quantitatively converted to HCHO at these lower flows, some further catalytic decomposition of the HCHO or other loss process may have occurred during its longer residence in the reactor. Increasing the time intermediate species remain in contact with the active sites on the catalyst surface can lead to secondary reactions including the re-adsorption of the HCHO formed. The recent work by *Kim et al., [2004]* points out that HCHO can be subsequently oxidized to carbon monoxide at low flow rates, although other products may also be formed [*Soares et al., 2005*].

3.7.3 Effect of carrier gas composition and total CH_3OH concentration

Conversion efficiency at a single reaction bed length, catalyst/quartz sand mixture, and catalytic converter temperature was tested using pure nitrogen rather than compressed air as the CH_3OH standard dilution gas. The result of removing oxygen from the catalyst bed was a reduction in efficiency by about 42% (Figure 3.6). This can be rationalised based on previously proposed mechanism for CH_3OH to HCHO conversion, one path of which involves formation of a methoxy radical intermediate [*Chu et al., 1997*]. However, HCHO is still produced and there is experimental evidence that oxygen from the lattice structure can participate in the CH_3OH to HCHO oxidation reaction [*Pernicone et al., 1969; Liberti et al, 1972*]. Thus, in the absence of oxygen in the reaction mixture, the catalyst surface becomes reduced, which decreases catalyst activity and selectivity. It is reasonable to expect that at some high CH_3OH mixing ratio, the exposed catalyst will become saturated with CH_3OH molecules. At this point, further increase in CH_3OH mixing ratio will not be accompanied by an increase in HCHO production and conversion efficiency will drop.

Figure 3.7 shows the conversion efficiency as a function of CH_3OH mixing ratio using a 12 cm reaction bed, a 1:4 ratio of catalyst/quartz sand, and a catalyst housing temperature of 345°C. Efficiency decreased significantly beyond CH_3OH mixing ratios of approximately 35 ppb suggesting that additional catalyst mixture may be required in environments with very high CH_3OH abundance. For more typical CH_3OH mixing ratios (up to 30 ppb), the current catalytic converter configuration is sufficient. For this configuration, Figure 3.7 shows the linear relationship between CH_3OH concentration and methanalyser response. The average r^2 (coefficient of determination) value for all calibration curves measured over a 6-month period was 0.986 suggesting a relative error of 1.4%. Combining this error with the stated 5% CH_3OH standard uncertainty leads to a CH_3OH measurement accuracy of better than 6% between 1 and 20 ppb.

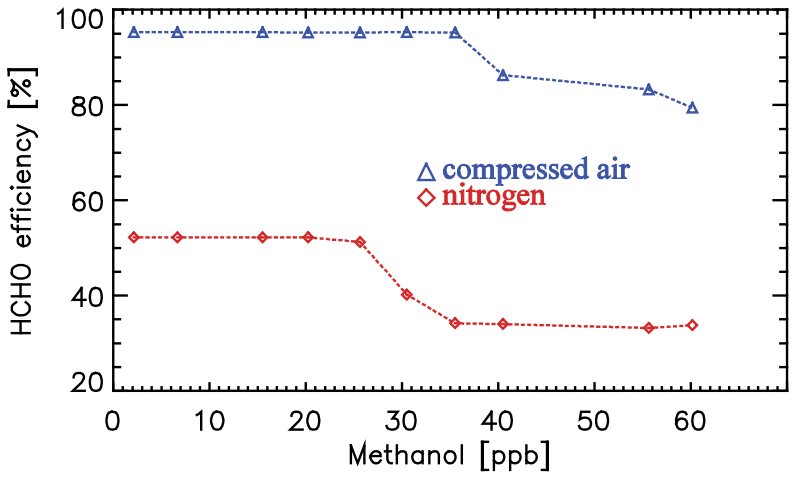

Figure. 3.6: *The HCHO yield for CH_3OH standard dilution in compressed air (blue) and nitrogen (red) as a function of CH_3OH volume mixing ratio.*

Related to the maximum working concentration of the catalytic converter is degradation of performance over time or the gradual poisoning of the catalyst. Possible mechanisms for catalyst deactivation are discussed in *Soares et al. [2001, 2003].*

3.7.4 Interference studies

For this work, repeated measurements of the conversion efficiency throughout a year (data not shown) indicate little or no degradation in performance. The following sections on interference studies will give more insights into the catalyst performance over extended time period. The catalyst converter was modified to suit various atmospheric conditions, based on the characterization experiments. These changes helped to attain higher detection limit and consistent efficiency over time.

3.7.4.1. CH_4 and VOC-I

The catalyst, though promising for effective and selective CH_3OH conversion, may also produce HCHO by the oxidation of other atmospheric trace gases. If methane, certain alkenes (e.g. isoprene), or another trace gas having comparable mixing ratio to CH_3OH was to produce HCHO upon contact with the catalyst, CH_3OH quantification could become problematic. Although a variety of studies have reported on the conversion of methane to CH_3OH and HCHO using supported ferric molybdate catalysts at temperatures around 400-500°C and pressures from 1-60 bar [*Brown et al., 1991; Chun and Anthony, 1993; Chellappa and Viswanath, 1995*], there are no reports describing methane conversion to HCHO at temperatures below 400°C. In studies where conversion is observed, catalyst surface areas were up to 50 times higher than those of the catalyst used here. The only literature the author could find describing alkene reactions using a catalyst similar to that used in this work [ethene; *Martin et al., 1993*] did not report HCHO production.

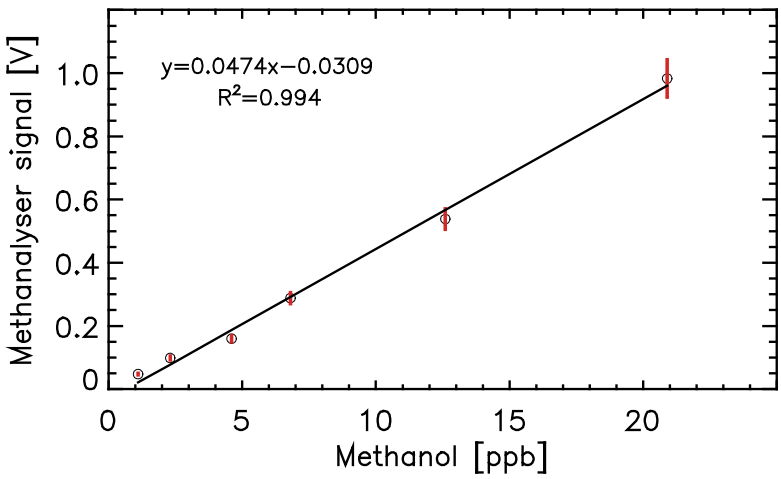

Figure 3.7: *Calibration curve of CH_3OH mixing from 1 to 20.5 ppb range at the estimated optimum catalyst temperature (345°C) and contact time (0.2 seconds).*

While possible reasons behind the selectivity of iron molybdate catalysts for CH_3OH is discussed in general in *Cheng et al. [1997]*, no other interference tests pertinent to our own studies were mentioned. Tests were performed with the catalytic converter to study any possible interference from methane and a variety of common atmospheric VOCs including isoprene, ethanol, benzene and acetone. For these experiments, either a standard tank containing methane (15 ppm, Linde, Germany) or a mixture of acetone, ethanol, benzene, and isoprene (23.1 ppm ± 5%, 5.82 ppm ± 3%, 10.7 ppm ± 2%, and 6.59 ppm ±10% respectively, Messer Griesheim, Germany) was diluted using synthetic air. Methane was diluted to final concentrations of 1.76 ppm and 1.06 ppm while the gas mixture was diluted to final isoprene concentrations of 2 and 55 ppb. These mixtures were then passed separately through the catalytic converter at a flow rate of 1.6 $Lmin^{-1}$under optimal catalytic CH_3OH conversion conditions.

The temperature of the catalytic converter housing was varied while monitoring the resulting HCHO mixing ratio, and the results of these experiments are illustrated in Figure 3.8. No appreciable conversion of methane to HCHO was observed at a representative methane mixing ratio of 1.76 ppm and catalyst temperatures up to 450°C. Above 460°C increasing methane to HCHO conversion was observed, suggesting new energetic access to an efficient conversion process. None of the other four VOCs tested produced any measurable amounts of HCHO, even at mixing ratios significantly higher than would be expected for these compounds in the atmosphere.

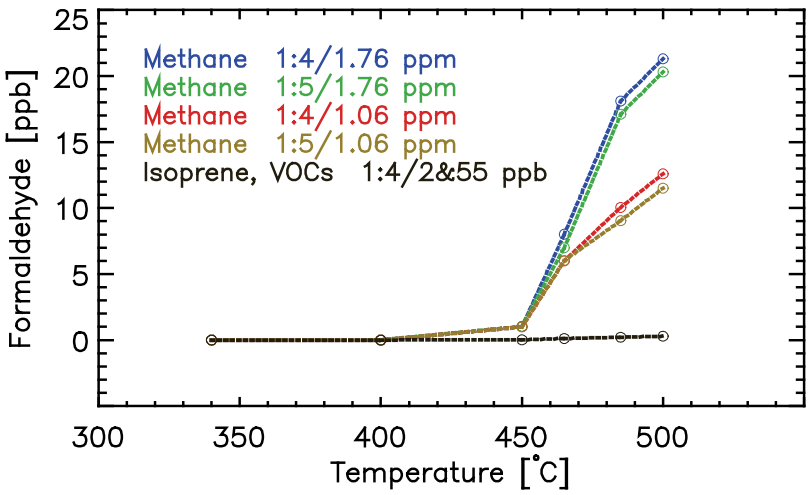

Figure.3.8: *Interference studies with methane and a mixture of common VOCs. Methanalyser response upon passage of CH_4, or the isoprene, ethanol, benzene and acetone standards diluted in synthetic air over the heated catalyst. The catalyst was tested using 2 and 55 ppb of isoprene and a mixture of acetone, ethanol, and benzene. The methanalyser signal is essentially at the noise level below 450°C.*

3.7.4.2. Effect of water addition on catalyst performance

Previous studies with iron molybdate catalyst have showed a marked inhibiting effect of water on the reaction rate for the HCHO formation, especially at higher water concentrations. This inhibiting effect could be explained in terms of competitive adsorption of water and CH_3OH on the free active catalyst surface [*Pernicone et. al., 1968*]. The effect of water vapour on feed gas mixture was studied with our reactor for a suit of trace gases including alkanes, alkenes, alcohols, aromatics, NH_3, SO_2 and CO_2 at reaction temperatures ranging from 125°C to 525°C.

Table 3.1*: The various compounds used for the interference studies conducted to study water effects in catalyst performance (EXP = Experiment).*

EXP: I	**EXP: II**	**EXP: III**	**EXP: IV**	**EXP: V**	**EXP: VI**	**EXP: VII**
HCHO	Ammonia	ALKENES	ALKANES	VOC-I	VOC-II	Methane
	Sulphurdioxide	Acetylene	1-Butane	Isoprene	Isoprene	
	Carbondioxide	Propene	Ethane	Ethanol	Acetaldehyde	
		Cis-Butene	Propane	Benzene	Benzene	
		Trans-Butene		Acetone	Acetone	
		1-Butene			Ethanol	

All the experiments with each feed gas type are performed continuously and repeatedly for a total of 5-10 h to test any possible deactivation of catalyst performance arising from catalyst poisoning or saturation. The experiments were done under widely varying conditions of feed gas composition. The results from the catalytic tests are presented together with those of the water free reference reaction. The different set of experiments with names of varying gas mixtures used for interference studies together with water vapour are shown in table 3.1.

HCHO

Results from the catalytic tests presented together with those of the water free interference for HCHO is shown in figures 3.9. The results from 6 set of repeated experiments are presented. The temperature of the catalytic converter housing was varied while monitoring the resulting HCHO mixing ratio in all experiments.It can be inferred that HCHO concentration in the feed mixture thermally decomposed into CO and CO_2 only at temperatures above 450°C. The conversion efficiency ranged from 78% (Humid air & dry air at 500°C) to 96% (Dry air & humid air mixtures below 475°C). The results are encouraging as no decay in the sample HCHO was detected when passed through the catalyst at the optimum temperature ranges, i.e., at 340-350°C. No appreciable conversion of HCHO to its byproducts was observed at a representative mixing ratios upto 25 ppb and catalyst temperatures up to 450°C. Water interference as a result of reaction site adsorption was also found to be negligible at temperatures below 500°C. The results are consistent as the product HCHO inside the reactor show little decomposition at the ambient levels found in normal atmospheric conditions. However, this result was contrary to the previous study done by *Jiru et al. [1966]* where HCHO concentration in the feed was observed to influence the reaction products and the reaction rate.

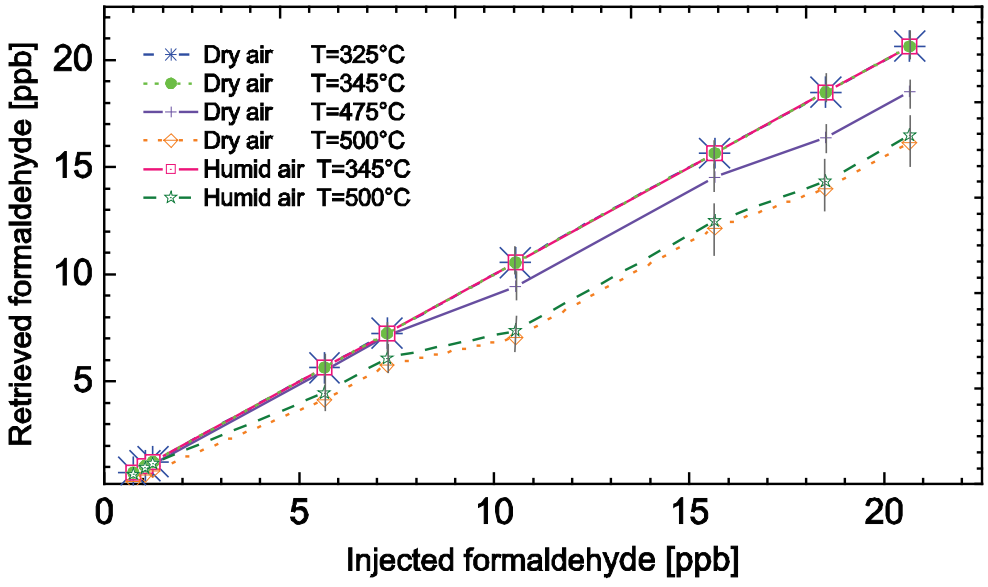

Figure 3.9: *Interferences from injected HCHO in the feed gas subjected to various levels of water concentration and catalyst reactor temperature.*

NH_3, SO_2 and CO_2

The same set of experiments repeated with NH_3, SO_2 and CO_2 as feed gas mixtures are shown in figure 3.10a, b and c respectively. The effect of these compounds on catalyst poisoning and deactivation was studied by passing mixtures of 5 ppb CH_3OH and individual compound at varying concentrations. Concentration level of each gas was selected according to their natural abundance and MAC (maximum accepted concentration) values in atmosphere. Each gas mixed with CH_3OH and synthetic gas was added independently into the reactor feed to analyse the effects on converter efficiency. At lower and operating temperatures below 400°C, the efficiency followed almost similar trend as for CH_3OH conversion. With higher temperature and concentration, catalyst poisoning was observed by these gases. This eventually decreased the reactor efficiency followed by catalyst deactivation when subjected to 5-7 h of sample gas flow. Though an increased deactivation of catalyst activity was observed with much higher concentration and duration of sample flow, the measurements at optimal temperature and at ambient levels were consistent and interference free. Catalyst deactivation due to SO_2 and CO_2 are found to be lower when compared with NH_3 mixture. However, measurements at higher concentrations can definitely decrease the catalyst activity due to active site poisoning.

Previous studies have also showed similar chemisorption of ammonia at catalyst surface resulting in poisoning [*Centi and Perathoner, 1998*]. Under oxidising conditions there are several basic means by which sulphur poisoning of catalyst occurs. The first way occurs at temperatures above 350°C and involves the conversion of SO_2 to SO_3, which then reacts directly with the catalytic components.

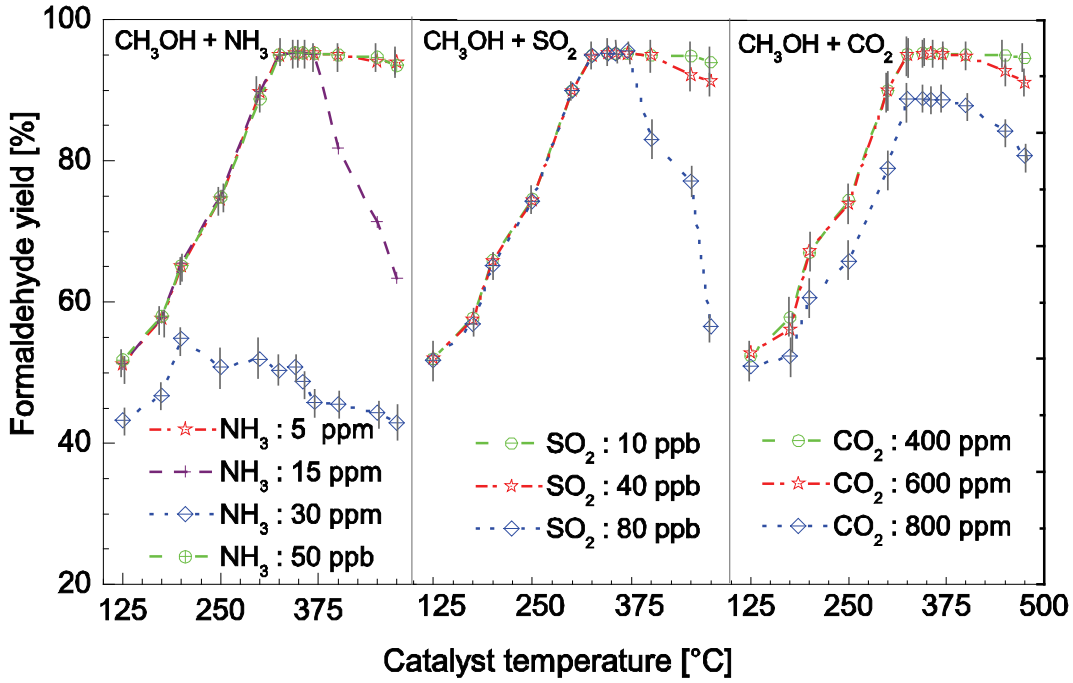

Figure 3.10: *Interferences studies with NH_3, SO_2 and CO_2 mixtures in the feed gas subjected to various levels of water concentration.*

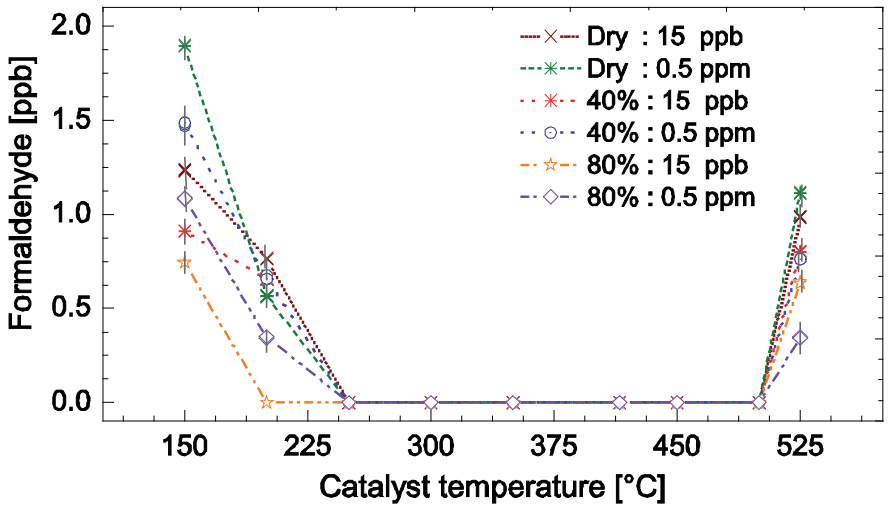

Figure 3.11: *Interference tests with ethylene mixture in the feed gas. Experiments are performed to study any interference from ethylene decomposition when passed through different catalyst temperature and humidity levels.*

The second mechanism is the chemisorption of SO_2 or SO_3 onto catalytic sites at temperatures <350°C, which prevents those sites from further catalytic action by either inaccessibility of active surface sites due to geometric blockages or changes in the structure of catalytic surface [*Ferrandon, 2001*]. As probability of occurrence of these trace gases at the levels reported in this study is very low under ambient conditions, any possible impairment and effect on atmospheric CH_3OH measurements can be easily ruled out.

Alkene mixture

The conversion of alkenes as a function of water concentration and temperature are shown in figure 3.11. Studies conducted with dry and humid ethylene mixture as feed gas shows interesting trend with respect to the catalyst temperature. Methanalyser response demonstrates a higher interference rate at lower and higher temperature ranges from 150 to 250 °C and above 500°C. The results shows that the catalytic gas phase oxidation of propylene in the mixture produced formaldehyde and acetaldehyde along with acrolein as found in previous studies with ferric molybdate catalysts [*Bhuvana et. al., 2005*]. The presence of water vapour lowered the HCHO formation rate significantly, especially at higher water concentration when compared to their corresponding dry mixtures. These results can be well explained in terms of competitive adsorption of water with CH_3OH on the free active catalyst site [*Deshmukh et. al., 2005*]. The absence of any interference at the 250-450°C range can be attributed to the presence of acetylene in the feed mixture.

At this temperature range acetylene has been proved to be refractory towards oxidation when passed through metal catalyst due to a large electron donor effect. Therefore it inhibits the oxidation of CO and all hydrocarbons [*Harmsen et. al., 2004*]. The increased catalyst temperatures beyond 500°C might have increased the decomposition of alkenes to acetaldehyde and subsequently to formaldehyde. The results suggest that interference from alkenes is highly temperature dependent and any production of HCHO is favoured only at very low and high energetic temperature levels.

Alkane mixture

Similar experiments with alkanes (1-butane, ethane and propane), shown in figure 3.12, at different humidity levels indicate signatures of interference at temperatures above 400°C only. Interference from product gas increased with feed gas concentration of alkanes and decreased with humidity levels. The oxidative production of HCHO quickly levels off when ~40% (v/v) or more of water was added to the feed. It should be noted that the effect of water on the activity towards HCHO is not linear. A maximum is observed at 35% of water in the feed at alkane concentrations of 15 ppb and 0.5 ppm. It clearly shows the water accelerated reaction mechanism has little influence on the conversion rate even when the gas concentration is increased. The performance of dry and humid mixtures of 1-butane, propane and ethane when passed through the catalyst affirms that the presence of water in the feed has negative effect on net conversion rate, where it reduces the conversion of alkanes to HCHO by masking the active sites or by preventing the oxidation cycle of compounds inside the reactor.

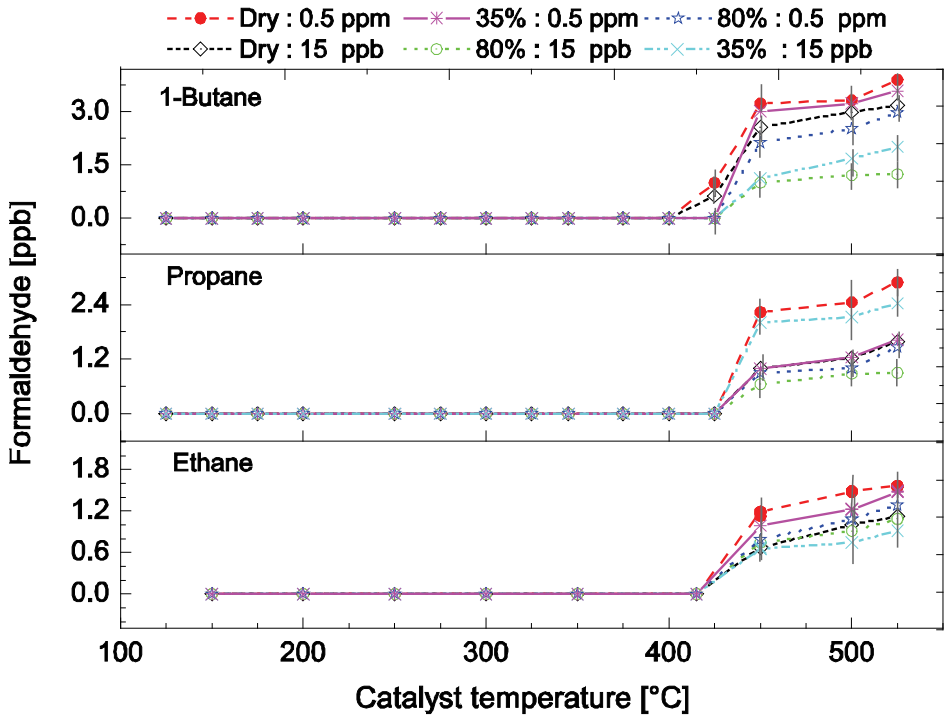

Figure 3.12: *Interference studies with 1-butane, propane and ethane in dry and humid sample feed. The methanalyser response is essentially at the noise level below 425°C.*

Methane, VOC-I and II

Interference studies with methane and VOC-I mixtures as feed gas are repeated under slightly varying conditions than the previously conducted experiments with methane and isoprene mixture (sec. 3.7.4.1). The results are depicted in figure 3.13 a, b and c respectively. Results show varying responses to humid and dry feed gas mixtures, where mixtures with 80% humidity and higher concentrations in the order of ppm produced fairly detectable range of interference at lower and higher temperatures compared to dry experiments. In contrast to the previous experiments with dry CH_4 feed, appreciable conversion of methane to HCHO was observed at a representative CH_4 mixing ratio above 0.5 ppm and catalyst temperatures below 300°C and above 420°C in the presence of water (figure 3.13).

Higher CH_4 to HCHO conversion above 420°C suggests new energetic access to an efficient conversion process at higher temperatures. None of the other two set of VOC mixtures produced any measurable amounts of HCHO at the optimum ranges, even at mixing ratios significantly higher than would be expected for these compounds in the atmosphere. The presence of water in the VOC-I feed increased the HCHO yield contrary to the dry experiments conducted with same mixture. The kinetic reactions leading to an increase in HCHO production in response to increased temperature, humidity and gas concentration is unknown. Compared to VOC-I, interferences from VOC-II were significantly higher even for dry feed mixture. This could be due to the presence of acetaldehyde in the mixture which could eventually undergo catalytic reduction to HCHO. The catalyst performance also indicated a decreasing trend with water content and increasing trend with mixture concentration.

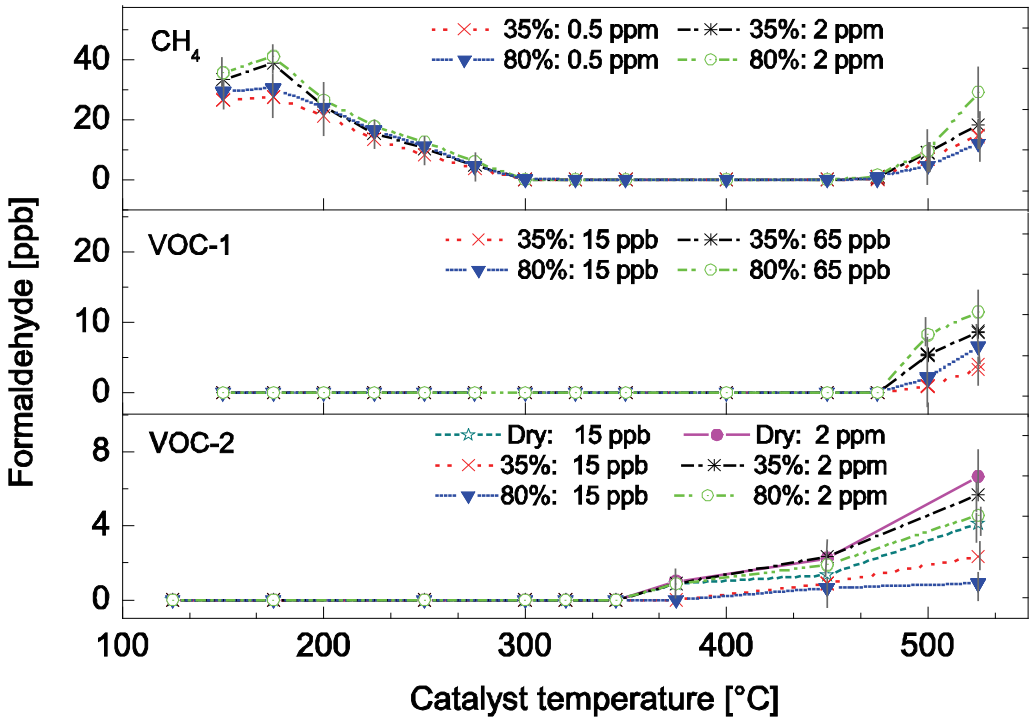

Figure 3.13: *Same as figure 3.8, but with methane. The experiment with water vapour in the sample feed to test for water adsorption effects in the active sites of catalyst.*

The results agree with previous studies, which have shown that the interaction of VOCs with the active centres of the metal catalysts can be accompanied by the deformation and the subsequent dissociation of individual bonds in the reacting molecules resulting in product molecules at higher temperatures [*Finnochio et. al., 1994; Centi et. al., 1988*]. Methane, in contrast to other hydrocarbons, is not adsorbed on the catalyst surface at higher reaction temperature. But is activated on impact against the surface, being converted into a methyl radical, which is desorbed and forms a methoxy-compound as a result of a secondary interaction with various forms of oxygen on the surface or with a OH group [*Krylov, 1993; Driscoll et. al., 1987*].

3.8 Atmospheric measurements

Atmospheric air sampled from the roof of the Institute of Environmental Physics building on the south side of the University of Bremen campus (53°50'N, 8°49'E) was analysed for CH_3OH and HCHO from 1 to 15 July 2004. The results are shown in Figure 3.14.

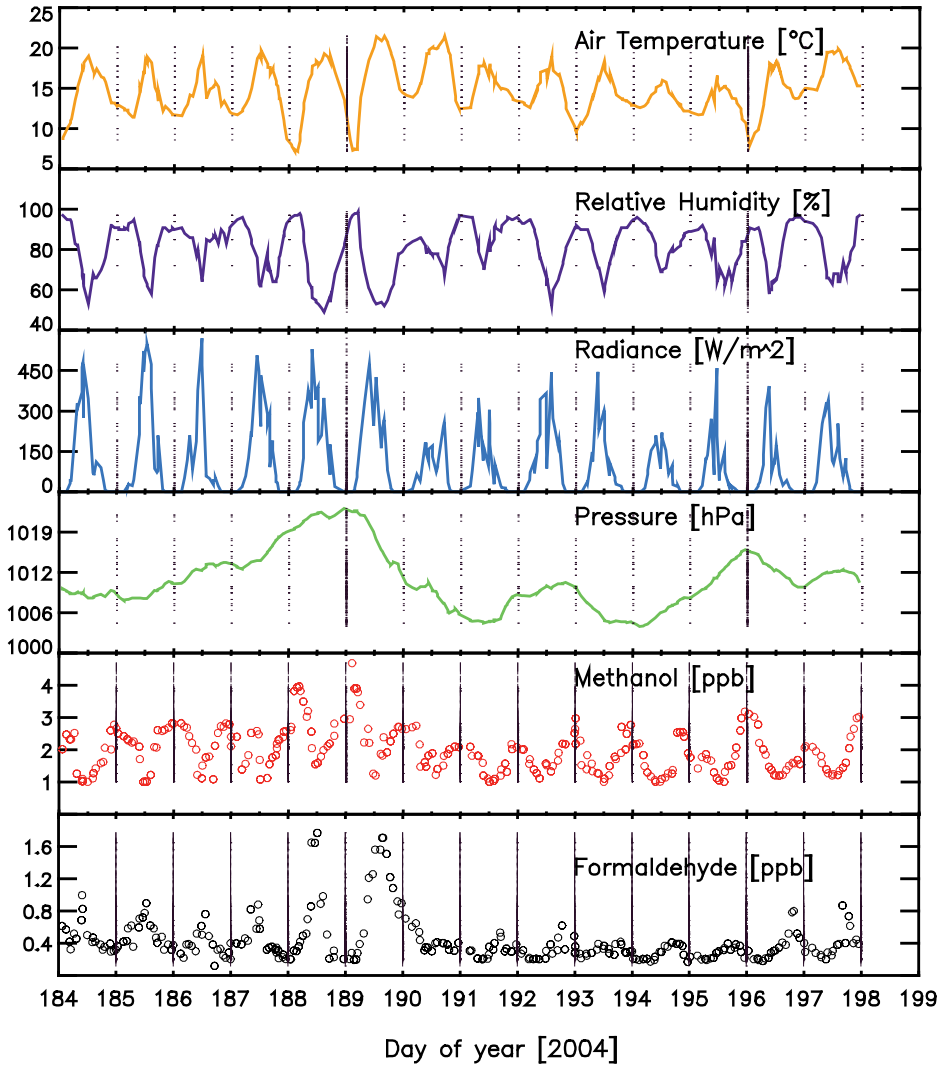

Fig. 3.14: *CH_3OH and HCHO mixing ratios measured from outside the laboratory window along with meteorological data collected at a nearby weather station provided by the DWD during 1-15 July 2004 (184–198 in Julian days).*

HCHO and HCHO-corrected CH_3OH mixing ratios for the complete period are presented. The respective meteorological data were provided by the Deutsche Wetterdienst (DWD) and were acquired from a weather station approximately 5 km to the Southwest. Though this period was unusually cold and rainy CH_3OH still showed a pronounced diurnal cycle. Mixing ratios of CH_3OH ranged from 1 to 5 ppb with peak values at night. Lower mixing ratios were observed during julian days 190-192 (7-9 July) and 194-195 (11–12 July). Both of these time periods were also associated with low atmospheric pressure. The nocturnal maxima were likely due to the prevention of efficient turbulent mixing in the night time boundary layer while CH_3OH emissions continued, a common feature also found for CH_3OH at other sites [*Holzinger et al., 2001; Schade and Goldstein, 2001; Schade and Custer, 2004*]. Since there are no consistent features in the data, contribution from anthropogenic sources such as car traffic can be neglected. However, the measurement location was not well suited for such an analysis. Rather, back trajectory analysis with the NOAA HYSPLIT (National Oceanic and Atmospheric Administration HYbrid Single- Particle Lagrangian Integrated Trajectory) model [*Draxler and Rolph, 2003*] is exploited to analyse large-scale features. The model results indicate a frontal passage over Bremen over days 191 and 192.

The change in air mass associated with passage of this low-pressure system was likely the origin of the decrease in CH_3OH mixing ratio during this time. HCHO also showed a prominent diurnal cycle. Its mixing ratio ranged from 0.2 to 1.6 ppb and peaked during midday. The midday maximum for HCHO is an expected result due to its photochemical source from the oxidation of hydrocarbons. Probably as a result of the relatively low ambient temperatures during this period, both CH_3OH and HCHO mixing ratios were low when compared to previous studies. In an attempt to connect CH_3OH and HCHO mixing ratios with the meteorological parameters, we carried out a simple factor analysis [*Lamanna and Goldstein, 1999*] whose results are given in Table 3.2.

Table 3.2: *Factor analysis performed to find associations of CH_3OH and HCHO mixing ratios with the meteorological parameters (loading values <0.3 omitted). Proportion variation defines the fraction of data explained by each factor. Cumulative variation is the sum of the proportion variation, indicating that nearly two thirds of observations are explained by these 2 factors. The chi square statistic is 15.06 on 4 degrees of freedom. The p-value (significant level) is 0.00457.*

	Factor 1	**Factor 2**
CH_3OH	-0.533	0.639
HCHO	0.501	
Temperature	0.852	
RelativeHumidity	-0.932	
Radiance	0.693	
Pressure		0.873
Sum square loadings	2.646	1.30
Proportion of variation	0.441	0.218
Cumulative variation	0.441	0.659

Interestingly, CH_3OH showed a significant correlation with pressure and relative humidity while HCHO correlated better with solar irradiance and temperature. As these CH_3OH measurements are consistent with previous long-term measurements [*Schade and Goldstein, 2001; Holzinger et al., 2001*], they support the notion that the atmospheric CH_3OH abundance is influenced more by the air mass origin and biogenic emissions than by anthropogenic emissions.

3.9 Summary

Gas phase conversion of CH_3OH to HCHO using an iron molybdate catalyst was investigated as a simple and accurate way to measure atmospheric CH_3OH using commercially available wet-chemical HCHO monitoring equipment. Maximum CH_3OH to HCHO conversion efficiency of 95% was obtained using a catalyst bed temperature of 345°C and an air/catalyst contact time <0.2 seconds. This high efficiency remained unchanged over a period of several months of measurements for which the catalyst was used.

Interference studies showed that neither methane nor a mixture of common atmospheric VOCs having significant ambient mixing ratios produced HCHO when passed as dry or humid mixtures over the Mo-Fe-O catalyst under optimum conditions. Studies with all potentially interfering atmospheric VOCs, mixture of a double 1-alkene (isoprene), alkenes, aromatic compounds (e.g., benzene), alcohols (e.g., ethanol), and carbonyls (e.g., acetone), did not produce any significant HCHO signals. Therefore, the optimised reactor coupled with the wet chemical HCHO detector proved to be an essentially bias-free method for most atmospheric sampling applications.

By applying the method, atmospheric measurements of HCHO and CH_3OH were conducted. Both CH_3OH and HCHO showed diurnal features consistent with previous atmospheric measurements of these VOCs, providing further confidence into the capability of the method.

Chapter 04

Validation of CH_3OH and HCHO measurements from M&M

Being an important subgroup that influences atmospheric photochemistry, reliable measurements of OVOCs are crucial for further analyses and understanding of atmospheric chemistry. However such measurements are highly variable and push the limits of technical feasibility, owing to the high reactivity of certain OVOCs. None of the techniques, ranging from liquid scrubbing chemical derivatization followed by chromatography to spectroscopic methods, had distinguished themselves as reliable for ambient carbonyl and VOC determination despite nearly a decade of analytical development. This chapter describes the first formal, rigorous, co-deployment/intercomparison of major techniques that have potential to provide broad characterization of OVOCs. Hence, this is an ideal opportunity to carry out the validation of the M&M measurements as well.

4.1 Overview

Within the framework of the integration task on "Quality assurance/Quality control (QA/QC)" the comprehensive formal instrument intercomparison campaign of OVOC measuring instruments, OVOCCOMP (OVOC Comparisons), was performed at the Forschungszentrum Jülich (Research Center Julich) on 17-28 January, 2005 under the supervision of an independent referee (*Eric Apel, National Centre of Atmospheric Research, CO, Boulder, USA*). The scientific motivation behind the ACCENT (Atmospheric Composition Change the European Network of Excellence) OVOC intercomparison activity includes:

1. Improvement of the methods for the measurement of OVOC in the atmosphere and foster analytical training,
2. Enhancement of the transfer of knowledge through scientific and technical communication among the participants,
3. Demonstration of the importance of regular proficiency tests to stay abreast of advancing technology.

Two week formal "blind" measurements of fifteen atmospherically significant OVOC species including aldehydes, ketones and alcohols, of both biogenic and anthropogenic origin were performed during the deployment. Two NMHC compounds (*n*-butane and toluene) were also included in the study to act as tracers in order to monitor the dilution of the chamber air, with toluene specifically chosen for the benefit of PTR-MS instruments, which are unable to detect short chain alkanes. The experiment used the large atmospheric simulation chamber as the sample reservoir, giving the ability to alter sample matrix, humidity and ambient ozone levels. Apart from M&M, fourteen other instruments from various scientific institutes took part in the intercomparison experiment.

4.2 The experimental setup and time line

The measurement campaign was conducted in two phases. In the first phase, the OVOC instruments were compared during two days of simultaneous ambient air measurements from the chamber. In the second phase, the actual intercomparison measurements were conducted under well-defined conditions in the SAPHIR chamber in order to investigate critical experimental parameters and possible interferences of the respective instruments. The second phase consisted of five different experiments, each having a single day in duration. Each day the conditions inside SAPHIR were varied so that the instruments sampled the OVOCs from a matrix of dry or wet synthetic air and with or without the presence of ozone. For the intercomparison experiments, trace gas delivery to the chamber took place via syringe injection of the liquid OVOCs into a heated injector port, which facilitated their volatilisation before entering the bag. Total time for OVOC injection was of the order of 1.0 h. Once inside the chamber, all gases were mixed by a series of mechanical fans. The chamber characterisation suggests a minimum mixing time of 30 min for the sample matrix to become homogeneous.

Table 4.1 *The intercomparison experiment plan and composition.*

Day 1	Day 2	Day 3	Day 4	Day 5
Dry and wet synthetic air with and without O_3	OVOCs in dry synthetic air	OVOCs in wet synthetic air, RH~75%	OVOCs in wet synthetic air, RH~75%, with O_3	Ambient air first, subsequently spiked with OVOCs

The precision of OVOC addition via this method is at best 20% [*Wegener and Holzke, personal communication, 2004*]. Ozone used in chamber experiments was supplied from a silent discharge ozonator held under pure O_2 in order to reduce possible impurities and contamination. Chamber humidification was facilitated by vaporising (Dampf-O-Mat) ultra pure deionised water (Milli-Q, Millipore), through which a continuous stream of high purity nitrogen (purity grade 7.0) was passed to remove dissolved trace impurities. The intercomparison exercise was designed such that four main experiments would be conducted, each approximately a single day in duration. The conditions of the synthetic air sample matrix were varied between experiments in order to explore the effects of humidity and ozone on the ability of the instruments to reliably monitor the target compounds. Details of the conditions employed during each experiment are shown in table 4.1. Consequently, each experiment was composed of three individual sub-experiments termed A, B and C, during which the compounds were sampled at mixing ratios of roughly 6–10, 2–3 and 0.6–1 ppb, respectively. Because of constraints imposed by SAPHIR and the minimum sampling time required by some participating instruments, the minimum length of each sub-experiment was set to 3 h. The total length of each daily experimental period was in the order of 12 h.

During each experiment chamber relative humidity was monitored using a frost point hygrometer (General Eastern model Hygro M4) and ozone concentrations were measured "on-line" (~90 s) through UV absorption (Ansyco O_3 41M). To maintain a given relative humidity and ozone mixing ratio throughout the entire day and hence to account for the effects of dilution, compensation injections were made during the flushing phases between sub-experiments. Ozone and OVOC concentrations and experiment duration were designed to be sufficiently low to ensure ozonolysis reactions, and hence susceptible OVOCs loss would be insignificant. All instruments start up with zero measurements followed by three hour sampling from the chamber, during which the chamber will be flushed with injected compounds. The total injection period i.e., the time taken to finish injecting all the compounds was nearly 20 min. Depending on the estimated chamber volume and flow rate, ~5 min is required for the uniform distribution of inject gas inside the chamber.

After each injection, all instruments simultaneously started the measurement for 3 hrs. After the first experiment, the chamber was flushed with synthetic purified air, which subsequently lowers the mixing ratio of compounds inside the chamber, by a factor of 2 to 3. The second set of measurements for 3 hrs starts soon after this chamber dilution. This procedure is repeated for the next set of experiments too, followed by 3 hr sampling period.

4.3 Deployment of instruments at SAPHIR

The large atmospheric simulation chamber SAPHIR is a tool for quantitative experimental investigation of tropospheric chemistry under natural condition and evaluation of photochemical models. These design criteria were met through the design as a double-wall Teflon foil cylinder of 5 m diameter and 20 m length providing a volume of 300 m^3 at a surface area of 324 m^2. The instruments were accommodated in 6 containers near the SAPHIR chamber with each container having separate manifolds from the chamber. The list of participants, instruments used and compounds measured are listed in table 4.2. The manifolds through which the sample air is flown to the individual system is kept at a flow rate of ~30 L/min. Periodic checking of manifolds and sampling lines were made by passing CO2 through the sample line and detecting its concentration at the end of sample port.

Time activity diary of each experiments and events are recorded individually as well as for the whole experiment. Each working group using liquid and gaseous calibration standards calibrated the respective instruments independently. A schematic of the measurement setup during the campaign was shown in figure 4.1.

***Table 4.2**: The list of the participating institutes, the instruments used, and the compounds measured during the experiments.*

PARTICIPANTS	INSTRUMENTS	COMPOUNDS INJECTED
University of Bristol, UK	Gas chromatography-Mass spectrometer (GC-MS)	Formaldehyde Acetaldehyde Benzaldehyde Butanal Hexanal Methanol Ethanol 1-propanol 1-butanol Methacrolein Methyl vinyl ketone Acetic acid Methyl ester Acetone 2-methyl-3-buten-2-ol
University of York, UK	Gas chromatography-Flame ionization detector (GC-FID)	
FAL Agroscope, Switzerland (Forschunganstalt für Agrarökologie und Landbau)	GC-FID PTR-MS (Proton Transfer Reaction Mass Spectrometry)	
EMPA, Switzerland (Swiss Federal Laboratories for Materials Testing and Research)	GC-MS	
Forschungszentrum, Karlsruhe Garmisch Patenkirchen, (IMK-IFU)	GC-MS Aerolaser-Hantszch method	
Forschungszentrum, ICG-II, Juelich (Institut für Chemie und Dynamik der Geosphäre-II)	GC-FID Aerolaser-Hantszch method PTR-MS, Broad band-DOAS	
University of Innsbruck, Austria	PTR-MS	
IUP-B, Germany (Institute of Environmental Physics-Bremen)	M&M (Methanol&Methanalyser)	
IFT Leipzig, Germany (Leibniz-Institute for Tropospheric Research)	High performance liquid chromatography (HPLC)	
NILU, Norway (Norsk Institutt for Luftforsknin)	Catridges, Solid phase microextraction	
CEAM, Spain (Centro de Estudios Ambientales del Mediterraneo)	GC-FID	
University of Leicester, UK	PTR-TOF-MS (Proton Transfer Reaction- Time of Flight-Mass Spectrometry)	

4.3.1 The M&M measurements

The air samples from the SAPHIR chamber (manifold 4) were automatically diverted using a 3-way PFA Teflon valve to pass either through or around the catalytic converter. Gas phase calibration to check the response of Methanalyser to HCHO was performed using a KIN-TEK gas standard generator (80±20% ng h^{-1}) and a standard of methanol in N_2 having a certified concentration of 20.4 nmol/mol. The estimated accuracy for HCHO during the measurement was ~4% and CH_3OH, it was ~6.6%.

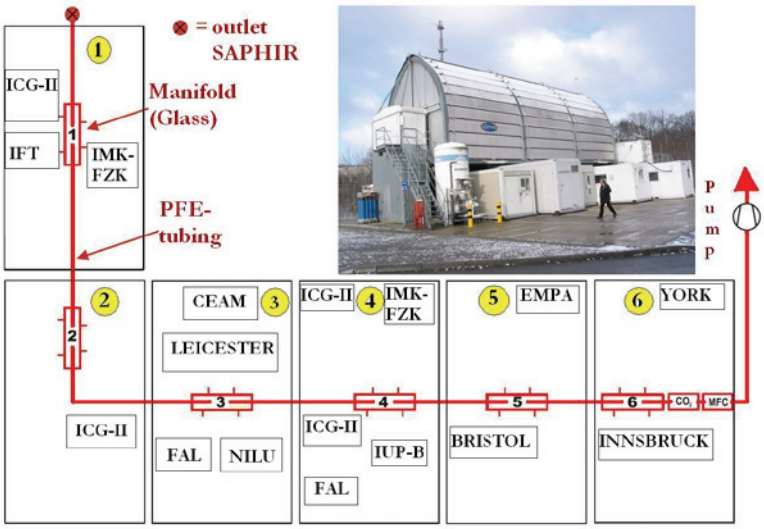

***Figure 4.1**: A pictorial representation of the deployment of various participating instruments at the SAPHIR simulation chamber. The gas manifolds and the sample gas supply through PFE tube to the instruments are also depicted.*

4.4 Results

In order to ascertain information regarding the ability of M&M to quantitatively measure the detected CH_3OH and HCHO both reliably and reproducibly, a comparison is performed between measured and estimated chamber values, which are determined from knowledge of the amount of liquid OVOC initially injected into SAPHIR and the air dilution rates over time. It should be noted; however, such estimated chamber values are not definitive and may vary from the actual ambient concentration of any given OVOC in the chamber at any point by no more than 20%. Effectively, the estimated chamber OVOC concentrations represent an upper limit of the true values [*E. Apel, personal communication, 2004*]. Except M&M, CIMS, Broad Band DOAS, Hantsczh measurement technique and DNPH-HPLC-UV/VIS were the other methods that measured CH_3OH and HCHO during the campaign.

4.4.1 The HCHO comparison

The M&M data are integrated over periods of ~15 min for each sub-experiment, producing 10 repeat measurements at each concentration to compare with the other correlative measurements. The results are shown in figure 4.2, for which the results from day 2 to 5 are given in figure 4.2a, b, c and d respectively. A good agreement among the M&M, PTR-MS-II, Hantszch and PTR-MS-I data was found on the day two. The DNPH data appear to be very low, which presumably is due the absence of water in the reactor.

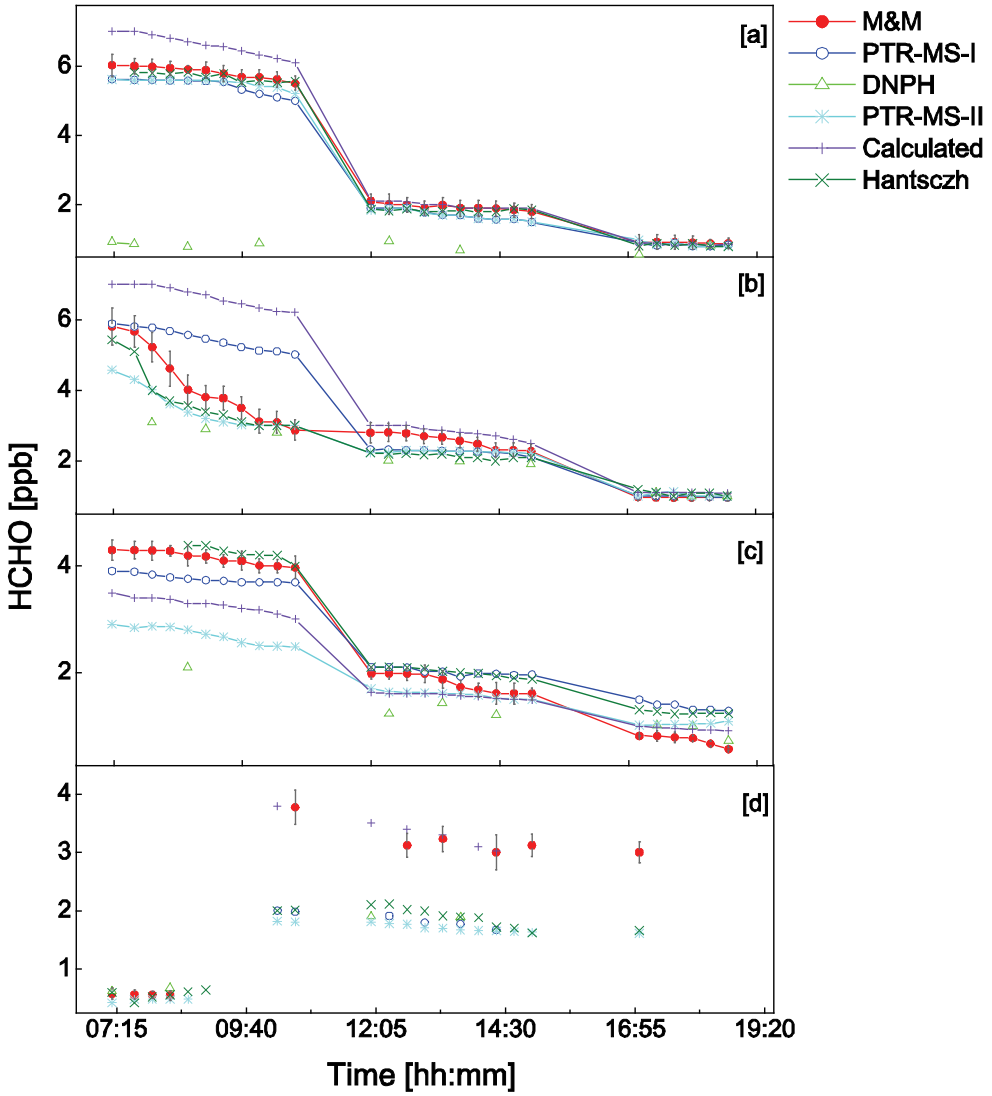

***Figure 4.2**: Comparison of HCHO measurements from various instruments during the deployment. (a) Results from the first day (25-01-05) experiment with dry synthetic air, (b) results from the second day (26-01-05) experiment with ~75% humid air mixed with OVOCs, (c) results from third day (27-01-05) experiment with ~75% humidity and O_3 mixed with OVOCs, and (d) results from the final day (28-01-05) ambient air measurement with subsequent spike by OVOCs .*

Since the DNPH reaction needs water, the yield for hydrazone formation is very low in the absence of water (5-35%; not reproducible and thus not correctable as well), which explains the reason for the low values in DNPH measurements. The calculated data (Referee) are somewhat high during the first plateau of experiment. This difference is occurred by a quantification error in the HCHO injection [*E. Apel, personal communication 2004*]. The HCHO injection method (heating of Para formaldehyde in a glass vessel, flushing into cold lines and cold chamber) induces an estimated loss of 20% of HCHO, which is the source of the aforesaid discrepancy.

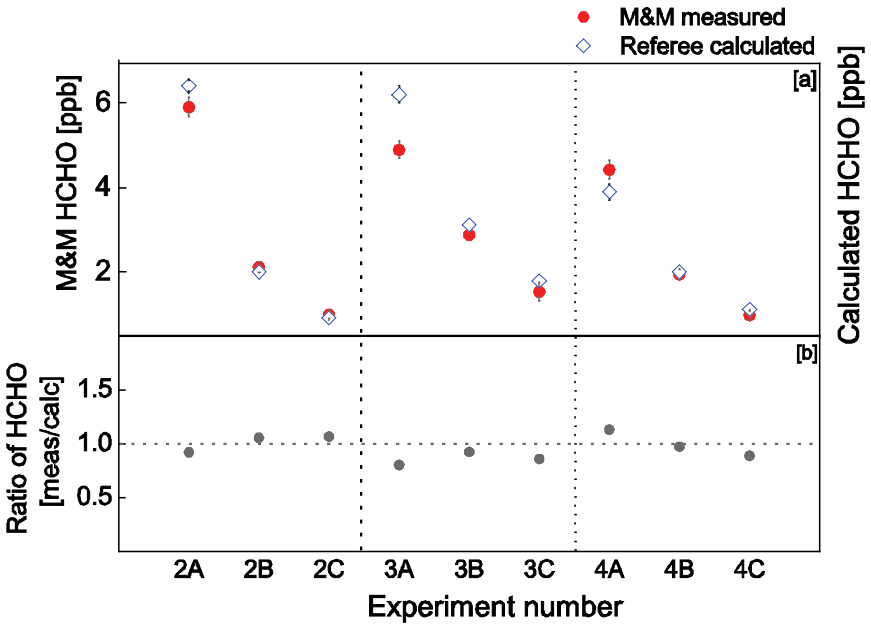

***Figure 4.3**: (a) Comparison between the measured and calculated (referee) HCHO for the measurements in day 2, day 3 and in day 4. The three measurement plateaus during each day is represented by A, B, and C respectively. (b) The ratio of calculated and measured HCHO.*

The intercomparison result from the day three is shown in figure 4.2b. A very good agreement is observed among the M&M, PTR-MS-II and Hantszch data. Relatively large discrepancies between the measured and calculated HCHO values are found in the morning measurements, where all instruments except PTR-MS-I show a sudden drop up to 2 ppb after ~40 minutes of measurement compared to the injected HCHO value. This drop could be due to condensation and subsequent HCHO scavenging inside the chamber. The measured RH was very high (95%) in this 1st plateau condition.

Apparently, the scavenged HCHO came back into the gas phase (when the chamber was flushed during the 1st dilution step) as there was no noticeable change in the concentration drop that would expect after the first dilution of chamber air. Although there is a good agreement between the M&M and Hantszch, an offset is found between the calculated and M&M values. Due to heterogeneous ozone reactions inside the chamber, some HCHO was already present in the chamber even before it was injected. This, obviously, explains the discrepancies in the calculated and measured data. Compared to M&M the DNPH data show low values for the 1st and the 2nd plateau. This could be due to the poor performance of the ozone scrubber inside the Leipzig instrument.

Figure 4.2d shows the measurement results from day five, in which the chamber was flushed with ambient air from outside and was sampled by the instruments without any injection of compounds into the chamber. The chamber was spiked with ambient air for an hour, followed by the routine measurement plateau. The DNPH measurements showed large unexplained variations and were omitted from the comparison. Compared to the measurements from other instruments, higher values

are observed in the M&M measurements after the spike. However, the M&M data consistently follow the calculated values.

The time averaged comparison of the measured and calculated values over the day two, day three and day four are shown in figure 4.3a. The measurements taken during the nine experiments with three sub-experiments in a single day, which is represented by A, B, and C respectively, are averaged here. A very good agreement is observed between the measured and calculated mixing ratios during the whole period. There is a slight difference in 3A, where the calculated value appears to be higher than the measured values. The calculation was badly affected by the scavenging effect of the HCHO inside chamber as explained previously (4.3.1 § 2). The measured to referee calculated HCHO ratio is shown in figure 4.3b. The ratio is ~1.0 in most cases, corroborates the very good agreement between the measured and calculated values of HCHO during the measurement period.

The correlation analysis of the measured and calculated HCHO data is shown in figure 4.4a, 4.4b, and 4.4c corresponding to day two, day three and day four respectively. The correlation coefficient (r^2) is averaged over the experiments 2, 3 and 4 here. The r^2 values are 0.99 for day 2 and day 3, shows the good concordance between the M&M and referee data. Nevertheless, the coefficient is relatively lower (0.80) for day 3, which is due to the aforementioned "scavenging" inside the chamber which was not taken into account in the calculated data.

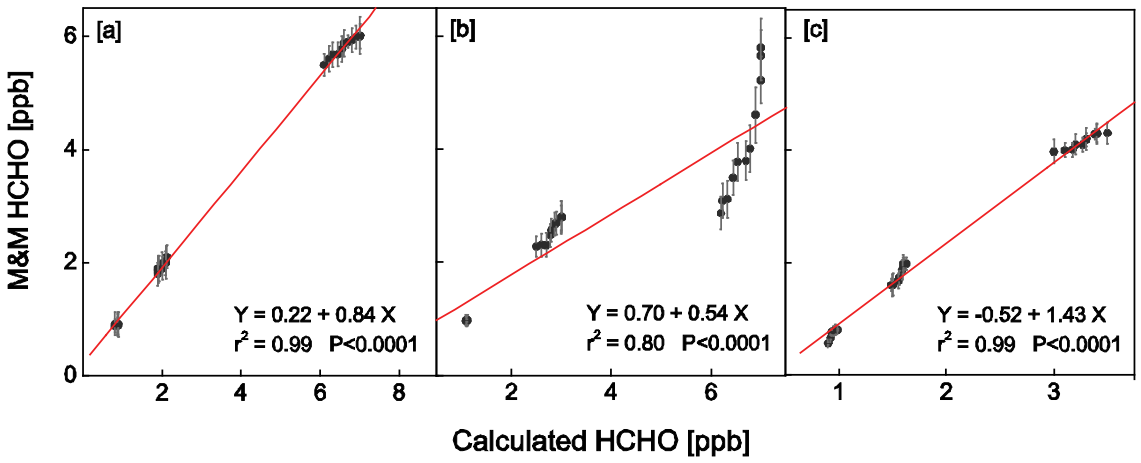

Figure 4.4: *The correlation between measured and calculated HCHO values during (a) day two, (b) day three, and (c) day four respectively.*

4.4.2 The CH_3OH comparison

The M&M measurements from day 2 to day 5 are compared with the GC-FID-I, GC-FID-II and PTR-MS-III data as well as with the calculated values, shown in figure 4.5. The M&M values show an offset from the calculated data by a factor of three for the day 2 measurements. This discrepancy is due to an error in setting the catalyst flow rate of M&M. This error in the flow rate calculation was rectified for the second plateau measurements that resulted into good accord with other measurements and calculations. The comparison for the day 3 also shows a good agreement among the M&M, GC-FID-I and the calculated values.

Nevertheless, there is a small offset in the PTR-MS-III dataset during the first and second plateau measurement for unknown reasons. The M&M data for day 3, day 4 and day 5 are in good agreement with measurements from other instruments, especially with the GC-FID-I and GC-FID-II data.

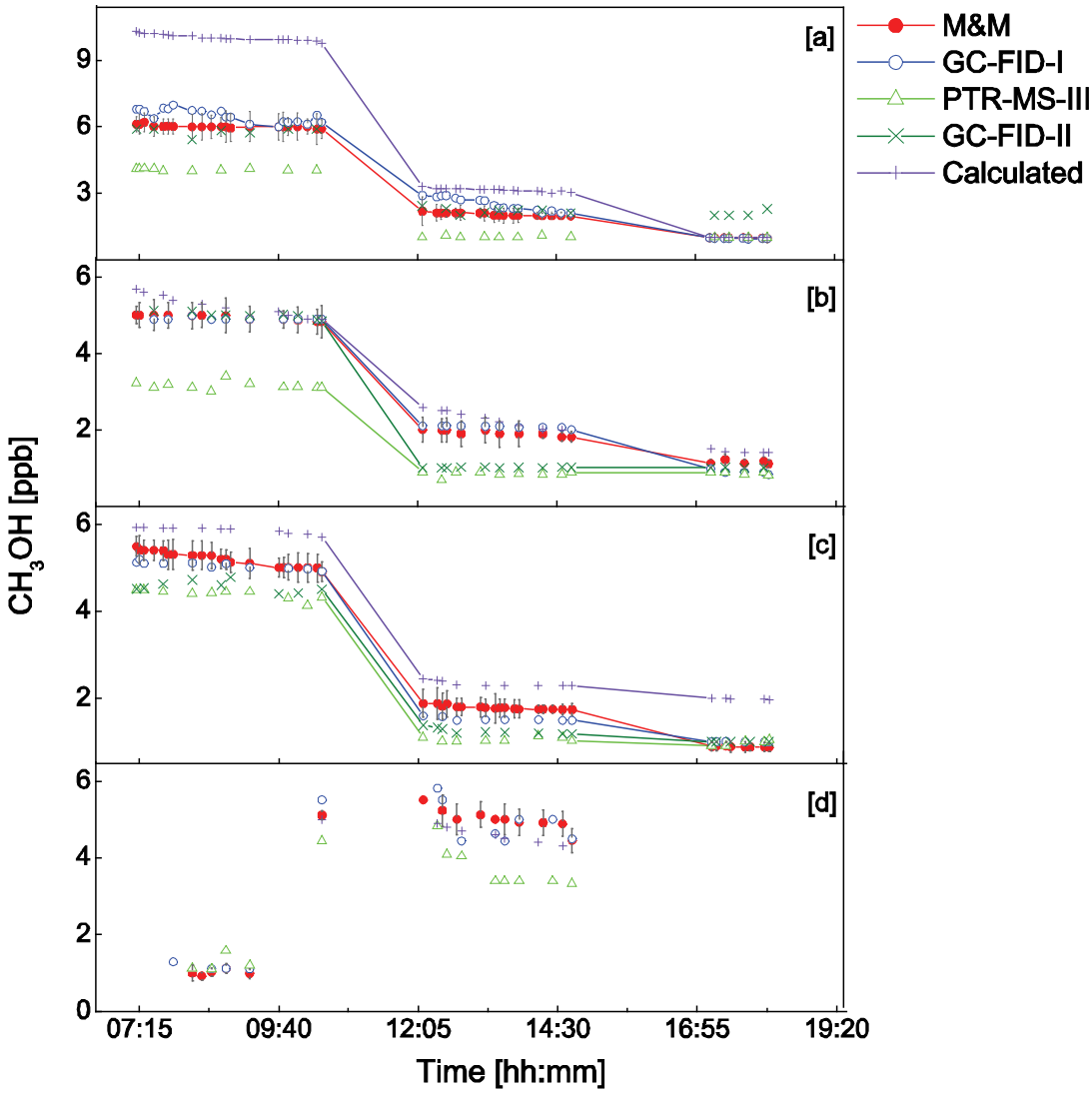

***Figure 4.5**: Same as figure 4.2, but for CH_3OH.*

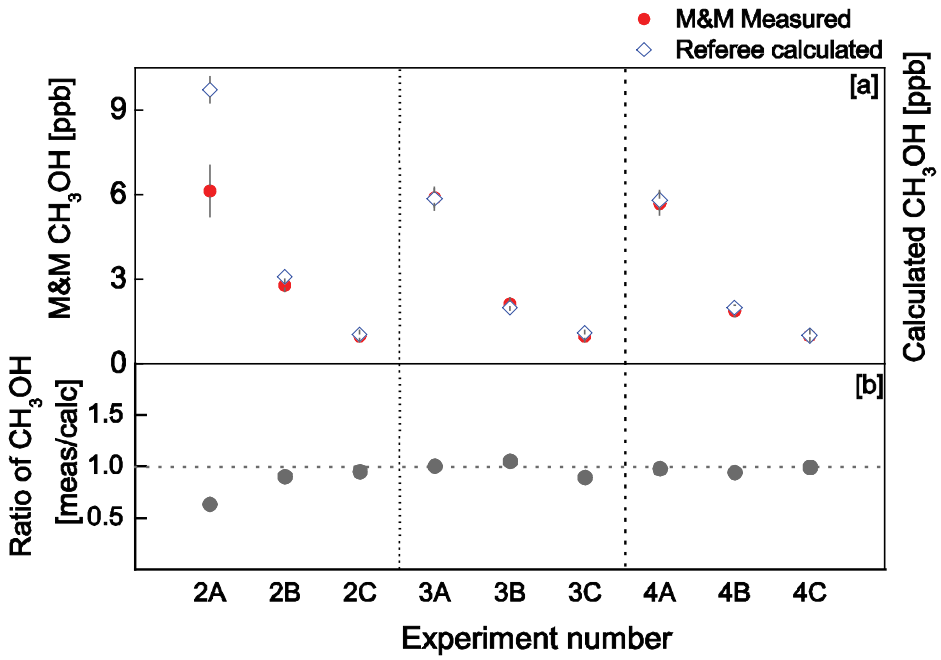

Figure 4.6: *Same as figure 4.3, but for CH_3OH.*

The calculated values for the third plateau measurement during day four are relatively higher than the measured values. This is due to the low levels of chamber flushing after the second plateau measurement in order to maintain the OVOC concentration inside the chamber above 0.6 ppb, which otherwise will affect the instruments with lowest detection limit higher than 0.6 ppb.

The time averaged comparison between measured and calculated values over the day 2, day 3 and day 4 are shown in figure 4.5a, b and c respectively. The values are averaged over the nine measurements taken during the three sub-experiments in a single day. The measured CH_3OH values are in very good agreement with the calculated data, except for 2A. The fine agreement is evident in the measured to calculated CH_3OH ratio, shown in figure 4.6b. The ratio is ~1.0 for most experiments except for 2A. The offset in the M&M vales in 2A is due to the error in the instrument flow rate as discussed previously.

This error in the flow rate calculation was rectified for the second plateau measurements that resulted into good accord with other measurements and calculations. The comparison for the day 3 also shows a good agreement among the M&M, GC-FID-I and the calculated values.

Nevertheless, there is a small offset in the PTR-MS-III dataset during the first and second plateau measurement for unknown reasons. The M&M data for day 3, day 4 and day 5 are in good agreement with measurements from other instruments, especially with the GC-FID-I and GC-FID-II data.

The calculated values for the third plateau measurement during day four are relatively higher than the measured values. This is due to the low levels of chamber flushing after the second plateau measurement in order to maintain the OVOC concentration inside the chamber above 0.6 ppb, which otherwise will affect the instruments with lowest detection limit higher than 0.6 ppb.

The time averaged comparison between measured and calculated values over the day 2, day 3 and day 4 are shown in figure 4.6a, b and c respectively. The values are averaged over the nine measurements taken during the three sub-experiments in a single day. The measured CH_3OH values are in very good agreement with the calculated data, except for 2A. The fine agreement is evident in the measured to calculated CH_3OH ratio, shown in figure 4.6b. The ratio is ~1.0 for most experiments except for 2A. The offset in the M&M vales in 2A is due to the error in the instrument flow rate as discussed previously.

The correlation analysis of the measured and calculated CH_3OH data is depicted in figure 4.7a, 4.7b, and 4.7c corresponding to day two, day three and day four respectively. The correlation coefficient (r^2) is averaged over the experiments 2, 3 and 4 here. The r^2 value is 0.99, 0.97, and 0.98 for day 2 and day 3 and day 4 respectively, which apparently show the good agreement between the measured and calculated data. The M&M response was found to be strongly linear over the concentration range investigated, with r^2 ranging between 0.975 and 0.998 for the chosen set of compounds under dry and humid sample conditions.

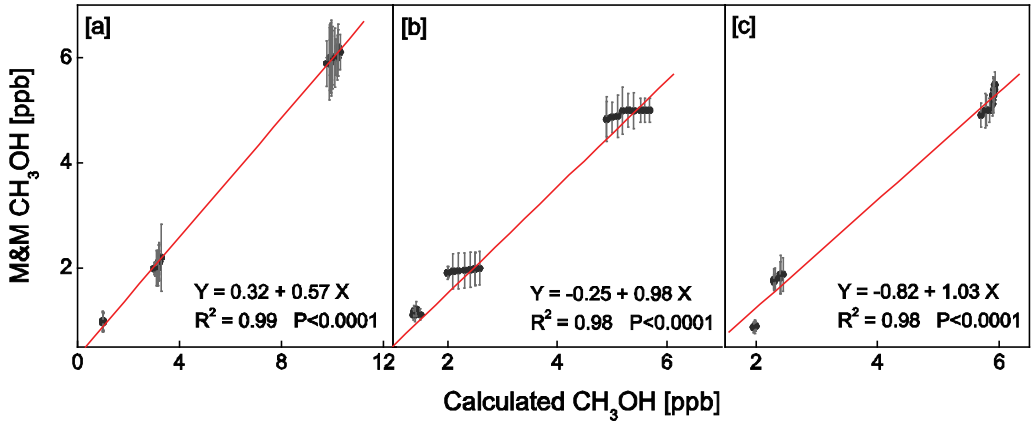

Figure 4.7: *Same as figure 4.4, but for CH_3OH.*

4.5 Discussion

The analyses indicate that a better accuracy, as compared to the reported one during the campaign, can be easily achieved with a precise HCHO calibrator. The results also point out that interference from O_3 or any other competent OVOCs inside the chamber have hardly any effect on methanol selective conversion by the newly constructed reactor. It should also be noted that humidity inside the chamber showed no detectable interference with reference to the catalyst active site adsorption.

Particularly high measurement accuracies were achieved for CH_3OH during all part B and C sub-experiments, where values were on average 6.5% for mixing ratios of the order ~1-4 ppb. The observed reproducibility throughout each experiment was generally high, with precision of the instrument in the order of ~6% or better for CH_3OH. Compared to HCHO, the CH_3OH measurements show good agreement with measurements from other instruments and with the calculated values. The precision values used (for HCHO and CH_3OH) are calculated from the ratio of the standard error of the mean in a given data set of repeats to that of the specific mean value. The relative accuracy of M&M with respect to other instruments is calculated using the root sum square (RSS) method for both CH_3OH and HCHO. The statistics showed a relative accuracy of 6.01% and 6.48% for HCHO and CH_3OH respectively.

4.6 Summary

In general HCHO and CH_3OH were measured by the M&M with an average accuracy of around 6.5% or better, with the compounds consistently measured with the greatest accuracy throughout the exercise. Particularly high measurement accuracies were achieved for these two compounds during all part B and C sub-experiments, where values were on average 5.7% for ~4-0.8 ppb. For HCHO, M&M consistently underestimated the derived chamber concentrations during all part of "A" measurements during day 2 and 3. This is clearly demonstrated by Figure 4.4 and verifies a roughly constant percentage difference between calculated values and those measured. Such findings are consistent with the presence of an unknown sink inside the chamber, presumably due to condensation out of the vapour phase enroute to detection. The possibility of sink/loss via this route is reinforced by consideration of the average ambient temperatures throughout the campaign, which were consistently low, in the range −1 to +4°C. Measurement reproducibility throughout each experiment was generally high, with compound specific precision of the order 6% or better for most plateaus. The M&M response was found to be strongly linear over the concentration range investigated, with correlation coefficients (r^2) ranging between 0.80 and 0.998 for HCHO and better than 0.97 for CH_3OH under dry and humid sample conditions. The results show the M&M is capable of detecting CH_3OH down to sub-ppb mixing ratios with high accuracy and precision.

Applications of M&M

Chapter 05

Plant emission budget studies: Counting the uncounted

While significant emissions of VOCs from plants are generally acknowledged, their budgets remain very uncertain and only few studies have addressed future global climate change related issues. Because VOC emissions exert a very significant influence on atmospheric chemistry, it is crucial to identify the responses and feedbacks of the terrestrial vegetation to anthropogenically induced climate change. This chapter describes the scientific results from the plant trace gas exchange studies, which was performed to elucidate the spectrum of VOCs emitted by Poplar plants and to identify and characterize physiological and environmental parameters controlling emissions/uptake.

5.1. Measurement setup

5.1.1 Materials and methods

All experiments carried out in this study were done with 2-years old cloned Grey poplar trees (*Populus x canescens* Aiton Smith), cultivated by micropropagation [*Leple et al., 1992*]. The plants were grown in plastic pots of 3.0 liters volume filled with a mixture of Perlite (Styroperl, LBS Horticulture, Lancashire, UK), fine quartz sand and commercial potting soil (John Innes No.2, Lincoln, UK) (2:1:1) (v/v/v), watered daily with tap water and fertilized every two weeks with a nutrient solution containing 3 g L^{-1} of a complete fertilizer (N:P:K, 15:30:15; Miracle-Gro®, The Scotts Company Ltd., Surrey, UK). Plants were kept under long-day conditions (light intensities 500 μmol m^{-2} s^{-1}) at day and night temperatures of 20°C±3°C and relative humidity of 40±10%.

All the plant materials for the analysis were placed in climate cabinets of 1 m^3 volume. A Li-Cor-6400 infrared gas analyzer was used to measure H_2O and CO_2 fluxes from plant. Gas exchange by the leaves of Poplar plant was determined using a modified dynamic flow-through system described by *Possell et al.* [*2005*]. It consisted of two identical glass cuvettes of 14.5 L volume. The cuvettes used for the experiments were mounted in temperature and humidity controlled housings. It was equipped with connections to introduce temperature and a light intensity sensor, PTFE tubes for gas-exchange analysis and air supply was also connected. Two fans ensured homogeneous mixing of the air inside the cuvette. Teflon (PFA or PTFE) tubes were used to minimise wall losses. Ambient air purified by drying devices (active charcoal) was pumped through the chambers at 2 - 4 L/min and was kept constant by mass flow controllers. Incident PAR (photosynthetically active radiation) was measured outside the enclosure with a light sensor (Delta T Dervices, Cambridge, UK), and leaf temperature was measured using a copper-constantan thermocouple (Omega Engineering Ltd., Manchester, UK) placed on the surface of the poplar leaves.

A single plant was placed into one of the cuvettes, whereas the other was kept empty and was used as a control. Both cuvettes were flushed with ambient air at flow rates of ~2 to 4 L min^{-1}. During experiments, flow rates, PAR, temperature, relative humidity, as well as the concentrations of CO_2 and

H_2O were measured continuously at the outlet parts of both chambers. Submergence of the roots ensured the emission of VOCs by the leaves and other plant parts only. The data were recorded on a logbook (Delta-T Devices Ltd, Cambridge, UK) connected to the system. The targeted compounds were sampled from the air leaving both cuvettes. At the end of each measurement all plant leaves from inside the cuvettes were harvested and subjected to determination of leaf area and fresh weight. BVOC flux rates as well as the rates of photosynthesis and transpiration were calculated by the concentration differences from the leaf and control cuvette by taking into account the flow rates through the cuvettes. The projected leaf area was determined using a leaf area meter (AM200, ADC Bioscientific Ltd., Herts, UK).

The purified ambient air at a known flow rate was passed through the cuvette containing plant material to be studied. Positive or negative fluxes were calculated by measuring the gas-phase concentration of the species of interest prior to entering the chamber (C_{in}) and then again upon exit (C_{out}) along with the flow rate of the gas added to the chamber (F).

$$Flux_{voc} = \frac{[F \times (C_{out} - C_{in})]}{A} \qquad \text{---------- 5.1}$$

5.1.2 Ozone treatments

The plants were exposed to short term, acute (4 h per day at 170±15 ppb) and chronic (4 h per day at 70±15 ppb) ozone concentrations under laboratory controlled conditions. Ozone was produced by UV dissociation (Opsis, Furulund, Sweden) of pure oxygen (BOC Gases, Surrey, UK) and it was monitored continuously inside both chambers by a photometric analyzer (Teledyne Instruments, San Diego, USA). The ozone fumigation and reactivity experiment were typically performed in the following sequence; starting with measurement of steady state VOC emissions in ambient air containing 20±5 ppb of O_3. This was followed by ozone addition into the plant chamber continuously for 4 hours. Once the ozone source was turned off, OVOC measurements were started immediately and continued till the next ozone fumigation experiment. Alternate blank cuvette measurements were carried out by switching an electric valve between the sample air from blank and plant cuvettes. Experiments to find any light and temperature dependence in OVOC synthesis were also done.

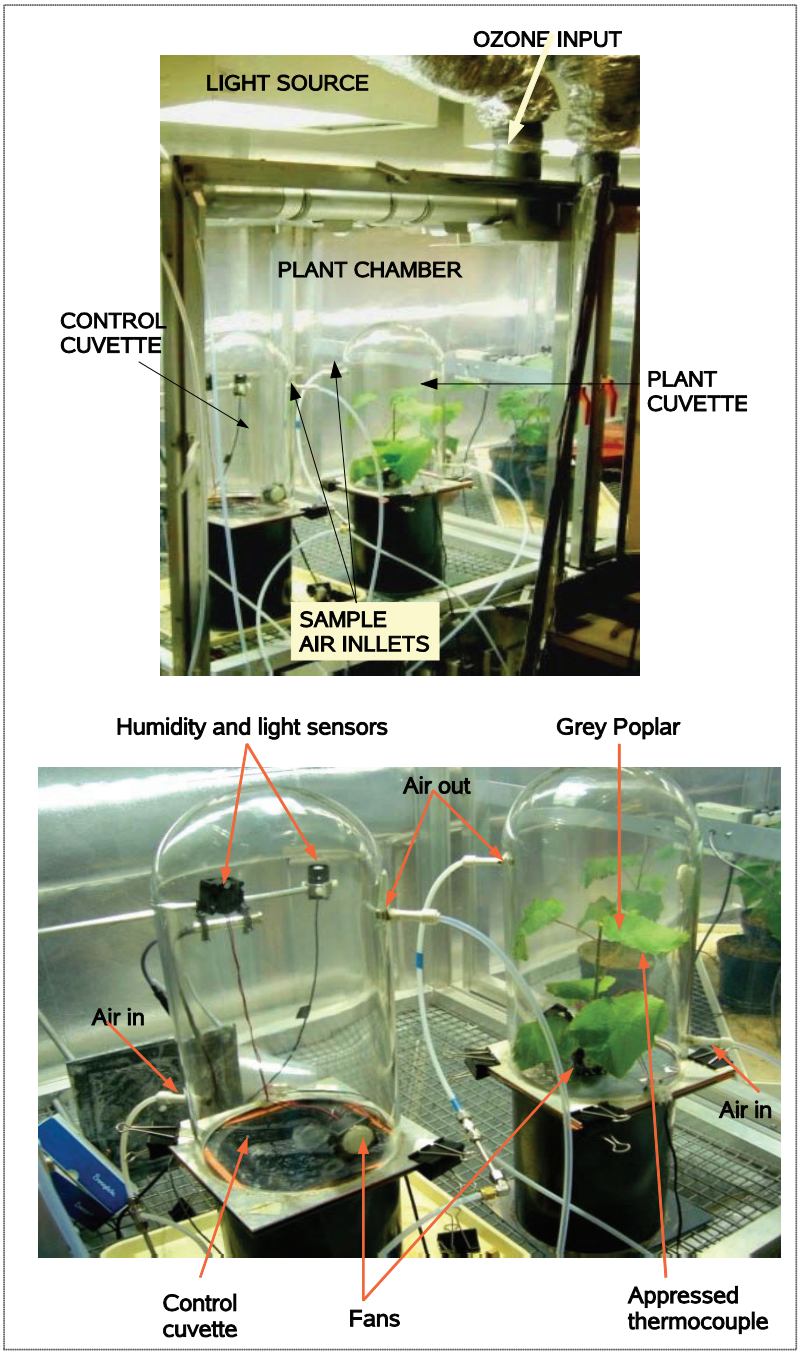

***Figure 5.1**: Pictures of plant and control cuvettes with temperature, humidity and light sensors attached.*

5.2 Plant physiological parameters

5.2.1 Net carbon assimilation [J_{CO2}]

Net carbon assimilation rates was calculated from the CO_2 concentration difference [ΔCO_2] between the cuvettes (plant and control), the gas flow rates [F] through the cuvettes and the leaf area [L_A],

$$J_{CO_2} = \frac{\Delta C_{co2} \times F}{L_A \times MV \times 60} \qquad \text{---------- 5.2}$$

[*Where,* J_{CO2}= *µmol.m*$^{-2}$*.s*$^{-1}$, *F= L.min*$^{-1}$, ΔC_{CO2} = *ppm,* L_A =*m² and Molar volume [MV] =L.mol*$^{-1}$]

5.2.2 Transpiration rate [J_{H2O}]

The transpiration rates were calculated in analogy to net carbon assimilation considering the difference in water vapour concentrations [ΔH_2O] between both cuvettes, the gas flow rates through the cuvettes and the leaf area using a similar equation as for CO_2 exchange,

$$J_{H_2O} = \frac{[\Delta C_{H_2O} \times F]}{L_A \times MV \times 60} \qquad \text{---------- 5.3}$$

[*Where,* J_{H2O} =*mmol.m*$^{-2}$*.s*$^{-1}$, ΔC_{H2O} =*ppm*]

5.2.3 Stomatal conductance [g_{H2O}]

It is defined as a measure of the limits on gaseous transport between the leaf and ambient atmosphere caused by the small pores (stomata) on the leaf surface. At a common partial pressure gradient between the atmosphere and leaf(ΔP), compound flux rate (F) increases linearly with increasing stomatal conductance (g_{H2O}), i.e.,

$$Flux_{voc} = [g_{H_2O} \times \Delta P] \qquad \text{---------- 5.4}$$

Leaf stomatal apertures vary strongly as plants track the ambient light, temperature and humidity conditions. In particular, water-stressed plants strongly reduce g_{H2O} to limit water loss. Gaseous transport also occurs through a waxy layer covering the rest of the leaf surface (cuticle), but the contribution of the cuticle to the passage of gases is small relative to stomatal transport. Under natural conditions net fluxes of VOCs, CO_2 and H_2O are regulated by the degree of stomatal opening. Thus stomatal conductance was determined taking into account of transpiration rates, temperature and relative humidity. Usually stomatal conductance is given in mm s^{-1}. As per the *Körner's* [*1979*] calculations (at standard temperature of 293 K and pressure of 105 Pa) division of stomatal conductance values calculated in mmol.m-^{2}.s-^{1} by a factor of 41 ensure conversion into mm s^{-1}.

$$g_{H_2O} = \frac{J_{H_2O}}{\Delta_{H_2O} \times 41} \qquad \text{---------- 5.5}$$

[*Where,* g_{H2O}=*mm s*$^{-1}$, Δ_{H2O}=*mol.m*$^{-3}$]

Δ_{H2O} is a measure of water vapour deficit in ambient air at a specific external temperature and relative humidity which was recorded in the control cuvette.

The water vapour saturation deficit was calculated using the MAGNUS formula [e_o = 610.78 x $e^{[(17.08085 \text{ x } T)/(234,175+T)]}$] at a specific temperature (T=°C) and water vapour concentration inside the cuvette.

5.2.4 Leaf area determination [T_{LA}]

At the end of each experiment all leaves from inside the cuvettes were harvested and are subjected to determination of leaf area and/or dry weight. All gas exchange parameters are calculated based on leaf area determination. The projected leaf area was determined using a video camera (TC2000 RCA, Lancaster, USA) adapted to an area-meter (Delta area meter, Delta-T devices, UK). The specific leaf area [T_{LA}] was calculated from the total fresh weight of the twig and a correction factor [C_{LA}=2.74]. With this correction factor conversion of projected leaf area to actual leaf area was achieved.

$$T_{LA} = \frac{[L_A \times C_{LA} \times 0.0001]}{FW} \qquad \text{---------- 5.6}$$

[*Where,* $T_{LA} = m^2 .g\, FW^{-1}$, *FW=fresh weight*]

5.3 Error analysis

The total errors of exchange rates (E_{ex}, in µg gFw^{-1} h^{-1}) from measurements were calculated by using an error propagation method (Equation 5.7), with absolute errors for the concentration measurements in the sample cuvette (E'_s, in ppb), the absolute errors in the reference or blank cuvette (E'_R, in ppb) and the concentration difference between sample and reference cuvette (ΔC),

$$E_{ex} = \sqrt{\frac{(E'_s)^2 + (E'_r)^2}{(\Delta C)^2} + E_Q + E_s} \qquad \text{---------- 5.7}$$

Relative errors for the VOC measurements were estimated to be ~1.1% for HCHO and 1.3% for CH_3OH and were obtained by parallel sampling from gas standards or from the permeation device. The error for the cuvette flow (E_Q) and the leaf area (E_A) were set to 4% and 0.15%, respectively.

5.4 Results and discussion

Leaf level measurements with potted plants performed in the laboratory were used to examine the plant processes controlling BVOC exchanges. Figure 5.2 to 5.6 shows significant emission of CH_3OH and HCHO fluxes when subjected to physical stress including O_3 and temperature stress and physiological parameters like transpiration and stomatal conductance (Figure 5.2a, 5.2b, 5.2c, and 5.2d). OVOC emissions from poplar tree were dominated by CH_3OH, along with significant amounts of HCHO. The diurnal fluxes of both compounds showed higher rates in the afternoon than at night. At some nights even uptake of HCHO was observed.

5.4.1 Influence of plant physiological parameters on CH_3OH emission

The results from the experiments performed to identify the relation of plant physiological parameters with poplar CH_3OH emission are represented in figure 5.2a, 5.2b, 5.2c and 5.2d. As seen in figure 5.2a and 5.2d, plant emission experiments show that CH_3OH closely flow the stomatal conductance and transpiration rate [*Fall et al., 1996]*. CH_3OH emission from leaves was positively correlated with light intensity, transpiration rate and with CO_2 assimilation (figure 5.2b)**.** Auxiliary HCHO results also showed an increase in emission in response to stomatal conductance and transpiration (figure 5.2c). In each case, poplar leaf CH_3OH emission rate increased and decreased with stomatal conductance but not exactly parallel to stomatal conductance. When stomata were induced to close, CH_3OH emission rate decreased considerably, although in most experiments the decline in CH_3OH emission rate lagged behind stomatal closure (Figure 5.2d). This lag may be due to a slower volatilization of some CH_3OH condensed on the leaf surface. Plant CH_3OH emission rate responses to changes in light intensity and stomatal conductance and to induced closure of stomata were find to be consistent. With most CH_3OH being produced inside leaves and emitted primarily through stomata. This aqueous pool then empties rapidly upon stomatal opening, correlating strongly with rates of transpiration. Following depletion of the pool, lower CH_3OH emissions reflect a dynamic balance among rates of production, phase partitioning, stomatal conductance and transpiration.

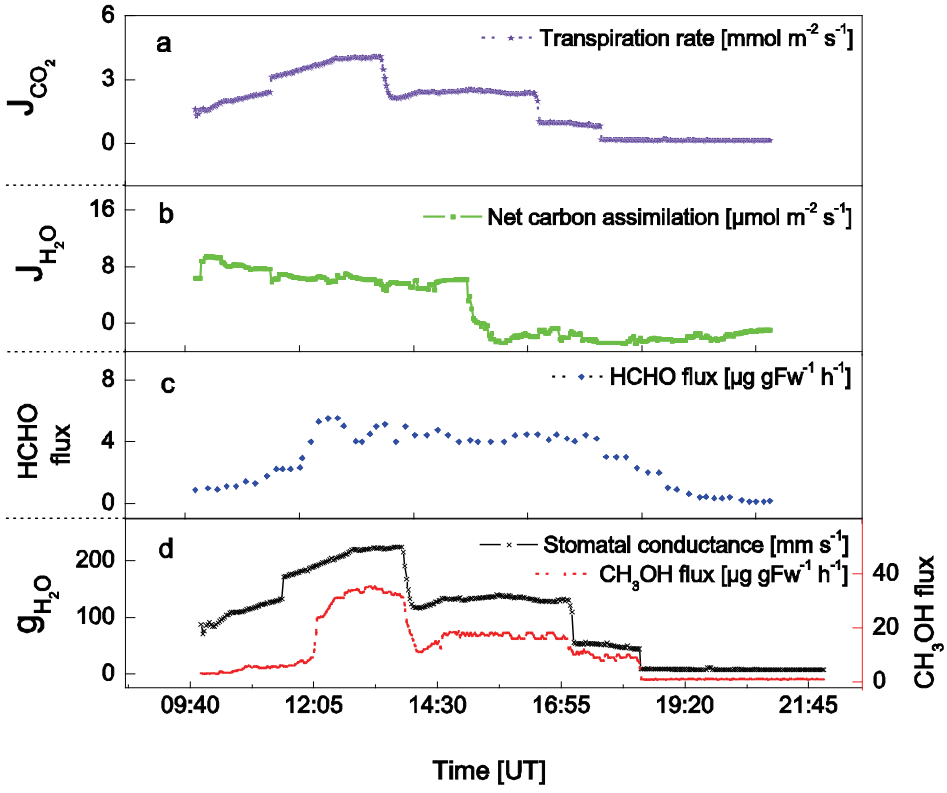

Figure 5.2*: Dependence of CH_3OH emission from poplars on physiological parameters as (a) transpiration rate, (b) net carbon assimilation and (d) stomatal conductance of poplar. (c) Auxiliary data of HCHO flux is also shown. CH_3OH flux closely followed the stomatal conductance with higher emission at higher stomatal opening and decreased at night due to stomata closure.*

CH_3OH emissions were decreased to very low levels after stomata were induced to close by either temperature or vapour pressure deficit. This indicates that free CH_3OH contained in the leaf air space exist in leaves and escapes along with transpired water vapour.

The emission rates decreased when the light was switched off in the evening and peaked in the morning when the light was turned on again. This pattern significantly correlated with diurnal rhythms of stomatal conductance, photosynthesis and transpiration. At night, assuming constant production and when stomatal conductance was low, gas phase concentrations increased and the size of the aqueous pool increased in response. It may be concluded that under conditions of diminished stomatal conductance, CH_3OH emission declines because its diffusive flux was reduced.

5.4.1.1 Correlation of CH_3OH and HCHO with environmental factors

Beside a direct comparison of daily trends of CH_3OH and HCHO emissions with physiological activities of the enclosed plant, correlation analysis of the emission rates with these parameters were also performed. During the measurements conducted in October-November 2005 ambient ozone concentration in non-fumigated control chamber varied between 2.5 to 50 ppb. The correlation graphs for CH_3OH and HCHO showing the regression coefficients as well as the significance levels with PPFD (Photosynthetic Photon Flux Density), transpiration rate, net carbon assimilation and stomatal conductance are shown in figure 5.3a, 5.3b, 5.3c and 5.3d respectively.

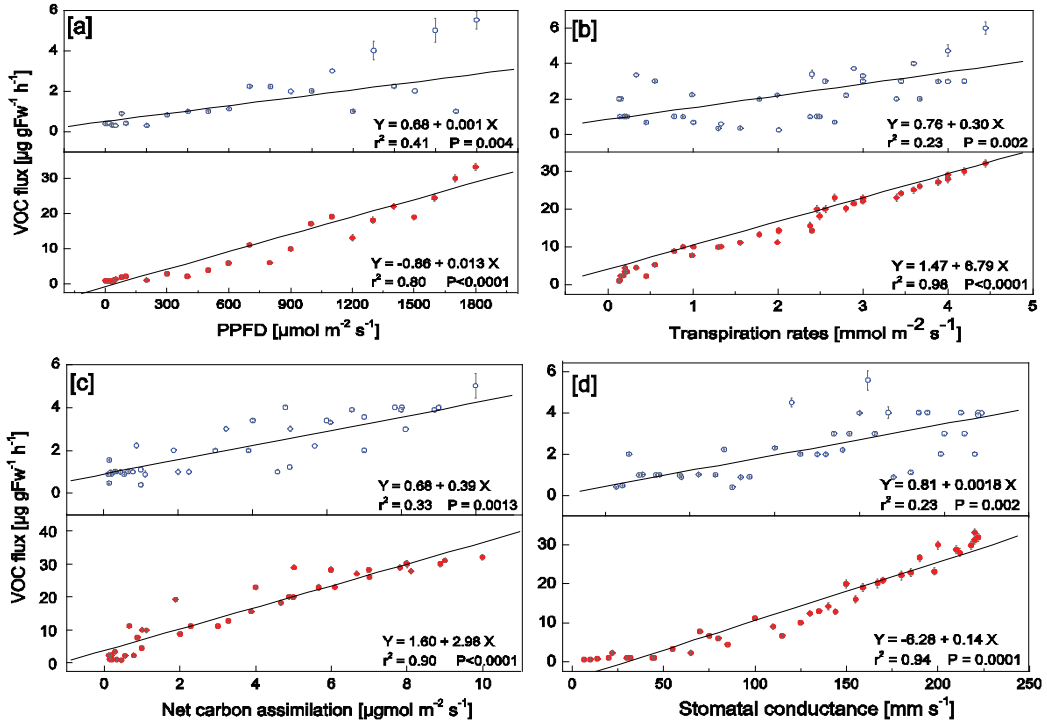

Figure 5.3: *Correlation of CH_3OH (red circle) and HCHO (blue open circle) emission rates of Grey poplars with (a) light intensity (PPFD) (b) transpiration rates, (c) net carbon assimilation and (d) stomatal conductance. The results of linear regression analyses (r^2 and Y) as well as the significance levels are shown.*

PPFD correlated significantly with CH_3OH (r^2 = 0.80; P<0.0001) emission rates with distinct early morning bursts. Compared to CH_3OH, the emission rates of HCHO from poplars (r^2 = 0.41; P = 0.004) were not strongly correlated with light intensity. Methanol was found to be emitted by the plant transpiration stream and hence the strong correlation (r^2 = 0.98; P<0.0001).

Formaldehyde emission rates were weakly correlated with transpiration rate (r^2 = 0.23; P = 0.002), net carbon assimilation (r^2 = 0.33; P = 0.0013) and stomatal conductance (r^2 = 23; P = 0.002) when compared to their respective CH_3OH correlations. The results shows that the stomatal aperture strongly affects the CH_3OH gas exchange between leaves and the atmosphere (r^2 = 0.94, P<0.0001). The CH_3OH pool inside the leaf structure is believed to be depend on the carbon assimilation process performed by the plants and this was illustrated by the strong correlation between CH_3OH emission and assimilation rates (r^2 = 0.90; P<0.0001).

5.4.2 Influence of meteorological parameters on CH_3OH emission

5.4.2.1 Plant Temperature

The relationship between plant leaf temperature and CH_3OH emission pattern are shown in figure 5.4. The correlations between the two parameters are given in figure 2a, where r^2 values and probability of the correlation are also shown. An artificial increase in ambient temperature induced an increase in CH_3OH emission rates. As seen from the measured emissions of CH_3OH exhibited near-exponential leaf temperature dependence between 10°C and 33°C (figure 2a and 2b). Figure 2b depicts a single sequence of temperature-emission relation out of several experiments (n = 7). Although emission of CH_3OH responds to variation in leaf temperature and incident light, the nature of the control was quite different. With increasing temperature, photosynthesis and related mechanisms inside plant cells enhances, and hence emitting a large amount of CH_3OH to the atmosphere.

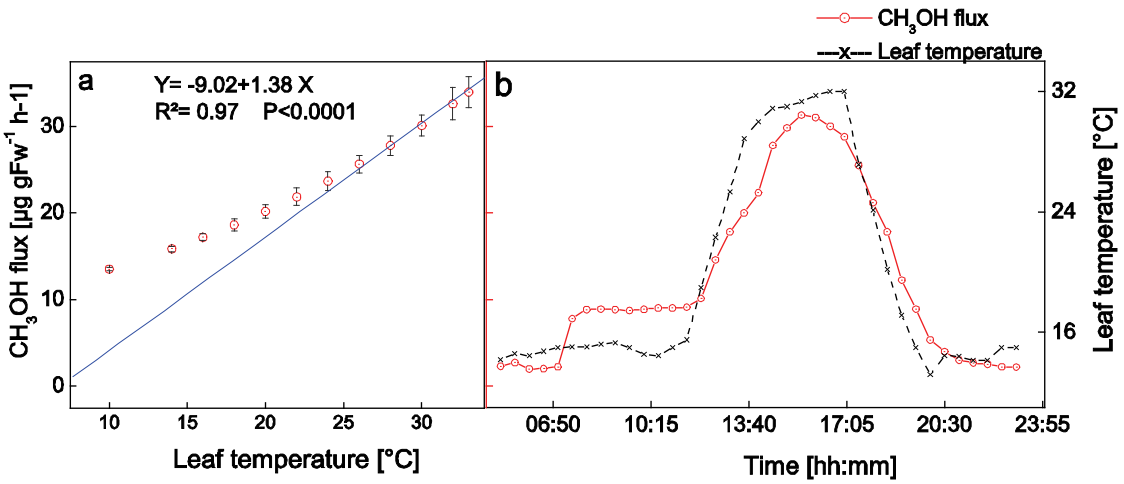

***Figure 5.4**: Effect of plant leaf temperature on CH_3OH emission. (a) Correlation of leaf temperature with CH_3OH emission from poplar leaves. (b) One typical temperature-emission sequence out of four independent experiments is shown.*

CH_3OH emissions were decreased to very low levels with very high temperature after stomata were induced to close either by temperature or vapour pressure deficit. This shows the relation of temperature with CH_3OH emission through the effects on stomatal conductance and evapotranspiration. The data analysis justify the conceptual model in which CH_3OH released in the demethylation of pectin partitions into the gas and liquid phases according to Henry's Law. Gas phase CH_3OH was then emitted through the stomata. However, CH_3OH emissions correlate more strongly with rates of evapotranspiration than with stomatal conductance and temperature (figure 5.3), suggesting that much of the CH_3OH was released from the dissolved pool along with the transpiration stream. The results are in accord with previous studies illustrating similar correlation for CH_3OH emission from plants [*Karl, et al., 2005; Fall 2003*].

The CH_3OH emission dependencies on temperature measured from poplars were analyzed on the basis of the following algorithm,

$$E = E_{st} \exp[\beta \times (T - T_{st})] \qquad \text{---------- 5.8}$$

where E is the emission rate at temperature T, E_{St} is the emission rate at a standard temperature T_{St} (usually 303 K*)*, and β is an empirical temperature coefficient (slope of ln dE/dT). This algorithm has been used to simulate the temperature dependence of monoterpene emissions [*e.g. Guenther et al., 1993*], and more recently the emission of oxygenated VOCs [*Schade and Goldstein, 2001; Karl et al., 2003a*].

The β-coefficient establishes the temperature dependence of the emission rate in equation 5.8. For monoterpenes an average value of 0.09 K^{-1} is commonly used [*Guenther et al., 1993*], and for CH_3OH, acetaldehyde and acetone values that vary from 0.04 to 0.13 K^{-1} have been calculated from field measurements at a pine forest in California [*Schade and Goldstein, 2001*] and a hardwood forest in Michigan [*Karl et al., 2003a*]. In the present study the factor β was set to 0.07 K^{-1} for comparing the predicted values derived from *Guenther [1993*] algorithm with the present data measured under standard conditions.

The comparison between measured and modelled CH_3OH emission rates with plant cuvette temperature is shown in figure 5.4. Calculations with this algorithm showed that the simulated emission rates closely followed the measured values for temperatures from 10-34°C. The algorithm overestimated the emission at temperatures higher than 35°C where the measured values showed a decreasing trend due to the stomatal closure with high temperature. This clearly indicates that the emission rates must also depend on stomatal opening and not just on external temperature.

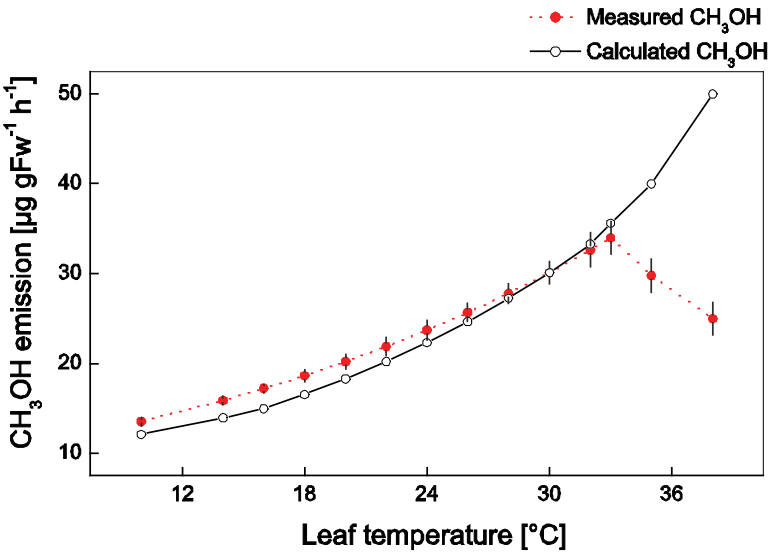

Figure 5.4*: The measured CH_3OH emission as compared to the calculated values using the algorithm developed by Guenther et. al. [1993]. The β-coefficient was set to 0.07 K^{-1} to identify the best compilation for predicting the emissions.*

5.4.2.2 Ozone stress response by Poplars

(a) Chronic ozone fumigation

Following 4-5 days of control measurements using ozone free air, poplar trees were fumigated for 5 consecutive days with chronic (70 ppb) or acute (170 ppb) ozone for 4 h per day followed by 3 days recovery measurements. Leaf temperatures were held constant at ~ 30°C, PAR at 500 µmol m^{-2} s^{-1} and RH at 40±10%. The results from two different sets of chronic experiments are shown in Fig. 5.5. The experiments performed with ambient air prior to fumigation cycle are represented as "control" days and the days following the fumigation as "recovery" days. An increase of CH_3OH and HCHO emissions immediately after ozone exposure was observed, which is clearly depicted in the figures.

Despite no clear physiological evidence of leaf damage after chronic exposure, CH_3OH emissions related to ozone damage were already triggered at these ozone concentrations. During the days following each 4h/day ozone fumigation cycle higher emission rates of CH_3OH and HCHO were observed. The results from chronic ozone stress experiments (figure 5.5) registered an approximate of 2-3 fold increase in CH_3OH and HCHO emission compared to control measurements. The four day control measurements clearly show bidirectional behaviour in both CH_3OH and HCHO flux. An increase in HCHO flux was observed during the recovery period, were CH_3OH showed a decreasing trend. It clearly shows that CH_3OH produced inside the plant cell was converted to HCHO as suggested by the formate cycle in plants [*figure 2.2*].

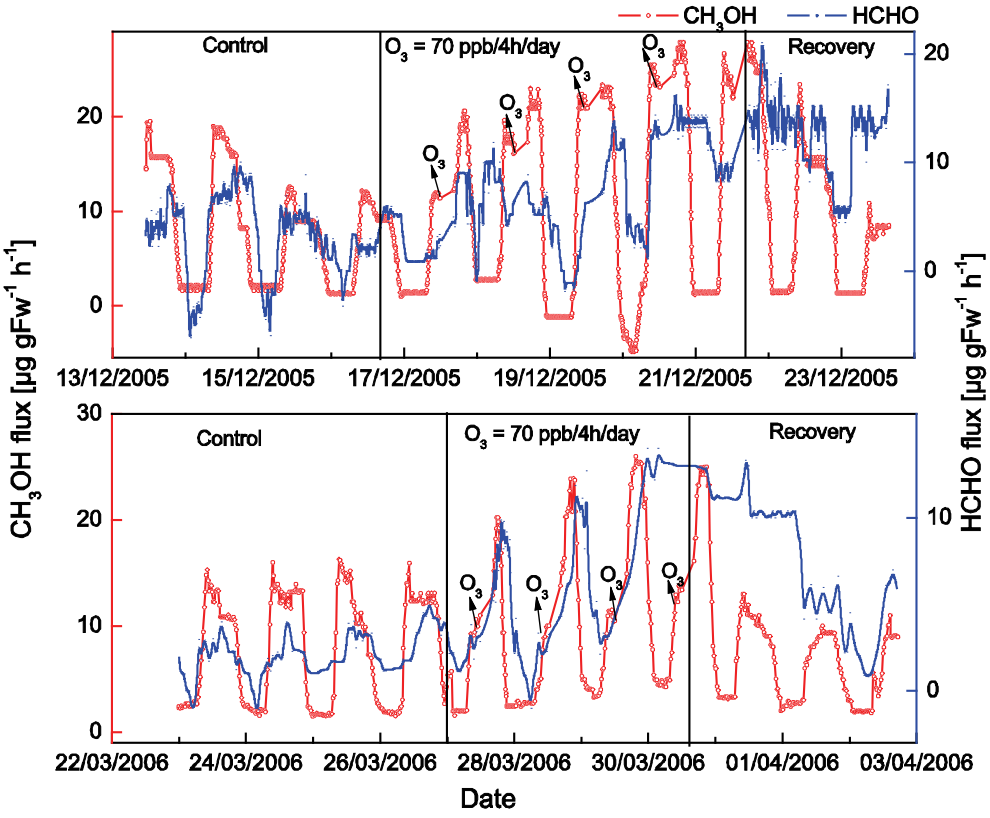

Figure 5.5*: CH_3OH and HCHO emission from plants during control, chronic fumigation and recovery days. Red dots denote HCHO emission rates and blue line shows the corresponding CH_3OH emission during the observation period.*

(b) Acute ozone fumigation

The CH_3OH and HCHO emission pattern during the acute short term fumigation experiment is shown in figure 5.6. Poplar plant was exposed to O_3 at a concentration of about 170 ppb for 4 h each day. As shown in the figure 5.6, there were a pre-fumigation control day measurements and post-fumigation recovery day measurements as in the chronic fumigation experiments. The amount of CH_3OH emitted after the acute stress was ~7-9 times greater than the ambient air measurement days. During this experiment CH_3OH and HCHO were emitted with maximum rates of about 100 µg gfw^{-1} h^{-1} and 22 µg gfw^{-1} h^{-1} respectively. The general emission pattern showed a decreasing trend at the night when lights were off. Even though physiologically significant changes were not obvious, the exchange rates of CH_3OH and HCHO at night were systematically higher on the days following 4 h of ozone fumigation as compared to the control experiment days. This argues that damage to cell wall responsible for CH_3OH metabolism might have already occurred at ozone concentrations at the 170 ppb range. These conditions often lead to decrease in transpiration rates and net photosynthesis, which implies reductions in stomatal aperture. Since O_3 was taken up through the stomata [*e.g. Neubert et al. 1993*], these reductions in stomatal aperture also lead to decreases of CH_3OH and HCHO fluxes at night.

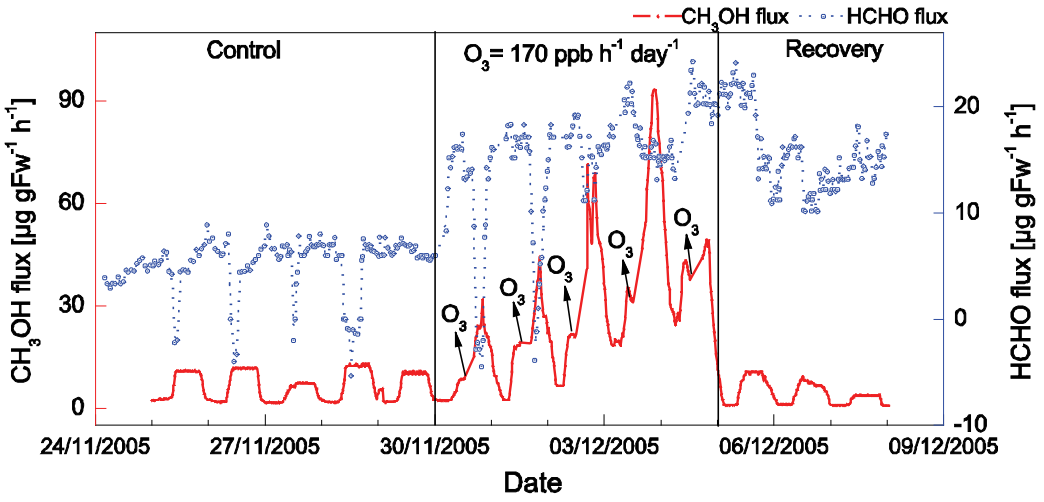

***Figure 5.6**: CH_3OH and HCHO emissions from plants during the acute ozone fumigation experiment (~170 ppb/4h/day). The red dots denote CH_3OH emission rates and the blue dots show the corresponding HCHO emission during the period.*

Figure 5.6 shows results from measurements conducted with the highest O_3 concentrations, in which this effect was most pronounced. In all cases related to the acute O_3 exposure induced VOC emissions, the necrotic spots on the older leaves became visible to the naked eye. The observed higher emission of CH_3OH due to ozone exposure might be due to leaf wounding and/or leaf cell damage. At C_{O3} below 40 ppb ie., at ambient control measurements, neither any physiological factors (increased VOC emissions, reductions in stomatal conductivity, decreases in the net rates of photosynthesis), nor any visible symptoms of injury were observed. The VOC emissions induced by O_3 exposure were transient. The emissions did not start directly with the O_3 exposure but after variable lag times ranging from 10 min to 30 min, depending on type of exposure and VOC. The CH_3OH emissions increased first, followed by those of HCHO and isoprene. In all cases when O_3 exposures induced additional emissions, the pattern of dominant CH_3OH emissions was similar.

The general CH_3OH and HCHO trend over the whole set of various measurements are shown as time weighted averages with standard deviations for each day in figure 5.7. Figure 5.7a depicts the weighted averages of emission (4 days each in 2 set of separate experiments) during the acute stress experiments in different phases, e.g., early morning bursts, night time emission, before and after the O_3 exposure etc. Figure 5.7b shows the same pattern as figure 5.7a, but for the chronic stress experiments. Two sets of chronic and acute experiments were conducted during the whole period, which are represented by number of experiments, “n”. The time weighted averages of ambient “control” measurements performed before each fumigation experiments are shown in figure 5.7c, with error bars representing 1 σ deviations from the mean value.

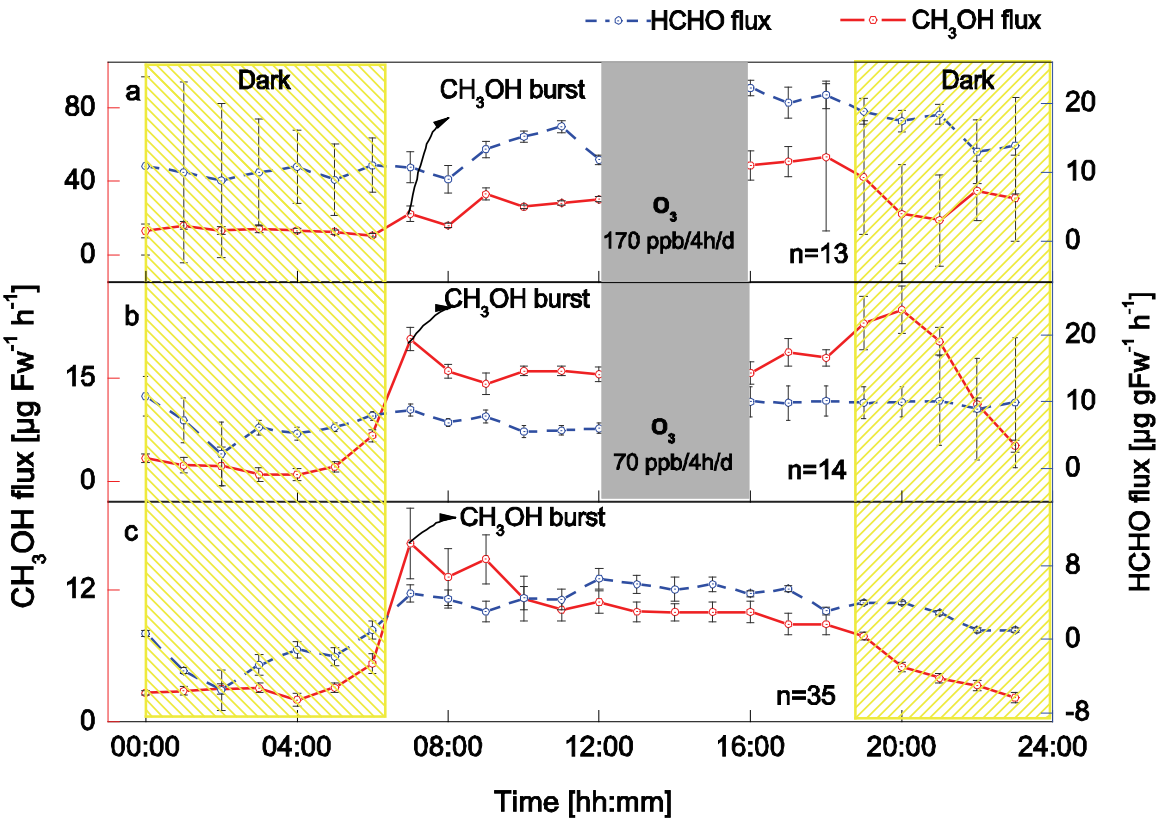

Figure 5.7*: Time averaged CH_3OH and HCHO emissions of poplar leaves during (a) acute ozone fumigation (b) chronic fumigation and (c) control days at ambient level ozone. At the time indicated by the yellow bar, the cuvette atmosphere was switched to dark conditions. The numbers of repeated measurements for each set of experiment is denoted by "n" at 1 σ level. The early morning CH_3OH burst is also shown. During the time indicated by the grey background, the plant was subjected to acute and chronic fumigations respectively.*

In the lab experiments some CH_3OH appears to be emitted from the cuticular surface; these fluxes were especially high early in the morning, which was indicated by the early morning burst in CH_3OH (figure 5.7). The control day measurements showed typically lower deviations from the mean values during day other than the early morning episodes. Our results showed significant emission and deposition of HCHO during control and fumigation periods from plants (figure 5.7), as shown by previous studies [*Cojocariu et al., 2005; Rottenberger et al., 2004*].

5.4.3 Compensation points

Several studies on the exchange of oxygenated compounds at the leaf level have directly shown the potential of trees to emit carbonyls, and also to take them up under certain environmental conditions [*Cojocariu et al., 2005; Kesselmeier et al., 2001; Kesselmeier and Staudt, 1999*]. Emissions of aldehydes and ketones have been observed from various plants, but in most cases only limited qualitative assessments are available above forests [*Steinbrecher and Rabong, 1994; Janson et al., 1999*].

***Table 5.1**: Leaf level compensation point measurements of CH_3OH and HCHO for Grey poplar. Values were derived from a linear regression analysis of observed HCHO or CH_3OH flux versus the reference mixing ratio. Slope (inferred from the compensation point regression analysis), and CP (compensation point, x axis intercept of regression line) are summarized in columns.*

No:	Slope (µg gFw^{-1} h^{-1} ppb^{-1})	CP (ppb)
CH_3OH before O_3 fumigation	-0.56±0.11	5.1±0.13
CH_3OH after O_3 fumigation	-1.23±0.09	6.9±0.09
HCHO before O_3 fumigation	-0.75±0.10	4.3±0.10
HCHO after O_3 fumigation	-0.58±0.17	5.2±0.23

Compensation point and canopy scale measurements of OVOCs are still extremely scarce [*Karl, et al., 2005; Kesselmeier, 2001*]. There are, however, no quantitative descriptions of the relations between carbonyl emission rates and factors controlling these emissions such as temperature, light intensities, relative humidity and plant physiological activities. In order to determine the exchange pattern of CH_3OH and HCHO compensation point measurements on Grey poplars were performed, which are listed in Table 5.1.

Figure 5.8 illustrates a typical example of the exchange of CH_3OH and HCHO plotted versus the concentration of outgoing air for poplar plant before and after fumigation with 70 ppb ozone (180µmol m^{-2} s^{-1}, 25°C, ~50% relative humidity). For this purpose CH_3OH and HCHO were blown into the chamber at levels ranging from 0-6 ppb and 0-4 ppb respectively [*Cojocariu et al., 2005*]. As expected, increasing ambient concentrations led to decreased emissions and finally to an uptake in Grey poplars. The VOC exchange varied as a function of mixing ratios in all experiments conducted.

In the observed concentration range, deposition of HCHO and CH_3OH increased with increasing mixing ratios, emissions occurred only at very low mixing ratios. During the control period, the daily average compensation point mixing ratio, where emission balances deposition (*x* intercept), was found below 5.2 and 6.9 ppb for HCHO and CH_3OH respectively.

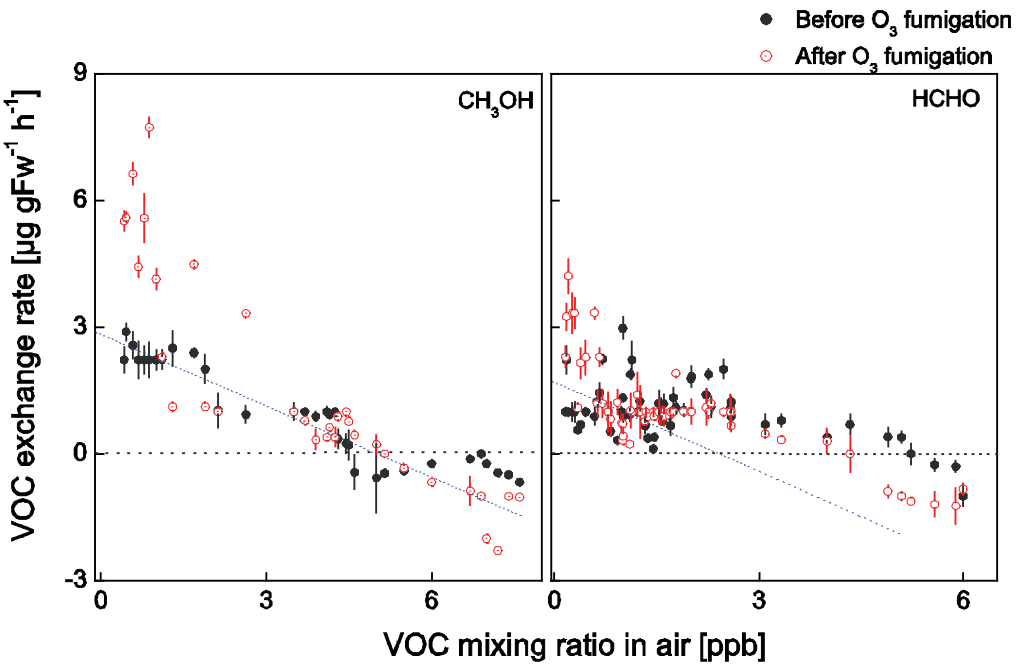

Figure 5.8: *Exchange of CH_3OH and HCHO in correlation with the ambient (reference) mixing ratios using Grey poplars before and after 70-170 ppb ozone exposures. The plots show measured data and the absolute error as estimated by the error propagation method (Equation 5.7). The compensation point represents the x-axis intercept of the regression line.*

A significant increase in CH_3OH and HCHO emission rate was observed at 70 ppb ozone where the post fumigation compensation point mixing ratio varied to 4.3 and 5.1 ppb for HCHO and CH_3OH respectively. The multiple regression of exchange rates on mixing ratios and stomatal conductance for data of both species showed a significant effect of mixing ratios (P_{CH3OH}<0.0001; P_{HCHO} = 0.0014) and stomatal conductance (P_{CH3OH} <0.0001; P_{HCHO} = 0.002 for HCHO).

5.5 Summary

A laboratory experiment on the emission of CH_3OH and HCHO under ambient and stressed conditions was conducted. CH_3OH and HCHO fluxes were found to be controlled by stomatal opening as indicated by strong correlations with stomatal conductance. CH_3OH flux also increased near-exponentially with leaf temperature similarly as shown in previous studies. The fumigation results show increased response of poplar leaves to chronic short term ozone exposure with respect to CH_3OH emissions. Acute exposure to 170 ppb ozone for the same time duration per day lead to even more drastic increases in CH_3OH emissions, possibly as a result of an internal re-structuring repair mechanism. The effects of ozone on production of CH_3OH are unknown, although emissions, and presumably production, continue through the night at reduced rates. Assuming that elevated temperature and ozone confers damage to cell walls, both cell degradation and new cell growth due to these stresses may explain the observed CH_3OH flux increase [*Kreuzwieser, et al., 1999*], a process that abate when the cause of damage is removed. HCHO emissions were highest at midday, amounting

up to ~15 μg gFw^{-1} h^{-1}. During darkness uptake was also observed. Fumigation of poplar plants with ozone indicated a compensation point of 5.1±0.09 ppb for CH_3OH and 4.3±0.23 ppb for HCHO.

The present findings support the view that CH_3OH emission by poplar is related to cell wall destruction and repair mechanisms, as previously shown for tree seedlings under controlled conditions. The basis of HCHO emission by poplar is still unclear and remains to be studied in further experiments. In a climate change scenario with increased boundary layer ozone abundance, higher HCHO emissions could further enhance ozone formation, while higher CH_3OH emissions can lead to higher upper tropospheric ozone formation, creating a "teleconnection" between the boundary layer and the upper troposphere. More work is needed to establish connections and feedbacks such as study in order to avoid further unpleasant "surprises" that anthropogenic climate change may bring on.

Chapter 06

Evaluation of occupational exposure to VOC concentrations in an indoor workplace environment: Implications for health effects

In recent years, increased attention has been paid by the scientific community to understand and improve indoor workplace atmospheres. Considerable concern has been voiced over plausible health effects from exposures to pollutants in indoor air, especially to VOCs. This chapter gives an overview of the indoor air quality measurements conducted inside the glasshouse and office rooms at the Institute of Environmental Physics, University of Bremen, Germany.

6.1 Indoor air: Beware of the knowledge gaps!

Indoors air quality is considered to be governed by high levels of outdoor pollutant concentrations, pollutant sources and sinks, and movement of air between the building interior and outdoors. There has been substantial scientific enquiry in determining personal exposures to pollutants as the individuals in developed countries spend more than 90% and individuals in developing countries spend more than 70% of their time indoors [*Jones, 1999*]. Although indoor pollution is not per second more dangerous than outdoor pollution, concentrations of indoor contaminants are often higher than those encountered outside, most of which can be attributed to human activities and to type of building [*Lee et al., 2002; Wallace, 1996*]. Health awareness studies conducted on the cancer risk assessment in various environments show about 70% of the estimated cancer risk was due to exposure to polycyclic aromatic hydrocarbons, HCHO, and benzene [*Guo et al, 2004; Morello-Frosch et al. 2000; Nexo, 1995*]. A study conducted in urban areas of Germany provides strong evidence of seasonality as a characteristic for indoor VOC VMRs [*Schlink et al., 2003*]. A recent review by *Weschler* [*2001*] reports possible reactions among indoor pollutants in both the gas and particle phases, producing secondary pollutants. During the past few decades a large number of new furnishing materials have also been introduced, such as fibre board and plastic carpeting, resulting in new emission sources and exposures that have not previously been encountered.

Indoor air pollution exposure can vary strongly with various interdependent factors including outdoor sources, cooking, smoking, building materials and furnishings, heaters, office equipment, type of building and the building air exchange rate. Despite a variety of studies on air quality and occupant health, the effectiveness of ventilation for controlling concentrations of gas phase pollutants in office buildings remains an open question. Environmental Tobacco Smoke (ETS), which is primarily derived from side stream smoke, is found to be a major contributor to indoor air pollution, wherever smoking occurs [*IARC, 1998*]. As the relation between indoor air quality (IAQ) and perceived health is a complex issue, it is often difficult to simply define and measure an ideal indoor environment since the concept of good IAQ may differ depending on the occupant. The present study was based on two experiments, designed to investigate issues on the role of indoor ETS, ventilation rate, and office types

and materials on indoor air pollution in their respective indoor premises during normal indoor activities.

6.2 Sampling and analysis

6.2.1 Site description

The indoor sampling area was located in the Department of Physics and Electrical Engineering building on the south side of the University of Bremen campus (53’ 5°N, 8’49°E), near the main road characterised by moderate traffic density. The cross-shaped building recently received a five-storey, new addition completed in 2004. The experimental environments selected included the glass-domed entrance courtyard between two of the old building’s wings, which is frequently used as a smoking area by the employees, corridors, an office room in the old building tract (“old room”), and an office room in the new building tract (“new room”). The measurements took place for 14 consecutive days under routine building operations in August 2005. The experiment days were characterised by cloudy and cool-temperate meteorological conditions as summarized in Table 6.1. Since the sampling was

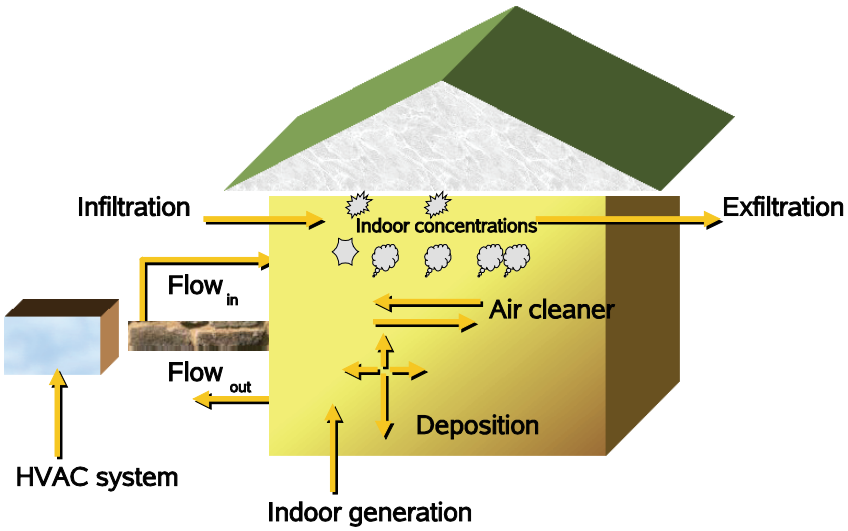

***Figure 6.1**: A schematic representation of the sampling site and the possible physical factors that affect indoor pollutant concentration.*

carried out during the summer break, student population was smaller than normal, likely to affect the results. A schematic representation of the sampling site and various factors influencing the pollutant concentration are shown in figure 6.1. The old building is a 45 year old four-storied building. Its entrance area has a footprint of roughly 440 m² with its slanted glass roof extending from the top floor. Adjacent to the ground floor entrance is a student study room, a small restaurant, and a mechanical workshop. Several potted small trees and flowering plants are permanently housed in the courtyard including European Fan Palm (*Chamaerops humilis*), Areca Palm (*Chrysalidocarpus lutescens*), and Ficus *(Ficus benjamina*). There are corridors opening from each floor to this courtyard with smoking corners at each end of the floor. Corridors and doorways separate the interior zones from the

courtyard. Ventilation of the glass-domed courtyard with outside air is provided by natural exchange through 16 windows (80x50 cm^2) in the glass roof and two normally/automatically closed entrance doors. No changes in ventilation of the courtyard occurred during the study period, with 6 windows in the roof kept open. Ventilation of the corridors and the office rooms were controlled by infiltration and natural ventilation from windows. The pollutant sources in the two offices varied with respect to office equipment and furnishings. Detailed metadata was collected for helping the interpretation of the time series analyses as well. A series of sensitivity tests prior to the experiment were also carried out to examine the uniformity of the air in the sampling area.

6.2.2 Analytical methods

Target compounds included BTEX (Benzene, Toluene, Ethylbenzene, Xylene), carbonyls, and other major components of tobacco smoke like, styrene and acetonitrile. The instrumentation used for the continuous measurements of air pollutants included PTR-MS for VOC measurements and M&M, for CH_3OH and HCHO measurements. The experimental setup for indoor measurements during the measurement period was as follows. Ambient air was sampled through a 2 μm Teflon-filter at a rate of ~15 L min^{-1} with a membrane pump through 6.4 mm ID Teflon PFA tubing, then sub-sampled at ~ 1.7 L min^{-1} into M&M and at ~100 mL min^{-1} into PTR-MS. The air samples were automatically diverted using a 3-way PFA Teflon valve for alternate sampling between indoor and outdoor air on a 30 min cycle. The sampling line of M&M was interfaced to another 3-way PFA Teflon valve to pass air either through or around the catalytic converter for alternate measurements of CH_3OH and HCHO.

The quantification of VOCs measured using PTR-MS and M&M were based on calibration standards of HCHO, CH_3OH, acetonitrile, acetone, acetaldehyde, benzaldehyde, benzene, toluene and isoprene. The responses of compounds, which were not directly calibrated for, were calculated directly from the PTR-MS data.

6.3 Results and discussion

6.3.1 Overview

Twenty-five VOCs were measured in the outdoor and indoor air, of which twenty compounds were unambiguously or tentatively identified. Metadata for the sampling sites are shown in Table 6.2. The temporal pattern and trends of selected compounds inside the glass-domed courtyard, is depicted in Figures 6.1 to 6.4, clearly indicate differences in pollutant concentrations between weekdays and weekends and between indoor and outdoor environments. Almost all pollutants exhibited diurnal cycles with maxima around noontime and minima at night, likely because of anthropogenic and/or temperature-driven source emissions and pollutant removal at night. Maximum levels for each compound in the courtyard were 2-15 times above the mean concentrations in outdoor air, and were significantly higher than those found in other microenvironments (old and new office rooms). Also the mean ratios of indoor to outdoor concentrations (I/O ratio) of the VOCs in both offices and the courtyard were greater than or equal to one. Among the pollutants measured benzene and HCHO are

high priority chemicals categorised under group I (carcinogens, e.g., HCHO, benzene, styrene) by the European Union (EU) and therefore, prone to health problems like cancer. The population exposure and risk assessment of the employees working with the university was determined by analysing the pollutant levels in indoors. The total exposure per day and for the whole period was determined from the concentration recorded per hour inside the building. Pollutant exposure indoors is estimated from:

$$\text{Exposure} = \text{Concentration} \times \text{Time exposed}$$

A simple model on how indoor pollutants impose health risk on the occupant is shown in figure 7.2. Human or occupant exposures to the pollutants generally vary with the population and time of occupation indoors.

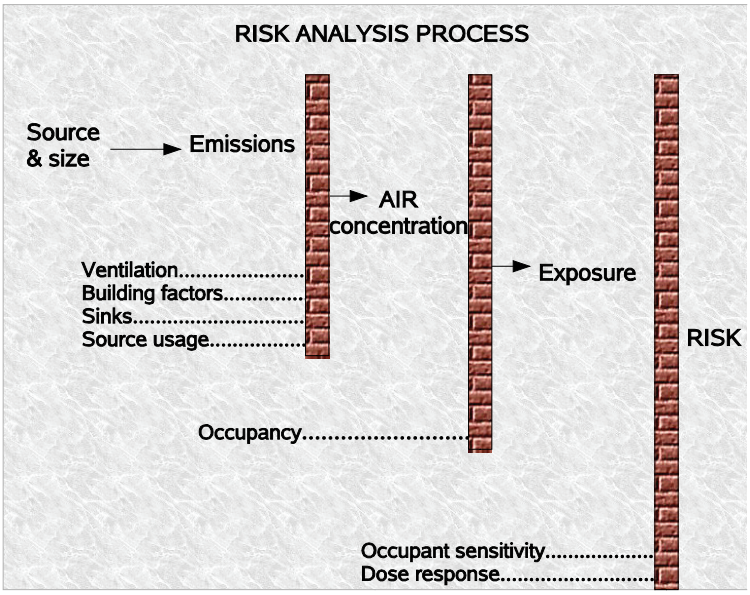

***Figure 6.2**: A schematic representation showing the relationship among sources and sink, and pollutant concentration on human exposure and health risk.*

6.3.2 Carbonyl compounds

The carbonyl compound time series from the experiment are depicted in Figures 6.3 and 6.4 in the form of hourly mean values. To a first approximation, the I/O ratio for weekend indicates emissions from within the building without people. Formaldehyde VMRs ranged from 5.5 to 87.5 ppb (Geometric Mean [GM] = 33.2 ppb), acetaldehyde from 4.4 to 79.1 ppb (GM = 20.2 ppb), benzaldehyde from 0.1 to 4.9 ppb (GM = 1.0 ppb; note that this represents an upper limit because C_8-aromatics such as xylenes contribute to the measured abundance at m/z = 107), and acetone from 3 ppb to 6 ppb (GM = 3.9 ppb).

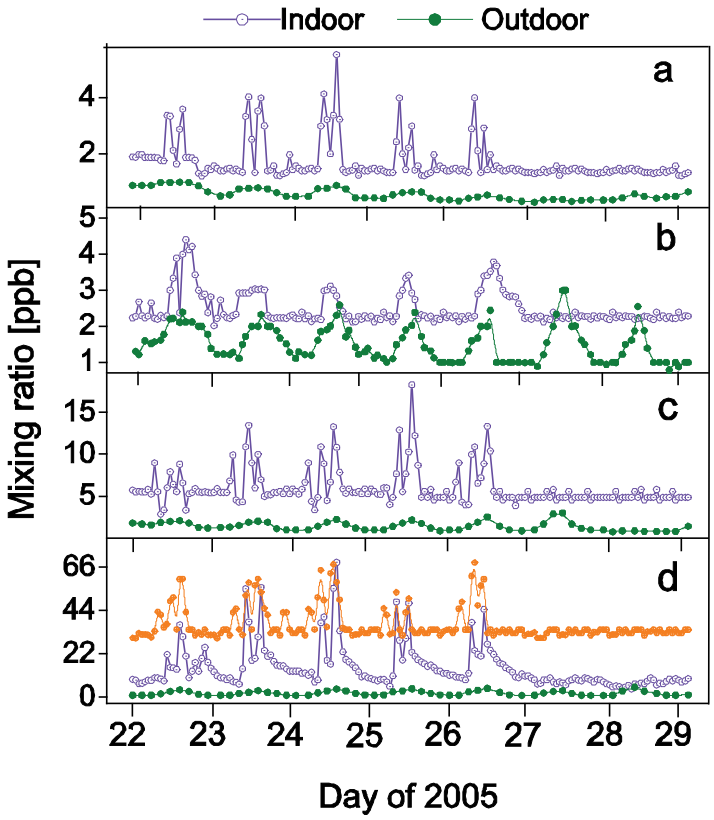

***Figure 6.3**: Time series of (a) m/z 45 (acetaldehyde), (b) m/z 59 (acetone), (c) m/z 107 (benzaldehyde and C_8-aromatics), and (d) HCHO with m/z 42 (acetonitrile as an ETS tracer) in the background (not to scale).*

All indoor carbonyl levels measured with PTR-MS showed elevated but rather flat values at night, which is typical for surface active compounds such as VOCs degassing from building surfaces or the sampling tubing itself. Another explanation for this phenomenon is method-related: besides the assigned VOC for a certain m/z value, numerous other indoor unidentified VOCs may have contributed to the mass measurements at m/z 45, 59, and 107, leading to a more or less constant background contamination. It should be noted that, there is no such contamination in the HCHO data since the measurements were carried out by an independent and highly selective method. Hence, the PTR-MS carbonyl data in Figure 6.3 should be viewed with caution when interpreting the lowest measured values, while the HCHO data are unaffected. For office rooms and courtyard, the average indoor HCHO levels were found to be more variable than the other carbonyls, with maximum concentrations in the courtyard typically exceeding 50 ppb during the smoking periods (Fig. 6.3a, Table 6.2).

Smoking was typically identified in the PTR-MS data from the signal at m/z 42 (acetonitrile, Fig. 6.3d), a known tracer of smoking [*Prazeller et al., 1998*]. Smoking-related VOCs such as HCHO [*Morrison and Nazaroff, 2002; Shaughnessy et al., 2001*] correlated with acetonitrile, and strongly with each other.

***Table 6.1**: The meteorological situation during the experiment days. The data is taken from the DWD (German Weather Office) station in Bremen (http://www.dwd.de/en/FundE/Klima/KLIS/daten/online/nat/index_tageswerte.htm).*

Date in August 2005	Mean Temp [°C]	Relative Humidity [%]	Wind speed, Winddirection [Bft]	Sunshine [hours]	Precipitation [millimetre]	Pressure [hPa]
22	17.8	88.0	3, N	5.6	0.0	1013.9
23	16.8	84.0	3, W	1.7	0.0	1012.7
24	14.9	74.0	2, SW	10.2	1.1	1011.7
25	14.6	86.0	3, S	0.0	13.5	1002.8
26	12.1	83.0	3, SW	6.9	1.3	1011.7
27	14.2	81.0	2, S	7.8	0.0	1016.9
28	15.4	81.0	2, SW	5.8	0.0	1020.9

*N= north, S= south, W= west, SW= southwest

All carbonyl concentrations seemed to be affected significantly by smoking as reported by previous studies [*Khoder et al., 2000*]. In the courtyard microenvironment, the time activity diary shows that the smoking was habitual and cyclic (Table 6.2). Absence of peak values during the weekend and the high variability during the smoking periods clearly points to smoking as the most significant source of carbonyls in this indoor environment, possibly also contribute to the constant background. All carbonyl compounds were 5-7 times higher during the active smoking period compared to their average VMR during the day.

Assuming that the spikes in HCHO abundance are solely related to smoking and HCHO thereafter decays only as a result of natural ventilation, its exponential decay after the last smoking period can be used to calculate the air exchange rate (k) of the courtyard. The hourly data shown in Figure 6.3d are used to calculate *k* in

$$x_{(t)} = (x_0 - x_{ref}) \times E^{(-k \times t)} + x_{ref} + P \qquad \text{---------- 6.1}$$

from a non-linear least squares regression of the afternoon decay of x(t) = [HCHO] versus t for x_0 = x(t=0) and x_{ref} = [$HCHO_{outdoors}$] on all five weekdays. *P* was included to account for any other possible sources or sinks within the courtyard. In all cases a significant additional source *P* was found, as expected from comparing the outdoor values to the lowest courtyard values. The exchange rate *k* was calculated to 0.36±0.08 h^{-1} (2 × standard deviation, N = 5). Though this may appear high, the value was likely to be influenced by the fact that air was sampled from the upper quarter of the courtyard closer to the glass roof, not accounting for a possible vertical gradient throughout the four-storey hall. At warmer days, when more roof windows are open, the air exchange rate of the courtyard may be higher and thus leading to more effective pollutant removal. However, during winter semesters with a relatively higher student population and fewer open windows for ventilation, significantly higher exposures of the employees to smoking-related pollutants are expected. If the smoking rate was

doubled from the 60-70 cigarettes per day (Table 6.2), while halving the air exchange rate, four times higher HCHO levels can be expected, i.e. exceeding 50 ppb on average every day.

6.3.3 Other anthropogenic VOCs

Commonly measured VOCs in a previous European study included acetone, toluene, xylenes, trimethylbenzene, limonene and isoprene [*Bernhard et al., 1995*]. Apart from the carbonyl compounds, the most abundant VOCs observed in this study were benzene, toluene, CH_3OH, styrene and isoprene, in which the BTEX compounds, shown in Figure 6.4, are regarded as being of anthropogenic origin.

Note that these BTEX compounds are less surface active compared to carbonyl species, which may account for their significantly lower levels of "background contamination" compared to the carbonyls (Figure 6.3 and Figure 6.4). Among the aromatic VOCs, benzene has been the main focus of interest because of its known carcinogenicity even at typical ambient concentrations [*WHO, 1993*]. Additionally, it is a genotoxic carcinogen and hence no safe level of exposure can be recommended. Comparing the indoor and outdoor levels, benzene was detected in slightly higher amounts in the courtyard, can be due to ETS. The median VMR of measured benzene was generally less than 6 ppb, and the I/O ratios were less than 1.0 in the old and new office rooms. However, benzene in the new office room was approximately twice of those measured in the old office rooms, which could be due to the emissions from boards and carpets containing styrene-based materials used for furnishing.

The most significant indoor source for benzene was previously found to be ETS, with its VMR increasing up to 50% compared to non-smoking environments [*Wallace and Pellizzari, 1986*] or intrusion of outdoor air. This was confirmed by our courtyard measurements, showing that benzene also peaked at the active smoking periods (Figure 6.4a). The concentrations of benzene associated with an excess lifetime risk for developing cancer of $1{:}10^3$, $1{:}10^4$, and $1{:}10^5$ are approximately 5.3, 0.5 and 0.05 ppb [*Guo et al., 2003*], respectively.

Table 6.2*: Auxiliary data for the indoor study sites namely the glasshouse, new and old office rooms.*

Code	Glasshouse (restaurant/study room)	New room	Old room
Footprint (m^2)	440 (volume of ~10560 m^3)	12	10
Smoking rate (cigarettes/day)	≥64 (from bud collection)	NA*	NA
Active smoking periods	11.30 -12.30 am 2.30 -4.00 pm	NA	NA
Cleaning period	6.30 -7.45 am	7.00-8.00 am	7.00-8.00am
Ventilation type	Infiltration, windows		
Indoor temperature (°C)	29 to 10	24 to 20	24 to 18

**NA= Not applicable*

Average urban outdoor benzene levels in the EU are 1.3±1.0 ppb with a 90th percentile of ~3.6 ppb [*IARC, 1998*]. This study also shows comparable outdoor benzene levels. However, the indoor levels often exceeded the 1:10^3 cancer risk even under moderate smoking and relatively high ventilation conditions during this experiment. It also indicates that under winter semester conditions the risk value can be exceeded at all times.

After HCHO, toluene was the second most abundant VOC indoors with an average mixing ratio of approximately 35 ppb, which was 20 times higher than its mean outdoor value. While smoking was obviously also a source of toluene, a very significant constant source, only slightly less active during the weekend must have been present. Sources may have been the restaurant kitchen, the workshop, or the numerous chemical laboratories in the building. Similar circumstances may apply to m/z 105 (styrene), m/z 107 (C_8-aromatics and benzaldehyde), and m/z 121 (C_9-aromatics). All these have significantly elevated levels indoors as compared to outdoors. Styrene in particular showed highly elevated indoor levels even during night and on weekends, suggesting numerous indoor sources besides smoking such as the linoleum floors [*Parreira et al., 2002; ATSDR, 1992*].

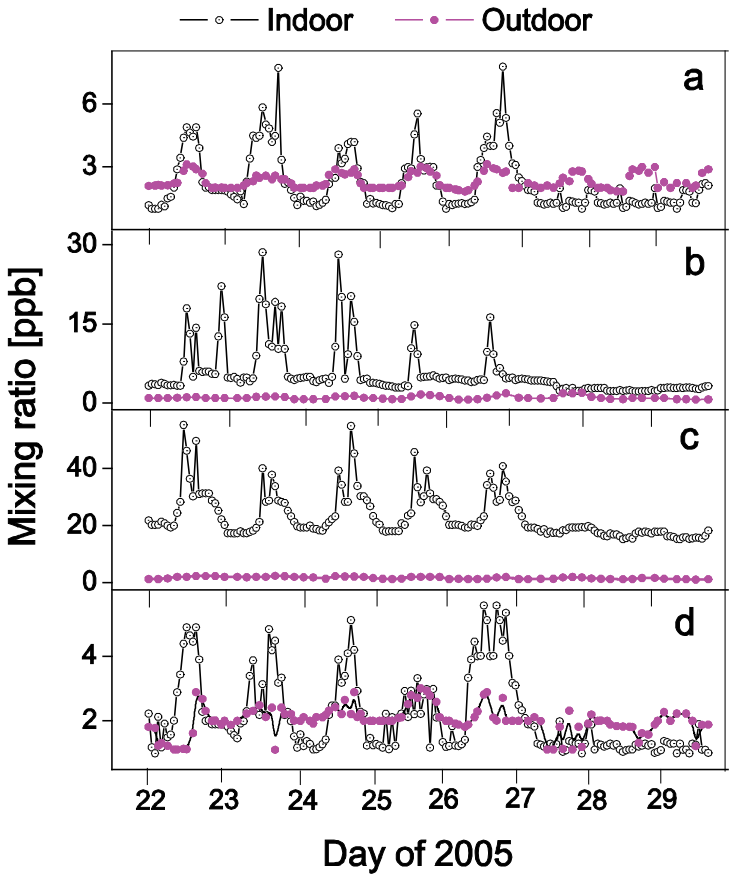

***Figure 6.4**: Same as Figure 1 but for typical aromatic VOCs contained in ETS, (a) m/z 79 (benzene), (b) m/z 93 (toluene), (c) m/z 105 (styrene), and (d) m/z 121 (C_9-aromatics).*

6.3.4 Biogenic VOCs

Measurements of selected biogenic VOCs in indoor and outdoor environments during our experiment are depicted in Figure 6.5. The highest abundances were found for m/z 33 (CH_3OH), followed by m/z 69 (isoprene), and m/z 137 (monoterpenes). The early morning peak of m/z 137 (Figure 6.5b) indicates that cleaning acts as the dominant source and hence, this too is an anthropogenic source. Fragranced and scented products including cleaners, air fresheners, lotions, soaps and detergents represent significant sources of human exposure to indoor VOCs. A wide spectrum of VOCs emitted from such sources and their health concerns are summarized in Nazaroff and *Wechsler* [*2004*]. Indoor concentrations of VOCs quantified in previous studies were in general considerably below the odour threshold but often exceeded outdoor levels by up to 5 times [*Wallace, 1991*]. The fast disappearance of m/z 137 suggests that the monoterpenes contributing to this signal were removed not just by dilution with outside air, but may have had short chemical lifetimes against reaction with ozone, such as in the case of limonene, which is typically added to cleaners as a fragrance. Methanol (Figure 6.5c) was the most abundant biogenic VOC in the indoor environments, with permanently elevated values as compared to outdoors.

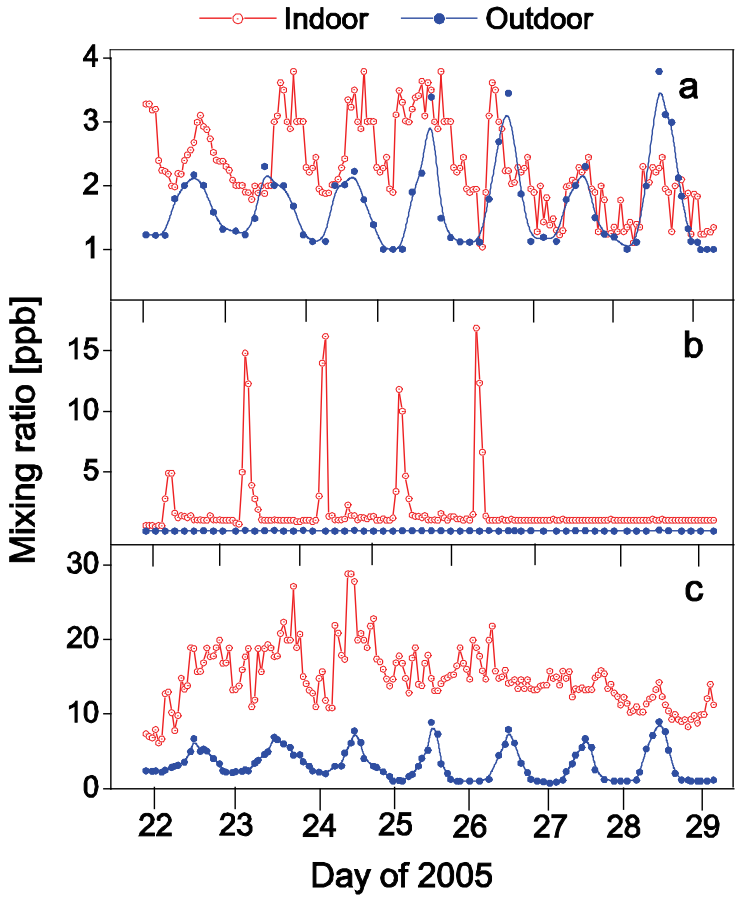

Figure 6.5: *Hourly mean abundances of selected biogenic VOCs, (a) m/z 69 (isoprene), (b) m/z 137 (monoterpenes), and (c) m/z 33 (*CH_3OH*).*

Its indoor sources may have been the courtyard plants, the kitchen, and the building occupants' breath; all related to the demethylation of plant or food pectin. The potential role of the courtyard plants was demonstrated by elevated values during the removal and replanting of green plants (e.g. on Wednesday, 24 August 2005), which could be associated with the disturbance and removal of plant litter and soil organic carbon [*Warneke et al., 1999*]. The potential role of the kitchen and the building's occupants is demonstrated by the significantly lower weekend values.

Isoprene (Figure 6.5a) is often the dominant VOC detected on m/z 69 in ambient air. Our measurements generally showed higher indoor values as compared to outdoors. A high population of isoprene emitting oak trees in this part of Bremen can readily be identified as the source of the outdoor isoprene, and the highest values were recorded during the warmer days when the wind was blowing from the largest park in Bremen to the SW of the university. Indoor isoprene was likely to be emitted by the courtyard plants. In contrast, outdoor isoprene has a much longer lifetime in indoors due to lack of oxidants, in particular the OH radical, which could explain the isoprene's higher indoor abundance albeit its much more limited leaf surface source. However, the fact that m/z 69 is not reduced to outdoor levels at night suggests that another VOC may have contributed to its indoor abundance, possibly even dominating over isoprene at times. A lower weekend indoor abundance to m/z 69 points to isoprene in human breath or another VOC coming from the restaurant kitchen as a source.

6.3.5 Office measurements

A comparison of median measured abundances of VOCs in three different indoor environments as compared to outdoors is depicted in Figure 6.6. Highest median levels of all the smoking-related VOCs were recorded inside the courtyard followed by the new office room and the old office room, clearly points to ETS as a significant source with room for abatement. Not too surprising, generally higher concentrations in the new compared to the old office room suggest significant out gassing from materials such as carpets, textiles, or furniture was ongoing [*Zhang et al., 1994a, b*].

New buildings often contain VOC levels that can be several orders of magnitude higher than outdoor levels [*Wallace, 2001*]. As an example, the rate of emission of indoor HCHO varies according to temperature and humidity, which usually exceed the observed outdoor values. A study conducted in a number of Danish homes by *Anderson et al.* [*1975*] measured the average HCHO concentration of 500 ppb. Similar findings have subsequently been reported for Germany by *Prescher and Jander* [*1987*], and for Finland by *Niemala and Vaino* [*1985*]. Though there is conclusive evidence that HCHO is an animal carcinogen [*Morgan, 1997*], none of the previous studies except that by *Vaughan et al.* [*1986*] found very strong evidence for an additional human cancer risk. Nevertheless, the mean and maximum values of HCHO that we measured in indoor air are significant as it has previously been shown to have health problems at concentrations below 1.0 ppm [*Koeck et al., 1997*].

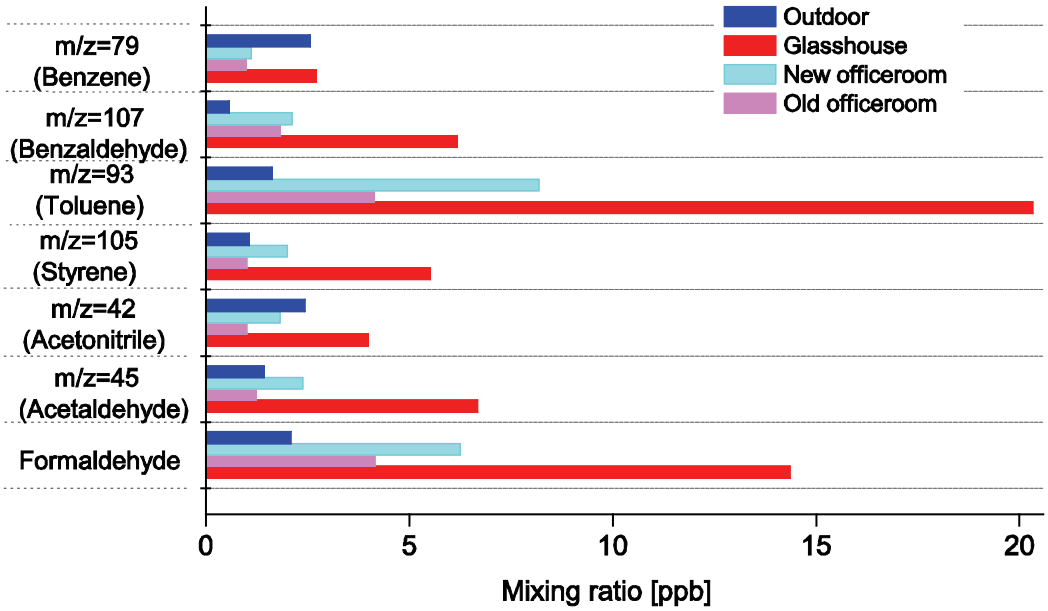

***Figure 6.6**: Median abundances of selected VOCs during the study in three different indoor environments compared to outdoors.*

The fact that the two biogenic VOCs (CH_3OH and isoprene) were also found in higher mixing ratios in the courtyard environment compared to outdoors was possibly related dominantly to plant sources since no significant differences were found in the new versus old office rooms, without plants. As expected, all commonly identified VOCs from sources in furnishings or building materials were found to be elevated in the new versus old office rooms.

6.4. Summary

The indoor survey inside a highly frequented university building identified several indoor pollutants and analysis of their abundances affirms that long-term exposure might cause adverse health effects. The VOCs concentrations in the building's glass-domed entrance hall were strongly influenced by smoking, with a sharp increase of mixing ratios up to 10 times when compared to the baseline level of each compound. As the courtyard is a preferred gathering place of both smoking and non-smoking students and employees, and many offices have "outdoor" windows to the courtyard, passive smoking is a major nuisance and concern in this environment. Particularly during winter semesters, smoking-related exposure can be higher than the measured levels during this study due to lower air exchange rates and higher smoking rates. VOCs with known health effects such as HCHO (median value [MV] = 26.5), benzene (MV = 2.75) as well as less toxic VOCs like toluene, (MV = 20.31) or benzaldehyde (MV = 4.6), were less abundant in the office rooms, where smoking is generally not tolerated and most of the work hours are spent.

However, as all corridors and many offices in the older part of the building investigated are linked to the courtyard, and nearly all employees in the building must traverse through the courtyard at least twice a day, higher exposure levels are unavoidable, but could not be evaluated in depth within the focus of this study. Nevertheless, this study confirms that even small amounts of ETS can significantly, and in the short term drastically increase the pollutant level in a large enclosed volume of air. It further shows that an abatement of ETS exposure by sending smokers into designated areas may fail to protect non-smokers effectively, unless smokers are sent outdoors or the ETS is actively removed from the building. In this particular case, smoking cannot currently be banned from the glass-domed courtyard because it is legally regarded as being outside the building. Airborne VOCs that were measured such as CH_3OH and acetone, which have both biogenic and anthropogenic sources, were not previously studied in indoor areas in detail, also showed elevated indoor levels at most times during this study. However, this was not likely to be caused by anthropogenic sources like, out gassing from the building, but was rather related to the occupant's breath, a local kitchen, and indoor plants.

Conclusions

1. A methanol to formaldehyde catalytic converter system was developed for the measurement of CH_3OH in the atmosphere. Maximum CH_3OH to HCHO conversion efficiency of 95% was obtained using a catalyst bed temperature of 345°C and an air/catalyst contact time of less than 0.2 seconds. This efficiency remained consistent and high over a period of a year of measurements without any impairment in catalyst performance. A wide range of chemicals are tested against catalyst performance to diagnose interference. The results are promising that the temperature and flow rate range of maximum conversion was found to be interference free in all the set of experiments with varying conditions.

2. VOCs (including CH_4, alkenes, aromatic compounds, alcohols, and carbonyls) with mixing ratios comparable to CH_3OH and with the potential to produce HCHO upon oxidation should exhibit no interference. The efficiency retardation effect from water content in feed mixture was also tested by passing water mixed feed mixture over the catalyst reactor. The results are encouraging as interference from water induced active site masking in the catalyst occurring only at very low and high temperatures (<300°C and >425°C). At intermediate temperatures from 300-400°C the presence of water vapour in the feed showed to have improved CH_3OH selectivity of catalyst by blocking adsorption sites for CH_3OH. The water saturation in the feed mixture seems to retard the re-oxidation of the catalyst at temperatures above 450°C and when subjected continuously for more than 78 h, which is responsible for the acceleration of its deactivation. The possible catalyst poisoning by NH_3, SO_2 and CO_2 was checked for different mixing ratios and found to be negligible <350°C. Therefore from the wide spectrum of characterisation experiments performed, the optimised reactor coupled with the wet chemical HCHO detector proved to be an essentially bias-free method for most atmospheric sampling applications.

3. By applying the method, atmospheric measurements of HCHO and CH_3OH were conducted at the Bremen University campus. Both CH_3OH and HCHO showed diurnal features consistent with previous atmospheric measurements of these VOCs, providing further confidence into the capability of the method. Hence, this selective catalytic conversion technique shows great promise as a simple, efficient, transportable, and very affordable method for atmospheric CH_3OH measurements.

4. The M&M system was validated against the measurements from existing state-of-art instruments during the first ACCENT OVOC measurement campaign at the SAPHIR chamber, Juelich. The estimated accuracy of the instrument is ~6.7% and particularly consistent accuracy was achieved even at lower mixing ratios of ~5 ppb to 0.5 ppb. The variability in accuracy was attributed to the error in permeation source used during the

campaign for HCHO calibration, which otherwise would have been better than 6.4%. The measurement reproducibility throughout the experiment was high and the precision of the instrument was recorded of the order of 6% or better for most plateaus. The RSS (root sum square) analysis of M&M measurements with other instruments showed a relative accuracy of 6.01% and 6.48% for HCHO and CH_3OH respectively. The correlation between M&M and calculated values was found to be linear with correlation coefficient values ranging from 0.80 and 0.99 for HCHO and better than 0.97 for CH_3OH. Therefore, this study affirms that M&M is a highly effective tool for the real-time analysis of CH_3OH and HCHO in complex trace gas mixtures such as atmospheric air with good precision and accuracy.

5. In the application level the instrument was used for various studies to expose different atmospheric processes leading to the formation and deposition of methanol and formaldehyde. The plant dynamic chamber experiment with Greypoplars demonstrates a strong relationship between CH_3OH emission and plant physiological and environmental parameters. Methanol flux was found to be controlled by stomatal opening as indicated by strong correlations (r^2 = 0.94) with stomatal conductance. The flux increased near-exponentially with leaf temperature with a correlation coefficient of about 0.97. The fluxes also well correlated with net carbon assimilation by the plant, transpiration rates and light intensity with r^2 values 0.90, 0.98 and 0.80 respectively. The multiple regression analysis showed strong dependence of CH_3OH flux with all physiological parameters. Compared to CH_3OH, HCHO fluxes from Grey poplars exhibited no significant correlation with any of these physiological parameters and the significance level was always P>0.0001.

6. The effect of elevated tropospheric O_3 on VOC emission from plants was asserted by ozone fumigation experiments at levels ranging from ambient (~20-40 ppb), to chronic (~70 ppb) and acute (~170 ppb) concentrations. The results are important with respect to the future changes in atmospheric composition of tropospheric trace gases and its plausible impacts on plant emissions. The plant responded to the chronic ozone levels, for 4 h/day, by emitting CH_3OH and HCHO at a rate of 2-3 times higher than the ambient conditions. The acute exposures to 170 ppb ozone for the same time duration per day lead to even higher emissions of CH_3OH at a range of ~80-100µg gFw^{-1} h^{-1}, 8-10 times higher than the ambient levels. The recovery day measurements recorded higher HCHO emissions when CH_3OH level went down suggesting the conversion of CH_3OH to HCHO inside the plant cell. Both CH_3OH and HCHO (~ 10 µg gFw^{-1} h^{-1}) showed diurnal variations with higher emissions at midday.

7. Bidirectional fluxes of both CH_3OH and HCHO were observed at nights especially during days following fumigation periods. The increased CH_3OH and hence HCHO emission was found to be related to cell wall destruction due to high ozone stress which subsides when the stress is removed. The present findings suggest that cell wall destruction and repair

mechanisms resulting from plant injury are responsible for the elevated CH_3OH emission from plants under stressed conditions. The study affirms that CH_3OH and HCHO produced by plants for the purposes of defence against environmental stress are volatile and leak into the lower atmosphere. The study is significant as the increased emission rates of CH_3OH and HCHO as observed could further enhance upper tropospheric ozone formation and thus can induce anthropogenic climate change in future.

8. The indoor survey as part of a case study designed to investigate the impact of the chemical industry on human exposures to VOCs identified several pollutants including carcinogens like benzene and formaldehyde. The environmental tobacco smoke inside the glass domed entrance hall proved to be the major source of BTEX compounds and HCHO during the weekdays. The air exchange rate (k) of the courtyard was calculated to 0.36 ± 0.08 h^{-1} by taking into account the exponential decay of HCHO after the last smoking period inside the hall. The results suggest that smoking-related exposure and risks can be higher at winter semesters than the measured levels during this study due to lower air exchange rates and higher smoking rates. VOCs with known health effects such as HCHO (MV = 26.5), benzene (MV = 2.75) as well as less toxic VOCs like toluene, (MV = 20.31) or benzaldehyde (MV = 4.6), were less abundant in the office rooms when compared to courtyard due to the absence of smoking inside the office rooms. This study confirms that even small amounts of ETS can increase pollutant levels inside the courtyard and the higher occupant exposure cannot be avoided efficiently unless it is banned from the hall. The biogenic VOCs measured inside the hall and office rooms also showed elevated indoor values contributed mostly by anthropogenic sources. Therefore the regulatory and statutory efforts to improve the quality and health effects of air within our office environment should be based on sound science and research.

References

- Adkins, H., Peterson, W, R; J. Am. Chem. Soc., 53(4); 1512-1520, 1934.
- Anderson, L. G., Lanning J. A., Barrel R., Mityagishima J., Jones R. H., and Wolfe P., Sources and sinks of formaldehyde and acetaldehyde: An analysis of Denver's ambient concentration data. *Atmos. Environ.,* 30, 2113-2123, 1996.
- Anderson, I, Lundquist G R, Molhave L: Indoor air pollution due to chipboard used as a construction material: Atmos Environ., 9: 1121-1127, 1995.
- Andreae, M. O., and Crutzen, P. J.: Atmospheric Aerosols: Biogeochemical Sources and Role in Atmospheric Chemistry, *Science*, 276, 1052-1058, 1996.
- Anthoni, P. M., Knohl, A., Rebmann, C., Freibauer, A., Mund, M., Ziegler, W., Kolle, O., and Schultze, E. –D.: Forest and agricultural land-use-dependent CO2 exchange in Thuringia, Germany, *Global Change Biology*, 10, 2005-2019, 2004.
- Arey, J., Winer, A. M., Atkinson, R., Aschmann, S. M., Long, W. D., and Morrison, C. L.: The emission of (Z)-3-hexen-1-ol, (Z)-3-hexenylacetate and other oxygenated hydrocarbons from agricultural plant species, *Atmos. Environ.*, 25A (5/6), 1063-1075, 1991.
- Arlander D. W., Brüning D., Schmidt U., and Ehhalt D. H., The Tropospheric Distribution of Formaldehyde During TROPZ II. *J. Atmos. Chem.*, 22, 251-268, 1995.
- Altshuller A. P., Production of aldehydes as primary emissions and from secondary atmospheric reactions of alkenes and alkanes during the night and early morning hours. *Atmos. Environ.*, 27, 21-31, 1993.
- Atkinson, R.: Atmospheric chemistry of VOCs and Nox, *Atmos. Environ.*, 34, 2063-2101, 2001.
- Atkinson, R. and Arey, J.: Atmospheric Chemistry of Biogenic Organic Compounds, *Accounts Chem. Res.*, 31, 574-583, 1998.
- ATSDR (Agency for Toxic Substances and Disease Registry). Toxicological Profile for Styrene. U.S. Public Health Service, U.S. Department of Health and Human Services, Atlanta, GA; 1992.
- Baker, B., Guenther, A., Greenberg, J., Goldstein, A, H., and Fall, R.: Canopy fluxes of 2-methyl-3-buten-2-ol over a ponderosa pine forest by relaxed eddy accumulation: Field data and model comparison, *J. Geophys. Res.,* 104, D21, 26107-26114, 1999.
- Beauchamp, J., Wisthaler, A., Hansel, A., Kleist, E., Miebach, M., Niinemets, Ü., Schurr, U., and Wildt, J.: Ozone induced emissions of biogenic VOC from tobacco: Relationships between ozone uptake and emission of LOX products, *Plant, Cell and Environ*., vol, 1-9, 2005.
- Bernhard C A, Kirchner S, Knutti R, Lagoudi A: Volatile organic compounds in 56 European office buildings, In: Proceedings of the Healthy Buildings ’95, Milan 1995; Vol. 3:1347–1352, 1995.
- Braun, O.L., Lohmann, M., Maksimovic, O.,Meyer, M., Merkovic, A., Messerschmidt, E., Riedel, A. & Turner, M. Potential impacts of climate change effects on preferences for tourism destinations. A psychological pilot study. *Climate Research* 11: 247–254, 1999.

- Brasseur, G. P., Orlando, J. J., and Tyndall, G. S., Atmospheric chemistry and global change: Oxford University Press, Oxford, 1999.

- Brickus L S R, Cardoso J N, Neto F R D A: Distributions of Indoor and Outdoor Air Pollutants in Rio de Janeiro, Brazil: Implications to Indoor Air Quality in Bayside Offices, Environ Sci Technol. ,32: 3485-3490, 1998.

- Brown, M. J. and Parkyns, N. D.: Progress in the partial oxidation of methane to methanol and formaldehyde, Catal. Today, 8(3), 305–335, 1991.

- Carlier P., Hannachi H., and Mouvier G., The chemistry of carbonyl compounds in the atmosphere. *Atmos. Environ.*, 20, 2079-2099, 1986.

- Chameides, W., Lindsay, R., Richardson, J., and Kiang, C.: The role of biogenic hydrocarbons in urban photochemical smog: Atlanta as a case study, *Science*, 241, 1473-1475, 1987.

- Chappelka, A, H., and Samuelson, L. J.: Ambient ozone effects on forest trees of the eastern United States: A review, *New Phytologist*, 139, 91-108, 1998.

- Cardenas, L., Brassington, D. J., Allan, B. J., Coe, H., Alicke, B., Platt, U., Wilson, K. M., Plane, J. M. C., and Penkett, S. A.: Intercomparison of formaldehyde measurements in clean and polluted atmospheres, *J. Atmos. Chem*., 37, 53–80, 2000.

- Chellapa, A. S. and Viswanath, D.: Partial oxidation of methane using ferric molybdate catalyst, *Ind. Eng. Chem. Res*., 34, 1933–1940, 1995.

- Cheng, W.-H.: Methanol and formaldehyde oxidation study over molybdenum oxide, J. Catalysis., 158, art. no. 0047, 477–485, 1996. Chu, P. M., Thorn, W. J., Sams, R. L., and Guenther, F. R.: On-demand generation of a Formaldehyde-in-air Standard, *J. Res. Natl. Inst. Stand and Technol.*, 102(5), 559–568, 1997.

- Chun, J. W. and Anthony, R. G.: Catalytic oxidation of methane to methanol, *Ind. Eng. Chem. Res.*, 32, 259–263, 1993.

- Clemitshaw, K. C.: A Review of Instrumentation and Measurement Techniques for Ground-Based and Airborne Field Studies of Gas-Phase Tropospheric Chemistry, *Crit. Rev. Env. Sci. Tech.*, 34, 1–108, doi:10.1080/10643380490265117, 2004.

- Conrad, R., and W. Seiler: Influence of temperature, moisture, and organic carbon on the flux of H2 and CO between soil and atmosphere: field studies in subtropical regions, *J. Geophys. Res.*, 90, 5699-5709, 1985.

- Crump DR and Gardiner D: Sources and concentrations of aldehydes and ketones in indoor environments in the UK: *Environ Int.,*15: 455–462, 1989.

- Custer, T. G., Kato, S., Fall, R., and Bierbaum, V.M.: Negative ion mass spectrometry and the detection of carbonyls and HCN from clover, *Geophys. Res. Lett.,* 27, 3849-3852, 2000.

- Dasgupta, P. K., Dong, S., Hwang, H., Yang, H.-C., and Genfa, Z.: Continuous liquid-phase fluorometry coupled to a diffusion scrubber for the real-time determination of atmospheric formaldehyde, hydrogen peroxide and sulphur dioxide, *Atmos. Environ.*, 22, 949–963, 1988.

- Dasgupta, P. K., Genfa, Z., Poruthoor, S. K., Caldwell, S., Dong, S., and Liu, S.-Y.: High-Sensitivity gas sensors 5 based on gas-permeable liquid core wave guides and long-path absorbance detection, *Anal. Chem.,* 70, 4661–4669, 1998.

- Dasgupta, P. K., Genfa, Z., Li, J., Boring, C. B., Jambunathan, S., and Al-Horr, R.:Luminescence detection with a Liquid core waveguide, *Anal. Chem.*, 71, 1400–1407,doi:10.1021/ac981260q, 1999.

- DeBortoli M, Knoppel H, Pecchio E. and et al: Concentrations of selected organic pollutants in indoor and outdoor air in northern Italy, *Environ Int*. 1986; 12: 343-350.
- de Gouw, J. A., Howard, C. J., Custer, T.G., Baker, B. M., and Fall, R.: Proton-Transfer Chemical-Ionization Mass Spectrometry allows real time analysis of volatile organic compounds released from cutting and drying of crops, *Environ. Sci. Tech.*, 34, 2640-2648, 2000.

- de Gouw, J. A., Warneke, C., Karl, T., Eerdekens, G., van der Veen, C., and Fall, R.: Sensitivity and specificity of atmospheric trace gas detection by proton- transfer-reaction mass spectrometry. *Int. J. Mass Spectrom.*, 223/224, 365-382, 2003.

- Dong, S. and Dasgupta, P. K.: Solubility of gaseous formaldehyde in liquid water and generation of trace standard gaseous formaldehyde, *Environ. Sci. Tech*., 20, 637–640, 1986.

- Dong, S. and Dasgupta, P. K.: Fast fluorometric flow injection analysis of formaldehyde in atmospheric water, Environ. Sci. Tech., 21, 581–588, 1987.

- Draxler, R. R. and Rolph, G. D.: HYSPLIT (HYbrid Single-Particle Lagrangian Integrated Trajectory) Model access via NOAA ARL READY Website (http://www.arl.noaa.gov/ready/hysplit4.html), NOAA Air Resources Laboratory, Silver Spring, MD, 2003.

- Dockery DW and Spengler J D: Indoor-outdoor relationships of respirable sulphates and particles: *Atmos Environ.* ,15: 335-343, 1981.

- Duncan, B.N., J.A. Logan, I. Bey, R.V. Martin, D.J. Jacob, R.M. Yantosca, P.C. Novelli, N.B. Jones, and C.P. Rinsland, Global model study of the interannual variability and trends of carbon monoxide (1988-1997) 1. Model formulation, evaluation, and sensitivity, *J. Geophys. Res., 2004.*

- Fall, R.: *Cycling of methanol between plants, methylotrophs and the atmosphere. Microbial Growth on C1 Compounds*, edited by Lidstrom, M. E., Tabita, F. R., Kluwer Academic Publishers, The Netherlands, 1996.

- Fall, R.: *Biogenic emissions of volatile organic compounds from higher plants: Reactive Hydrocarbons in the Atmosphere*, edited by C. N. Hewitt, 41-96, 1999.

- Fall, R.: Abundant Oxygenates in the Atmosphere: A Biochemical Perspective, *Chem. Rev.*, 103, 4941-4951, 2003.

- Fall, R., and Benson, A., A.: Leaf Methanol-the simplest natural product from plants, Trends *Plant Sci.*, 1(9), 296-301, 1996.

- Fall, R., Karl, T., Hansel, A., Jordan, A., and Lindinger, W.: Volatile organic compounds emitted after leaf wounding: On-line analysis by proton-transfer-reaction mass spectrometry, *J.Geophys. Res.*, 104, 15963-15974, 1999.

- Fan, Q., and Dasgupta, P. K.: Continuous automated determination of atmospheric formaldehyde at the parts per trillion levels, *Anal. Chem.*, 66, 551–556, 1994.

- Fehsenfeld, F., Calvert, J., Fall, R., Goldan, P., Guenther, A. B., Hewitt, C. N., Lamb, B., Liu, S., Trainer, M., Westberg, H., and Zimmerman, P.: Emissions of volatile organic compounds from vegetation and the implications for atmospheric chemistry, *Global Biogeochem. Cycles*, 6, 389-430, 1992.

- Fukui, Y., and Doskey, P. V.: Air surface exchange of nonmethane organic compounds at a grassland site: Seasonal variations and stressed emissions, *J. Geophys. Res.*, 103, 13153-13168, 1998.

- Galbally, I. E., and Kirstine, W.: The production of methanol by flowering plants and the global cycle of methanol, *J. Atmos. Chem.*, 43, 195-229, 2002.

- Gerberich, H. R., Stautzenberger, A. L, and Hopkins, W. C.: Formaldehyde: Kirk-Othmer Encyclopedia of chemical technology, New York, John Wiley & Sons, 231–250, 1980.

- Gilpin, T., Apel, E., Fried, A., Wert, B., Calvert, J., Genfa, Z., Dasgupta, P. K., Harder, G. W., Heikes, B., Hopkins, B., Westberg, H., Kleindienst, T., Lee, Y.-N., Zhou, X., Lonneman, W., and Sewell, S.: Intercomparison of six ambient [CH2O] measurement techniques, *J. Geophys. Res.*, 102(D17), 21 161–21 188, 1997.

- Goldan, P. D., Kuster, W. C., Fehsenfeld, F. C., and Montzka, S. A.: Hydrocarbon Measurements in the South eastern United States - the Rural Oxidants in the Southern Environment (Rose) Program 1990, *J. Geophys. Res.*, 100, 25945-25963, 1995a.

- Goldan, P.D., Trainer, M., Kuster, W. C., Parrish, D. D., Carpenter, J., Roberts, J. M., Yee, J. E., and Fehsenfeld, F. C.: Measurements of hydrocarbons, oxygenated hydrocarbons, carbon monoxide, and nitrogen oxides in an urban basin in Colorado: Implications for emission inventories. *J. Geophys. Res.*, 100, 22771-22783, 1995b.

- Goldan, P. D., Kuster, W. C., and Fehsenfeld, F. C.: Nonmethane hydrocarbon measurements during the tropospheric OH photochemistry experiment, *J. Geophys. Res.*, 102, 6315-6324, 1997.

- Griffin, R.J., D.R. Cocker III, R.C. Flagan, and J.H. Seinfeld, Organic aerosol formation from the oxidation of biogenic hydrocarbons, *J. Geophys. Res*., 104, 3555-3567, 1999.

- Guenther, A., Hewitt, C. N., Erickson, D., Fall, R., Geron, C., Graedel, T., Harley, P., Klinger, L., Lerdau, M., McKay, W. A., Pierce, T., Scholes, B., Steinbrecher, R., Tallamraju, R., Taylor, J., Zimmerman, P.: A global model of natural volatile organic compound emissions, *J. Geophys. Res.*, 100, 8873-8892, 1995.

- Guenther, A., Geron, C., Pierce, T., Lamb, B., Harley, P., Fall, R.: Natural Emissions of nonmethane volatile organic compounds, carbon monoxide, and oxides of nitrogen from North America, *Atmos. Environ*., 34, 2205-2230, 2000.

- Guenther, A. B., Baugh, W., Davis, K., Hampton, G., Harley, P., Klinger, L., Vierling, L., Zimmerman, E., Allwine, E., Dilts, S., Lamb, B., Westberg, H., Baldocchi, D., Geron, C., and Pierce, T.: Isoprene fluxes by enclosure, relaxed eddy accumulation, surface layer gradient, mixed layer gradient, and mixed layer mass balance techniques, *J. Geophys. Res.*, 101, 18555-18567, 1996.

- Guo J, Rahn KA, Zhuang G: A mechanism for the increase of pollution elements in dust storms in Beijing: *Atmos Environ*. 2004; 38: 855-862

- Heath, R. L.: Possible mechanism for the inhibition of photosynthesis by ozone, *Photosyn. Res.*, 39, 439-451, 1994.

- Heggestad, H. E.: Origin of Bel-W3, Bel-C and Bel-B tobacco varieties and their use as indicators of ozone, *Environ. Polln.*, 74, 264-291, 1991.

- Heiden, A. C., Hoffman, T., Kahl, J., Kley, D., Klockow, D., Langebartels, C., Mehlhorn, H., Sandremann Jr, H., Schraudner, M., Schuh, G., and Wildt, J.: Emission of volatile organic compounds fro ozone exposed plants, *Ecol. Appl.*, 9, 1160-1167, 1999.

- Heikes, B. G., et al, Atmospheric methanol budget and ocean implication, *Global Biogeochem. Cycles*, 16(4), 1133, doi:10.1029/2002GB001895, 2002.

- Higgins, I. J., D. J. Best, A. P. Turner, S. G. Jezequel, and H. A. Hill. 1984. *Applied aspects of methylotrophy: bioelectrochemical applications*, purification of methanol dehydrogenase, and mechanism of methane monooxygenase, p. 297--305. In R. L. Crawford and R. S. Hanson (ed.), Microbial growth on C 1 compounds. American Society for Microbiology, Washington, D.C.

- Hoffmann, T., J.R. Odum, F. Bowman, D. Collins, D. Klockow, R.C. Flagan, and J.H. Seinfeld, Formation of organic aerosols from the oxidation of biogenic hydrocarbons, *J. Atmos. Chem*., 26, 189-222, 1997.

- IARC (International Agency for Research on Cancer): Overall Evaluations on Carcinogenicity to Humans, IARC Monographs, Vol. 1: Lyon, France; 1998.

- IPCC 2001,In: Houghton J T, Ding Y, Griggs D G, Nogeur M, van der Linden P J, Xiaosu D, eds, Climate change 2001: the scientific basis, Cambridge, Cambridge University Press.

- Jones, C. and Rasmussen, R. (1975) Production of isoprene by leaf tissue. *Plant Physiol*. 55, 982–987

- Jones A P: Indoor air quality and health, *Atmos Environ.* 1999; 33: 4535-4564.

- Jiru, P., Wichterlova, B., and Tichy, J. (1965) Mechanism of Oxidation of Methyl Alcohol to Formaldehyde on Oxide Catalyst. In Proceedings of 3rd International Congress on Catalysis; Amesterdam; Vol. 1, 199.

- Karacic V, Skender L, Bosner-Cucancic B, Bogadi-Sare A: Possible genotoxicity in low-level benzene exposure, *Am J Ind Med*.,27: 379–388, 1995.

- Kesselmeier, J., Ciccioli, P., Kuhn, U., Stefani, P., Biesenthal, T., Rottenberger, S., Wolf, A., Vitullo, M., Valentini, R. Nobre, A., Kabat, P., and Andreae, M.O.: Volatile organic compound emissions in relation to plant carbon fixation and the terrestrial carbon budget, *Global Biogeochem. Cycles*, 16, 1126, doi: 10.1029/2001GB001813, 2002.

- Kirstine, W., Galbally, I., Ye, Y. R., and Hooper, M.: Emissions of volatile organic compounds (primarily oxygenated species) from pasture, *J. Geophys. Res*., 103, 10605-10619, 1998.

- König, G., Brunda, M., Puxbaum, H., Hewitt, C. N., Duckham, S. C., and Rudolph, J.: Relative contribution of oxygenated hydrocarbons to the total biogenic VOC emissions of selected mid-European, agricultural and natural plant species. *Atmos. Environ.*, 29, 861-874, 1995.

- Kutsch, W., Liu, C., Hörmann, G., and M. Herbst, Spatial heterogeneity of ecosystem carbon fluxes in a broadleaved forest in Northern Germany, *Global Change Biology*, 11, 70-88, 2005.

- Khoder M I, Shakour A A, Farag S A, Hameed A A A: Indoor and outdoor formaldehyde concentrations in homes in residential areas in Greater Cairo: *J Environ Monit.* 2000; 2: 123-126.

- Koeck M, Pichler-Semmelrock F P, Schlacher R: Formaldehyde - Study of Indoor Air Pollution in Austria: Central European J Public Health. 1997; 5: 127-130.

- Lamb, B., Gay, D., Westberg, H., and Pierce, T.: A Biogenic Hydrocarbon Emission Inventory for the U.S.A. Using a Simple Forest Canopy Model, *Atmos. Environ*., 27A, 1673-1690, 1993.

- Lamanna, M. S., and Goldstein, A. H.: In situ measurements of C_2-C_{10} volatile organic compounds above a Sierra Nevada ponderosa pine plantation. *J. Geophys. Res.*, 104, 21247-21262, 1999.

- Lebret E, van del Wiel HJ, Bos H, Noij D, Boleij JSM: Volatile organic compounds in Dutch homes: Environ Int. , 12: 323-332, 1986.

- Lee S C, Li W M, Ao CH: Investigation of indoor air quality at residential homes in Hong Kong-case study: *Atmos Environ.* , 36: 225–237, 2002.

- Li W M, Lee S C, Chan L Y: Indoor air quality at nine shopping malls in Hong Kong: *Sci Total Environ*., 273: 27-40, 2001.

- Li, J., Dasgupta, P. K., Genfa, Z., and Hutterli, M. A.: Measurement of Atmospheric Formaldehyde with a Diffusion scrubber and light-emitting diode-liquid-core wave-guide based fluorometry, *Field Anal. Chem. Tech.*, 5(1-2), 2–12, 2001.

- Lightfoot, P. D., Cox, R. A., Crowley, J. N., Destriau, M., Hayman, G. D., Jenkin, M. E., Moortgat, G. K., and Zabel, F.: Organic peroxy radicals: Kinetics, spectroscopy and tropospheric chemistry, *Atmos. Environ.*, 26A, 1805-1961, 1992.

- Lindinger, W., Hansel, A., and Jordan, A.: Online monitoring of volatile organic compounds at pptv levels by means of proton-transfer-reaction mass spectrometry (PTR-MS), Medical applications, food control and environmental research, *Int. J. Mass. Spectrom.*, 173, 191-241, 1998.
- Lindskog, A., and Potter, A.: Terpene emission and ozone stress, *Chemosphere*, 30, 1171-1181, 1995.

- Lipari F., Dasch J. M., and Scuggs W. F., Aldehyde emissions from wood-burning fireplaces. *Environ. Sci. Tech.*, 18, 326-330, 1984.

- Loreto, F. et al. (1998) On the monoterpene emission under heat stress and on the increased thermotolerance of leaves of Quercus ilex L. fumigated with selected monoterpenes. *Plant. Cell Environ*. 21, 101–107

- Loreto, F., Mannozzi, M., Maris, C., Nascetti, P., Ferrnati, F., and Pasqualini, S.: Ozone quenching properties of isoprene and its anti-oxidant role in leaves, *Plant Physiol.*, 126, 993-1000, 2001.

- Loreto, F., and Velikova, V.: Isoprene produced by the leaves protects the photosynthetic apparatus against ozone damage, quenches ozone products, and reduces lipid peroxidation of cellular membranes, *Plant Physiol.*, 127, 1781-1787, 2001.

- Loreto, F., Pinelli, P., Manes, F., and Kollist, H.: Impact of ozone on monoterpene emission and evidence for an isprene like antioxiadant action of monoterpenes emitted by Quercus Ilex leaves, *Tree Physiol.*, 24, 361-367, 2004.

- Lorenzini, G., and Panattoni, A.: an integrated, physico-chemical and biological, survey of atmospheric ozone in coastal Tuscany, Italy, *Rivista di Patologie Vegetale*, S IV 22, 130-164, 1986.

- Lowe D. C. and Schmidt U.: Formaldehyde (HCHO) measurements in the momurban atmosphere. *J. Geophys. Res.*, 88, 10844-10858, 1983.

- Mancinelli, R. L.: The regulation of methane oxidation in soil, *Ann. Rev. Microbio.*, 49, 581-605, 1995.

- Martin, C., Martin, I., and Rives, I.: Fourier-transform infrared study of the oxidation of ethane on MoO3/TiO2 catalysts doped with alkali metals, *J. Chem. Soc. Faraday. Trans.,* 89(22),4131–4135, 1993.

- McKeen, S. A., Hsie, E. Y., and Liu, S. C.: A study of the dependence of rural ozone on ozone precursors in the eastern United States, *J. Geophys. Res.*, 96, 15377-15394, 1991.

- McKeen, S. A., Gierczak, T., Burkholder, J. B., Wennberg, P. O., Hanisco, T. F., Keim, E. R., Gao, R. S., Liu, S. C., Ravishankara, A. R.,and Fahey, D. W.: The photochemistry of acetone in the upper troposphere: A source of odd-hydrogen radicals, *Geophys. Res. Lett.*, 24, 3177-3180, 1997.

- Millet, D. B., Goldstein, A. H., Allan, J. D., et al.: Volatile organic compound measurements at Trinidad Head, California, during ITCT 2K2: Analysis of sources, atmospheric composition, and aerosol residence times, *J. Geophys. Res.*, 109, S16, doi:10.1029/2003JD004026, 2004.

- Montzka, S.A., R.C. Myers, J.H. Butler, J.W. Elkins, and S.O. Cummings,Global tropospheric distribution and calibration scale of HCFC-22. *Geophys. Res. Lett.,* 20:703-06, 1993.

- Morello-Frosch, R. A.; Woodruff, T. J.; Axelrad, D. A.; Caldwell, J.C. Air toxics and health risks in California: the public health implications of outdoor concentrations, *Risk Analy.* , 20: 273-291, 2000.

- Morrison, G C and Nazaroff, W W.: Ozone interactions with carpet: secondary emissions of aldehydes, *Environ Sci Technol.,* 36: 2185-2192, 2002.

- Morgan K T.: A brief review of formaldehyde carcinogenesis in relation to rat nasal pathology and human health risk assessment, *Toxicologic Pathology*, 1997; 25: 291-307.

- Nazaroff W W and Weschler C J.: Cleaning products and air fresheners: exposure to primary and secondary air pollutants, *Atmos Environ.*,38: 2841–2865, 2004.

- Niemala R and Vaino H.: Formaldehyde exposure in work and the general environment, *Scand J Work Environ Health*. 7: 95-100, 1985.

- Nguyen, H. T., Takenaka, N., Bandow, H., and Maeda, Y.: Flow Analysis Method for Determining the Concentration of Methanol and Ethanol in the Gas Phase Using the Nitrite Formation Reaction, *Anal. Chem.*, 72, 5847-5851, 2000.

- Palmer, P. I., D. J. Jacob, A. M. Fiore, R. V. Martin, K. Chance, and T. P. Kurosu, Mapping isoprene emissions over North America using formaldehyde column observations from space, *J. Geophys. Res.,* 108, doi:10.1029/2002JD002153, 2003.

- Parreira F V, de Carvalho C R, Cardeal Z de L.: Evaluation of Indoor Exposition to Benzene, Toluene, Ethylbenzene, Xylene, and Styrene by Passive Sampling with a Solid-Phase Microextraction Device, *J Chromato Sci.* 2002; 40: 122-126.

- Pasqualini, S., Batini, P., Ederli, L., Porceddu, A., Piccioni, C., Marchis, F. DE., and Antonielli, M.: Effects of short term ozone fumigation on tobacco plants: response of the scavenging system and expression of the glutathione reductase, *Plant, Cell and Environ.*, 24, 245-252, 2001.

- Pasqualini, S., Piccioni, C., Reale, L., Ederli, L., Torre, G. D., and Ferranti, F.: Ozone-induced cell death in tobacco cultivar Bel W3 plants. The role of programmed cell death in lesion formation, *Plant Physiol.*, 133, 1122-1134, 2003.

- Prasad, R. L., and Thakur, S. N.: Monitoring air pollution using infrared photoacoustic spectra of organic vapours. *J. Indian Chem.*, 80, 341-344, 2003.

- Peel, E. J., and Dann, M. S.: *Multiple stress induced foliar senescence and implication of whole plant longevity, In Responses of Plant to Multiple stresses* (eds H. A. Mooney, W. e. Winner and E. J. Peel), 189-204, Academic press, San Diego, CA, 1991.

- Penuelas, J. et al. (1995) Terpenoids: a plant language. *Trends Ecol. Evol.* 10, 289

- Penuelas, J., Llusia, J., Gimeno, B. S.: Effects of ozone on biogenic organic compounds emission in the Medeterranean region, *Environ. Pollut.*, 1005, 17-23, 1999.

- Penuelas, J., Llusia, J.: The complexity of factors driving volatile organic compound emissions by plants, *Biologia Planatarum*, 44, 481-487, 2001a.

- Penuelas, J., and Llusia, J.: BVOCs: plant defense against climate warming?, *Trends in Plant Sci,* 8, 105-109, 2003.

- Pernicone, N., Lazzerin, F., Liberti, G., and Lanzavecchia, G. (1969) On the Mechanism of CH_3OH Oxidation to CH_2O Over MoO_3-$Fe_2(MoO_4)_3$ Catalyst., *J. Catal.,* 14: 239.

- Prazeller, P.; Karl, T.; Jordan, A.; Holzinger.; R. Hansel, A.; Lindinger, W. Quantification of passive smoking using proton-transfer-reaction mass spectrometry, *Int J Mass Spectrom*.,178: L1-L4, 1998.

- Prescher, K.E. and Jander, K. Formaldehyde in indoor air, Bundesgesundheitsblatt,,30: 273-278, 1987.

- Qin, T., Xiaobai, X., Polk, T., Packova, V., Tulik, K., and Jech, L.: A simple method for the trace determination of methanol, ethanol, acetone and pentane in human breath and in the ambient air by preconcentration on solid sorbents followed by gas chromatography, *Talanta,* 44,1683-1690, 1997.

- Repond, P., and Sigrist, M. W.: Photoacoustic spectroscopy on trace gases with continuously tunable CO2 laser, *Appl. Optics*, 35, 4065-4085, 1996.

- Riemer, D., Pos, W., Milne, P., Farmer, C., Zika, R., Apel, E., Olszyna, K., Kliendienst, T., Lonneman, W., Bertman, S., Shepson, P., and Starn, T.: Observations of nonmethane hydrocarbons and oxygenated volatile organic compounds at a rural site in the southwestern United States, *J. Geophys. Res.*, 103, 28111-28128, 1998.

- Sandermann Jr, H., Ernst, D., Heller, W., and Langenbartels, C.: Ozone: an abiotic elicitor of plant defense reactions, *Trends Plant Sci.*, 3, 47-50, 1998.

- Sanz M.J. and Millán M. M. (1998) The dynamics of aged air masses and ozone in the Western Mediterranean: Relevance to forest ecosystems, *Chemosphere*, 36, 1089 . 1094.

- Schade, G. W., and Goldstein, A. H.: Fluxes of oxygenated volatile organic compounds from a ponderosa pine plantation, *J. Geophys. Res.,* 106, 3111-3124, 2001.

- Schade, G. W., and Custer, T. G.: OVOC emissions from agricultural soil in northern Germany during the 2003 European heat wave, *Atmos. Environ.*, 38, 6105-6114, 2004.

- Schnitzler, J. -P., Bauknecht, N., Brüggemann, N., et al.: Emission of Biogenic Volatile Organic Compounds: An Overview of Field, Laboratory, and Modelling Studies Performed during the 'Tropospheric Research Program' (TFS) 1997-2000, *J. Atmos. Chem.*, 42, 159-177, 2002.

- Schlink U, Rehwagen M, Damm M, Richter M, Borte M, Herbarth O.: Seasonal cycle of indoor-VOCs: comparison of apartments and cities, *Atmos Environ*.,38: 1181-1190, 2004.

- Shulaev, V. et al. (1997) Airborne signalling by methyl salicylate in plant pathogen resistance. *Nature* 385, 718–721

- Shaughnessy, R J, McDaniels T J, Weschler C J.: Indoor chemistry: ozone and volatile organic compounds found in tobacco smoke, *Environ Sci Technol.* 2001; 35: 2758–2764.

- Sharkey, T. D., and Singaas, E. L.: Why plants emit isoprene, *Nature*, 374, 769, 1995.

- Sharkey, T. D.: Emission of low molecular mass hydrocarbons from plants, *Trends Plant Sci.*, 1(3), 78-82, 1996.

- Sheldon L, Handy R W, Hartwell T D, Whitmore R W, Zelon H S, Pellizzari E D, Wallace L.: Indoor air quality in public buildings, Volumes II and II, EPA Report EPA/600/6-88/009a and EPA/600/6-88/009b; 1998.

- Sillman, S.: The relation between ozone, NOx and hydrocarbons in urban and polluted rural environments, *Atmos. Environ.*, 33, 1821-1845, 1999.

- Singh, H. B., Kanakidou, M., Crutzen, P. J., and Jacob, D. J.: High concentrations and photochemical fate of oxygenated hydrocarbons in the global troposphere, *Nature*, 378, 50-54, 1995.

- Singh, H., Chen, Y., Tabazadeh, A., and et al.: Distribution and fate of selected oxygenated organic species in the troposphere and lower stratosphere over the Atlantic, *J. Geophys. Res.*, 105, 3795-3805, 2000.

- Singh, H. B., Salas, L. J., Chatfield, R. B., Sandholm, S., and Fuelberg, H.: Analysis of the atmospheric distribution, sources, and sinks of oxygenated volatile organic chemicals based on measurements over the Pacific during TRACE-P, *J. Geophys. Res.*, 109, S07, doi:10.1029/2003JD003883, 2004.

- Skarby, L., Ro-Poulsen, H., Wellburn, F.A.M. and Sheppard, L.J. 1998. Impacts of ozone on forests: a European perspective. *New Phytologist* 139: 109-122.

- Sluis, M. K., Larsen, R. A., Krum, J. K., Anderson, R., Metcalf, W. W., and Ensign, S. A.: Biochemical, molecular and genetic analyses of the acetone carboxylases from Xanthobacter autotrophicus strain Py2 and Rhodobacter capsulatus strain B19, *J. Bacteriol.*, 184, 2969-2977, 2002.

- Smith, K. A., T. Ball, F. Cohen, K. E. Dobbie, J. Massheder, and A. Rey, Exchange of greenhouse gases between soil and atmosphere: interactions of soil physical factors and biological processes, *European Journal of Soil Science*, 54, 779-791, 2003.

- Snider, J. R., and Dawson, G. A.: Tropospheric light alcohols, carbonyls, and acetonitrile: concentrations in the southwestern United States and Henry's law data, *J. Geophys. Res.*, 90, 797-3805, 1985.

- Soares, A. P., Portela, M. F., Kiennemann, A., Hilaire, L., and Millet, J. M. M.: Iron molybdate catalysts for methanol to formaldehyde oxidation: effects of Mo excess on catalytic behavior, *App. Catal*. A, 206(2), 221–229, 2001.

- Soares, A. P. V., Portela, M. F., Kiennemann, A., and Hilaire, L.: Mechanism of Deactivation of Iron-Molybdate Catalysts Prepared by Co precipitation and Sol-Gel Techniques in Methanol to Formaldehyde Oxidation, *Chem. Eng. Sci.,* 58(7), 1315–1322, 2003.

- Solomon, S. J., Custer, T., Schade, G., Soares Dias, A. P., and Burrows, J.: Atmospheric methanol measurement using selective catalytic methanol to formaldehyde conversion, *Atmos. Chem. Phys. Discuss.*, 5, 3533-3559, 2005.

- Stefania, P., Claudia, P., Lara, R., Luisa, E., Guido Della, T., and Francesco, F.: Ozone-induced cell death in tobacco cultivar Bel W3 plants. The role of programmed cell death in lesion formation, *Plant Physiol.*, 133, 1122-1134, 2003.

- Tabazadeh, A., Yokelson, R. J., Singh, H. B., Hobbs, P. V., Crawford, J. H., and Iraci, L. T.: Heterogeneous chemistry involving methanol in tropospheric clouds, *Geophys. Res. Lett*., 31, doi: 10.1029/2003GLO18775, 2004.

- Tie, X., Guenther, A., Holland, E.: Biogenic methanol and its impacts on tropospheric oxidants, *Geophys. Res. Lett.*, 30 (17), 1881-1884, doi: 10.1029/2003GL017167, 2003.

- Tyndall, G. S., Cox, R. A., Granier, C., Lesclaux, R., Moortgat, G. K., Pilling, M. J., Ravishankara, A. R., and Wallington, T. J.: Atmospheric Chemistry of small organic peroxy radicals, *J. Geophys. Res.*, 106, 12157-12182, 2001.

- Vairavamurthy, A., Roberts J. M., and Newman, L.: Methods for determination of low molecular weight carbonyl compounds in the atmosphere: a reveiw, *Atmos. Environ*., 26A, 1965–1993, 1992.

- Vaughan T L, Strader C, Davis S, Daling J R.: Formaldehyde and cancers of the pharynx, sinus, and nasal cavity: II. Residential exposures, *Int J Cancer*. 1986; 38: 685-688.

- Wallace, L A. Human exposure to volatile organic pollutants implications for indoor air studies, *Annu Rev Energy Environ*.,26: 269–301, 2001.

- Wallace, L A. Environmental exposure to benzene: an update, *Environ Health Perspect*.,104: 1129-1136, 1996.

- Wallace, L A.; Nelson, W.C.; Ziegenfus, R. and et al. The Los Angeles TEAM study: personal exposures, indoor-outdoor air concentrations and breath concentrations of 25 volatile organic compounds, *J Expos Anal Environ Epidemiol.* , 1: 37-73, 1991.

- Wallace, L A.; Pellizzari, E.D.; Hartwell, T.D. and et al. The TEAM study: personal exposures to toxic substances in air, drinking water, and breath of 400 residents of New Jersey, North Carolina, and North Dakota, *Environ Res*., 43: 290-307, 1987.

- WHO (World Health Organisation), Updating and revision of the air quality guidelines for Europe, Meeting Report, 11-13 January, 1993.

- Warneke, C., Karl, T., Judmaier, H., Hansel, A., Jordan, A., Lindinger, W., and Crutzen, P. J.: Acetone, methanol, and other partially oxidized volatile organic emissions from dead plant matter by abiological processes: Significance for atmospheric HOx chemistry, *Global Biogeochem. Cycles*, 13, 9-17, 1999.

- Winer, A. M., Arey, J., Atkinson, R., Aschmann, S. M., Long, W. D., Morrison, C. L., and Olszyk, D. M.: Emission rates of organics from vegetation in California's Central Valley, *Atmos. Environ.*, 26A, (14), 2647-2659, 1992.

- Yokelson, R. J., Ward, D. E., Susott, R. E., Reardon, J., and Griffith, D. W. T.: Emission from smoldering combustion of biomass measured by open-path Fourier transform infrared spectroscopy, *J. Geophys. Res.*, 102, 18865-18877, 1997.

- Yokelson, R. J., Bertschi, I. T., Christian, T. J., Hobbs, P.V., Ward, D.E. and Hao, W.: Trace gas measurements in nascent, aged, and cloud-processed smoke from African savanna fires by airborne Fourier transform infrared spectroscopy (AFTIR), *J. Geophys. Res.*, 108, 8478, doi:10.1029/2002JD002322, 2003.

- Zhang J, He Q, Lioy P J.:Characteristics of aldehydes: concentrations, sources, and exposures for indoor and outdoor residential microenvironments, *Environ Sci Technol*.,28: 146–152, 1994a.